Oceanographic and Physical Setting

Arthur Desch[1], Timothy Wynne[1], Russell Brainard[2], Alan Friedlander[3,4] and John Christensen[1]

INTRODUCTION

The Northwestern Hawaiian Islands (NWHI) are set in a dynamic oceanographic and meteorological regime in the northern/central subtropical region of the Pacific Ocean (Figure 2.1). The boundary between the nutrient-poor surface waters of North Pacific Subtropical Gyre and the nutrient-rich surface waters of the North Pacific Subpolar Gyre frequently influence the NWHI region (Kazmin and Rienecker, 1996; Leonard et al., 2001; Polovina et al., 2001). This front shifts seasonally (Polovina et al., 2001) and migrates on interannual and decadal time scales, bringing colder and nutrient rich waters that are likely important to the productivity and ecology of the region (Polovina and Haight, 1999; Nakamura and Kazmin, 2003; Polovina, 2005). Longer-term changes, particularly those related to climate, are of concern since the reef ecosystems of the NWHI may not have encountered such conditions for hundreds, thousands or even millions of years (Rooney et al., 2008).

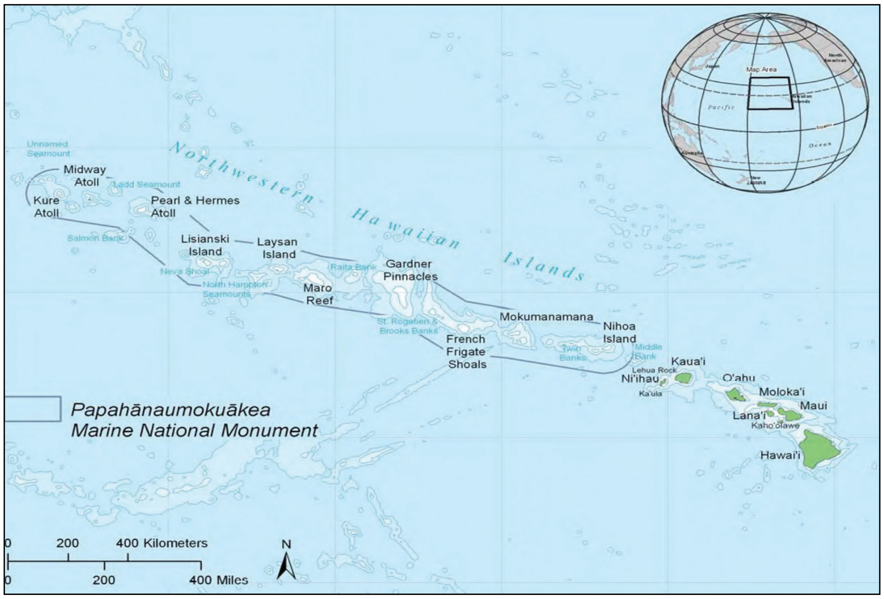

Figure 2.1. Hawaiian Archipelago Including the NWHI (Nihoa Island to Kure Atoll) and Main Hawaiian IslandsI (Hawaii to Kauai). Inset shows the Hawaiian Archipelago in the Pacific Ocean. Source: PMNM, 2008.

The health, functioning and biogeography of ecosystems of the NWHI are primarily controlled by the oceanographic processes and conditions, both physical and chemical, to which they are exposed. The Monument's diverse biological ecosystems, including fishes, corals and other invertebrates, algae, turtles, seabirds and marine mammals, is significantly influenced by ocean currents, waves, nutrients, temperature, and other measures of water quality and oceanographic conditions. The most important factors controlling the distribution and abundance of coral reefs in the NWHI are depth and shelter from large open ocean winter swell (Grigg. 1983).

This chapter provides a comprehensive analysis of ocean currents, waves, temperature, winds and productivity using satellite remote sensing data to offer a quantitative assessment of regional ocean climate. The objective is to capture spatial and temporal patterns in each of these parameters and to set context for the biogeographic assessment that follows. The Monument sits in a region of the Pacific Ocean that is dominated by large-scale circulation patterns that fluctuate over periods of years and decades. With that perspective, these data sets have been collected and analyzed over a spatial scale that includes much of the North Pacific Ocean. Large scale events and processes are the focus here. To illustrate this concept, Figure 2.2 provides a view of global sea surface temperature (SST), chlorophyll (ocean color), wind and sea surface height or SSH (proxy for currents). Each of these examples represents the average condition, worldwide, for the month of March. This view is provided as a reminder that while the NWHI cover a vast region, variability in oceanographic conditions as resolved by remote sensing platforms is most evident at basin-wide scales. That is, analysis of remote sensing data within the NWHI is not as variable as the Pacific basin as a whole. A short summary of regional cli-

1. NOAA/NOS/NCCOS/CCMA Coastal Oceanographic Assessment Status and Trends Branch
2. NOAA/NMFS/Pacific Islands Fisheries Science Center, Coral Reef Ecosystem Division
3. NOAA/NOS/NCCOS/CCMA Biogeography Branch
4. The Oceanic Institute

mate and oceanography is presented in advance of the quantitative analysis to provide points of reference for the results presented.

REGIONAL SUMMARY

Climate

The climate of the entire Hawaiian Archipelago features mild temperatures year-round, moderate humidity, persistent northeasterly trade winds and infrequent severe storms. Hawaii's climate is notable for its low day-to-day and month-to-month variability (Giambelluca and Schroeder, 1998). The climate is influenced by the marine tropical or marine Pacific air masses depending upon the season. During the summer, the Pacific High Pressure System dominates, with the ridge line extending across the Pacific north of Kure and Midway. This places the region under the influence of easterly winds, with marine tropical and trade winds prevailing. During the winter, especially from November through January, the Aleutian Low moves southward over the North Pacific, displacing the Pacific High (Grigg et al., 2008). The Kure-Midway region is then affected by either marine Pacific or marine tropical air, depending upon the intensity of the Aleutian Low or the Pacific High Pressure System (Amerson et al., 1974). The surrounding ocean has a dominant effect on the weather of the entire archipelago. Air temperature at the northern end of the archipelago varies between 11 and 33°C. Air temperature measurements made at six sites on Nihoa Island (23º N latitude) from March 2006 to March 2007 ranged between 16 and 34°C. Annual rainfall over the last 26 years has been 73.28 cm on average, ranging between 40.61 and 104.24 cm/year (PMNM, 2008).

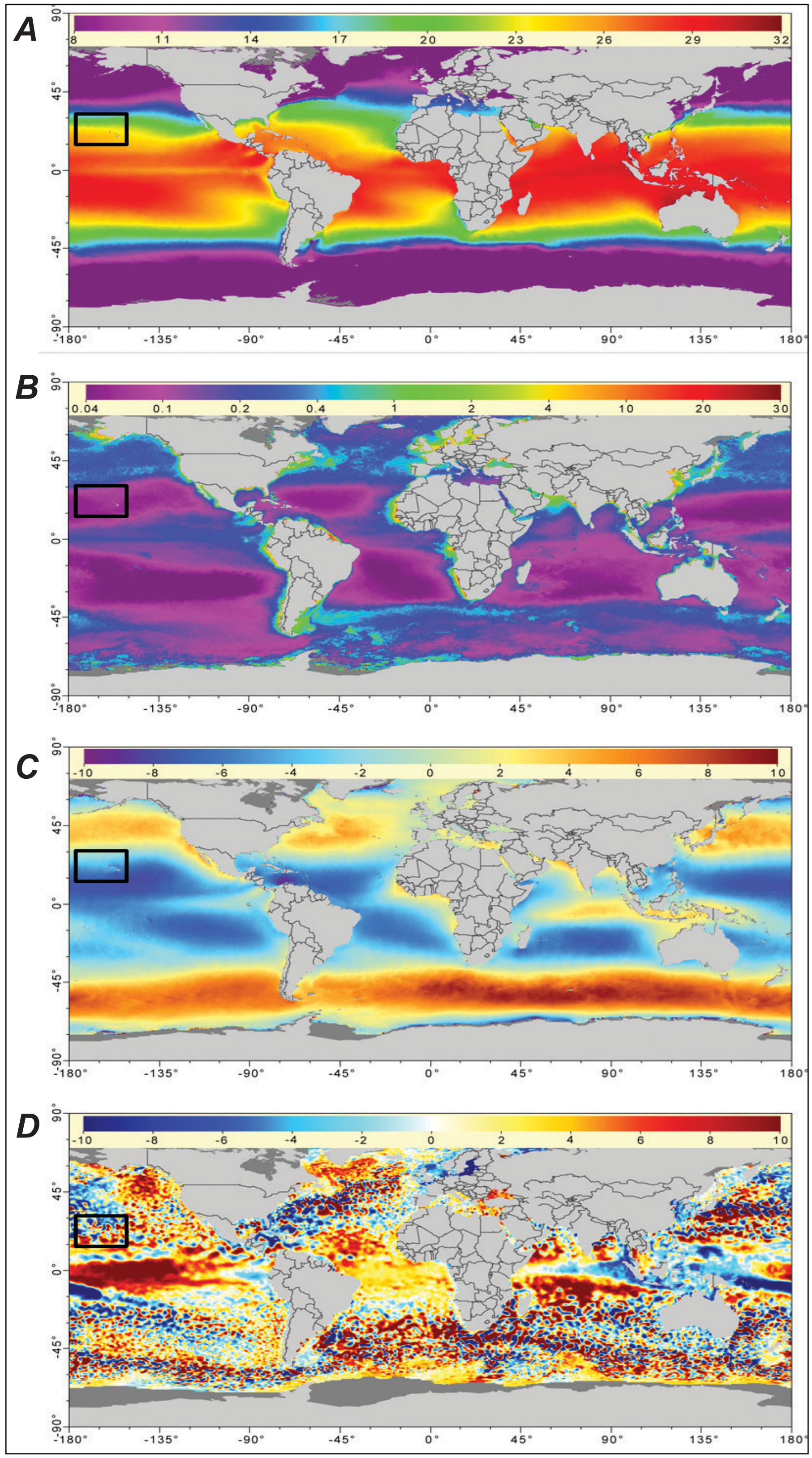

Figure 2.2. (A) Global climatological SST (ºC), (B) chlorophyll mg/m^3, (C) wind m/sec (D) and sea surface height anomaly cm estimates for the month of March. The NWHI study area is shown as a black box.

El Niño – Southern Oscillation (ENSO) and Pacific Decadal Oscillation (PDO)

ENSO is an interannual global climate phenomenon that results from the large-scale coupling of atmospheric and oceanic processes, which creates significant temperature fluctuations in the tropical surface waters of the Pacific and other oceans. The two distinct ENSO signatures in the Pacific Ocean are known as El Niño and La Niña. During El Niño events, the Aleutian Low pressure system tends to be more intense and extend further to

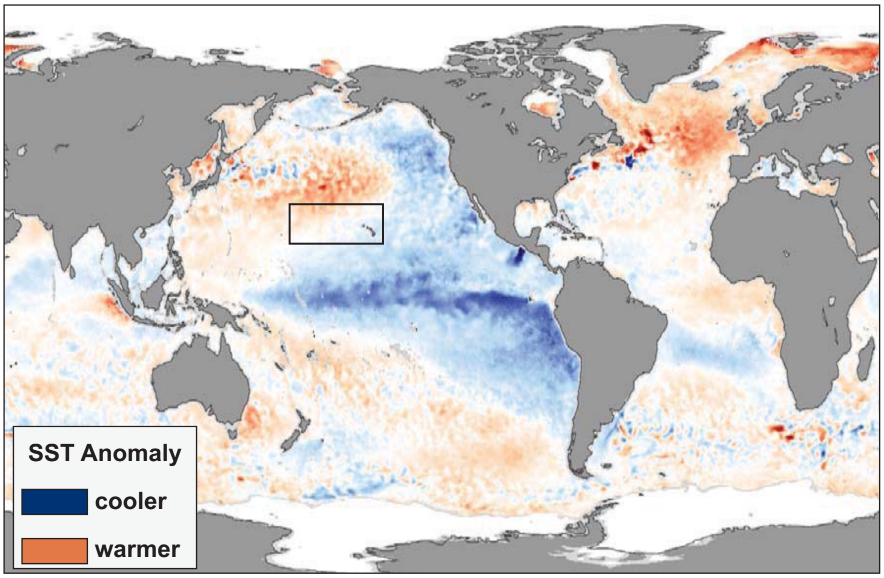

Figure 2.3. Diagram SST anomalies in November 2007 showing La Niña conditions. Blue tones indicate cooler than average surface temperatures, while orange tones indicate warmer than average. The Hawaiian Islands, including the NWHI are in the black box.

the south (closer to the NWHI), thereby producing stronger winds, larger waves and cooler water temperatures in the NWHI (Bromirski et al., 2005). During La Niña, SSTs in the eastern tropical Pacific are below average, and temperatures in the western tropical Pacific are above average (Figure 2.3). Leonard et al. (2001) and Rooney et al. (2008) have suggested that positive ENSO signatures (warming) correspond with southern extensions of the North Pacific subtropical front. A strong band of cool water (blue in false color range) appears along the Equator, particularly strong near South America. Warm conditions (orange in false color range) appear north and south of this strong blue band (Figure 2.3). The NWHI be seen straddling both warm and cold portions of the basin-wide temperature anomaly, highlighting complex regional thermal structure. Because biological communities are significantly influenced by spatially and temporally-varying ocean currents, temperature and nutrients (Polovina et al., 1995; Seki et al., 2002; Polovina et al., 2004), regional biogeography is equally complex and dynamic.

The PDO is a long-lived El Niño-like pattern of Pacific climate variability. While the two climate oscillations have similar spatial footprints, they have very different behavior in time. Two main characteristics distinguish PDO from ENSO are: 1) 20th century PDO events persisted for 20-to-30 years, while typical ENSO events persisted for 6 to 18 months; and 2) the climatic effects of PDO are most visible in the North Pacific, while secondary signatures exist in the tropics. The opposite is generally true for ENSO. Several independent studies provide evidence that two full PDO cycles have occurred over the past century, where cool regimes prevailed from 1890-1924 and again from 1947-1976, and warm regimes dominated from 1925-1946 and from 1977 through the mid-1990s. Additional research suggests that 20th century PDO fluctuations were most energetic in two general periodicities, one from 15-to-25 years, and the other from 50-to-70 years (http://jisao.washington.edu/pdo/).

Ocean Temperature

SST is an important physical factor influencing coral reefs and other marine ecosystems of the Monument. Maximum monthly climatological mean SST measured over the last 20 years at Kure is 27 ºC in August and September (NOAA Pathfinder SST time series; Hoeke et al., 2006), with monthly minimums in February at 19 ºC. The large seasonal temperature fluctuations at the northern end of the archipelago result in the coldest – and sometimes the warmest – SSTs in the entire Hawaiian chain (Brainard et al., 2004). At the southern end of the Monument, the annual variation in SST is much less, with French Frigate Shoals only varying between 23.3 and 27.5º C.

Winter temperatures tend to be 3-7°C cooler at the northerly atolls than at the southerly islands and banks as the subtropical front migrates southward. These cooler winter temperatures are thought to reduce coral growth rates (Grigg 1983, Grigg et al. 2008). In addition to the strong annual cycle, SST observations show significant interannual and decadal variability (Figure 2.4). The highest summer maximum SSTs at the northern atolls occurred during the summers of 1987, 1991 and 2002, possibly suggesting a teleconnection with ENSO events. Winter minimum temperatures at the northern atolls appear to oscillate over a longer time period, as indicated by a significant warming of winter SSTs beginning in 1999 and lasting for several years (Brainard et al., 2004). During the period between July and September 2002, ocean temperatures along the Hawaiian Archipelago were warmer than average.

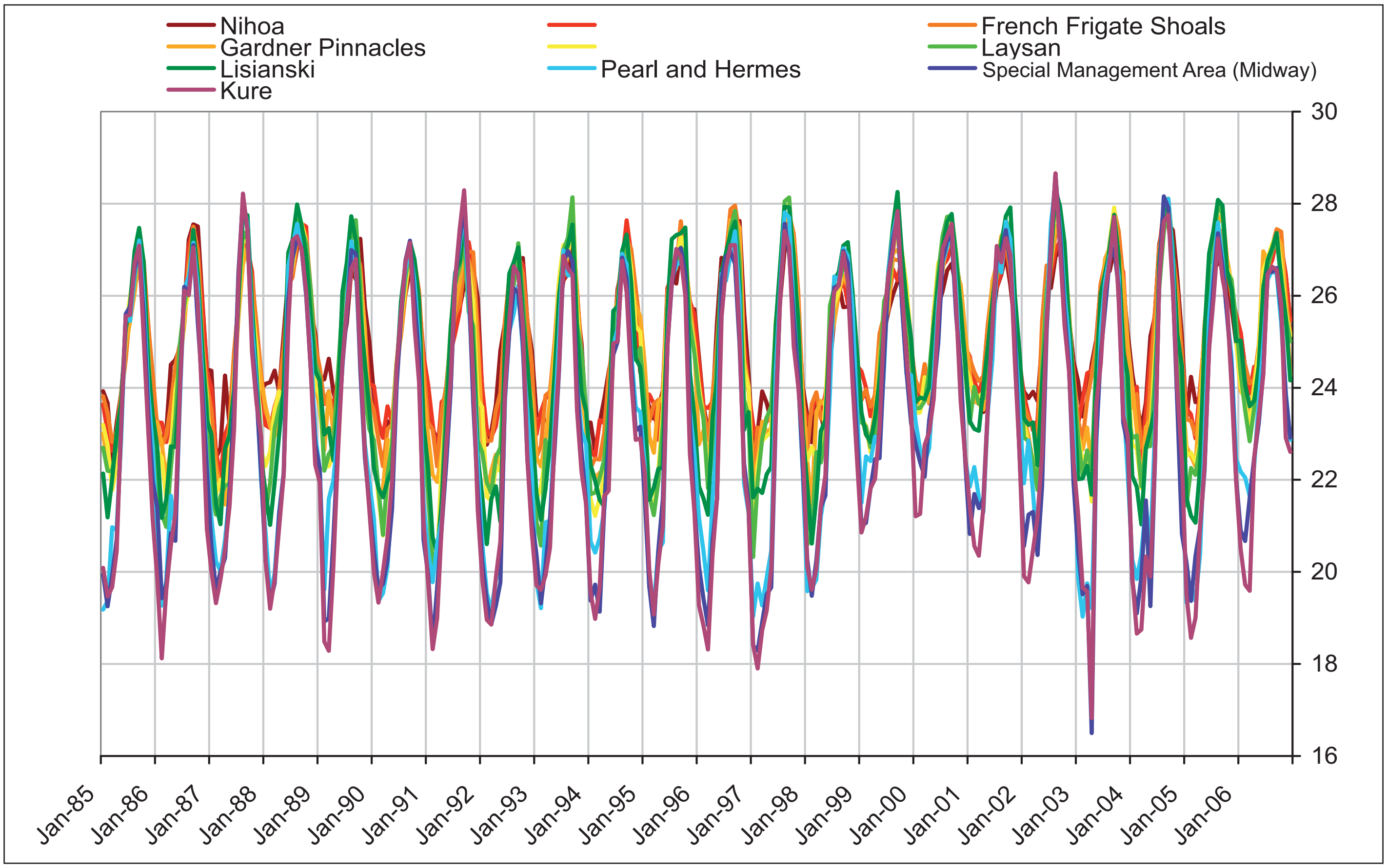

Figure 2.4. Pathfinder SST (^{o}C) time-series for islands, atolls and shoals throughout the Monument (1985-2006).

While coral bleaching can be caused by a wide range of environmental variables acting alone or in combination (Jokiel and Brown, 2004), the predominant cause of increasing incidences of coral bleaching globally is believed to be persistent warmer than average water temperatures (Jokiel and Coles, 1990; Kenyon et al., 2006a,b), and indeed a significant bleaching event was documented during the summer of 2002 (Friedlander et al., 2005; Hoeke et al., 2006, Kenyon et al., 2006a,b).

Ocean Currents

Ocean currents transport and distribute larvae among and between different atolls, islands and submerged banks of the NWHI, and also provide the mechanism by which species are distributed to and from the main eight Hawaiian Islands, as well as other regions (Polovina et al., 1995). The relatively low species diversity and high endemism of the NWHI are the result of the relative oceanographic isolation of the Hawaiian Archipelago (Grigg et al., 2008; Demartini and Friedlander, 2004; Friedlander et al., 2008).

Ocean currents are measured and monitored in the NWHI in many different ways. Since 1990, ocean current profiles along the Hawaiian Archipelago have been measured using Acoustic Doppler Current Profilers (ADCP) aboard the NOAA ships *Townsend Cromwell* (1990 to 2002) and *Oscar Elton Sette* (2003 to present) during routine transects along the archipelago to support a number of scientific cruises for NOAA's Pacific Islands Fisheries Science Center (PIFSC).

Based on 10 years of ADCP data (1990-2000), Firing et al. (2004a) demonstrated that upper ocean currents in the NWHI are highly variable in both speed and direction. Averaged over time, the resultant mean flow of the surface waters tend to flow predominantly from east to west in response to the prevailing northeast trade winds. The lack of coral reef ecosystems and low biodiversity to the east, or upstream, of the Hawaiian Archipelago explains the low species richness and high endemism (PMNM, 2008). Surface Velocity Program current drifters and autonomous profiling explorer drifters have also been deployed in the NWHI by PIFSC annually since 2001. These drifters provide indications of the Lagrangian (or water-following) flow, thereby representing potential larval pathways (Firing et al., 2004a).

Ocean Waves

Common throughout the region and perhaps more significant as a natural process affecting the geology and ecology of the Monument, are the extra-tropical storms and significant wave events that regularly move across the North Pacific in the boreal winter (Friedlander et al., 2008, Grigg et al., 2008). Among each of the islands, atolls and submerged banks of the NWHI, the distributions of species of corals and algae, and their associated fish and invertebrate assemblages are often determined not only by the ocean currents, but also by the exposure to ocean waves. Many species of corals and algae can only survive in sheltered or quiescent habitats. Other species; however, can survive or even thrive in the high wave-energy habitats on the northwestern facing reefs that are exposed to tremendous waves caused by winter storms across the North Pacific.

These large wave events, greater than 10 m, influence the growth forms and distribution of coral reef organisms (Dollar, 1982; Dollar and Grigg, 2004; Grigg et al., 2008) and affect the reproductive performance of winter-breeding seabirds nesting on low islets in the Monument. Most large wave events, 5 to 10 m, approach the NWHI from the west, northwest, north and northeast, with the highest energy generally occurring from the northwest sector. The southern sides of most of the islands and atolls of the NWHI are exposed to fewer and weaker wave events. Annually, mean wave energy and wave power (energy transferred across a given area per unit time) are highest (approximately 1.3 W/m) between November and March and lowest (approximately 0.3 W/m) between May and September (Figure 2.5). Extreme wave events, 10 m or higher, affect shallow water coral reef communities with at least an order of magnitude more energy than the typical winter waves (Grigg et al., 2008).

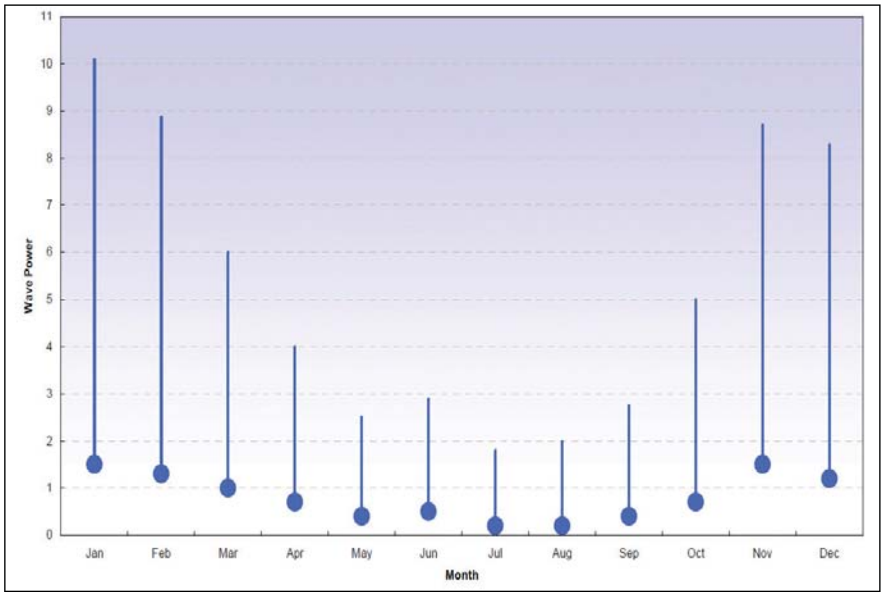

Figure 2.5. Diagram of Climatological values of wave power (W/m) derived from NOAA buoy # 51001 located near Nihoa Island from 1981 to 2003. Blue circles represent monthly means; blue lines represent wave power maxima. Source: NOAA NDBC.

Significant wave events vary over interannual and decadal time scales. This temporal variability of wave power allows expansions and retractions of the spatial and vertical ranges of the same species during relatively quiescent and turbulent years, respectively (Rooney et al., 2008). Over the past 20 years, wave measurements at NOAA buoy 51001 (near Nihoa Island in the NWHI) show a pattern of numerous extreme wave events during the periods 1985-1989 and 1998-2002 and low numbers of extreme wave events in the early 1980s and the period 1990-1996. This apparent decadal variability of wave power is possibly related to the PDO (Mantua et al., 1997). Studies have shown decadal oscillations of various components of NWHI ecosystems (lobsters, monk seals, seabirds, etc.) relate to larger scale climate shifts across the North Pacific (Polovina et al., 1995).

Primary Productivity / Ocean Color

Productivity in the NWHI is influenced by local and regional factors, and upwelling may occur in response to localized wind and bathymetric features (Friedlander et al., 2005). The Monument is located at the northern edge of the oligotrophic tropical Pacific, in the North Pacific central gyre ecosystem (Figure 2.6). Regional factors are largely influenced by the position of the subtropical front and associated high chlorophyll content of waters north of the front (PMNM, 2008). High chlorophyll waters intersect the northern portions of the NWHI during southward winter migrations of the subtropical front. The influx of nutrients to the NWHI from these migrations is considered a significant factor influencing different trophic levels in the NWHI (Polovina et al., 1995). It is near the 18°C isotherm, a major ecological transition zone in the northern Pacific. This boundary, also known as the "chlorophyll front", varies in position both seasonally and annually, occasionally transgressing the

Monument boundary and surrounding the northern atolls of Kure and Midway (PMNM, 2008).

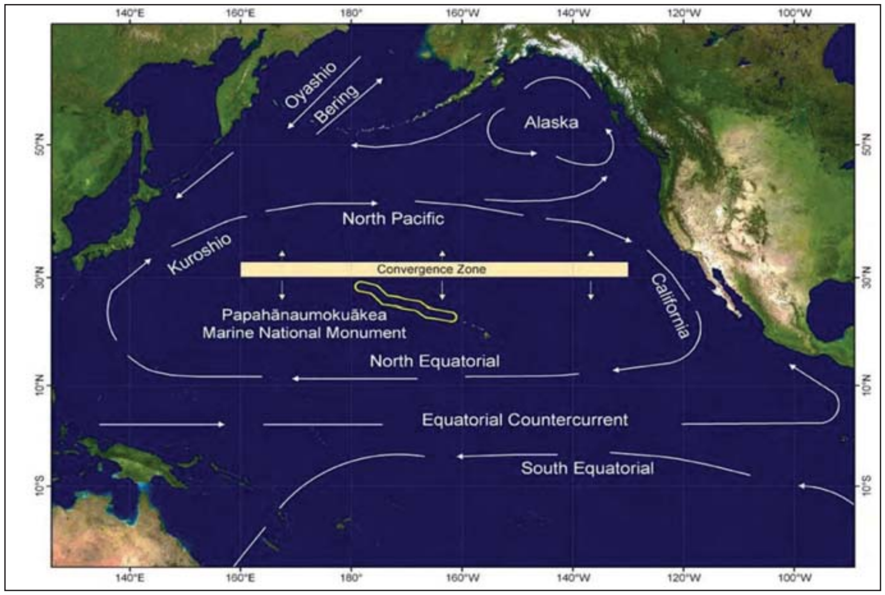

Figure 2.6. Diagram of Central Pacific Gyre. The North Pacific, California, North Equatorial, and Kuroshio currents along with atmospheric winds generate the North Pacific Subtropical Gyre. The subtropical Convergence Zone, an area where marine debris is known to accumulate, shifts seasonally between 23ºN and 37ºN latitude.

Movement of this front influences overall ocean productivity, and resultant recruitment of certain faunal elements such as Hawaiian monk seals and Laysan and Black-footed Albatrosses (Polovina et al., 1994). The northernmost atolls also are occasionally affected by an episodic eastward extension of the Western Pacific warm pool, which can lead to higher summer ocean temperatures at Kure than are found in the more "tropical" waters of the MHI further south (Hoeke et al., 2006). This interplay of oceanography and climate is still not completely understood, but is a dynamic not seen in most other tropical atoll ecosystems. As a result, it provides a useful natural laboratory for understanding phenomena such as periodic coral bleaching and the effects of El Niño and La Niña ocean circulation patterns (see ocean temperature).

Satellite observations of ocean color from the National Aeronautics and Space Administration's (NASA) Sea-viewing Wide Field-of-view Sensor (SeaWiFS) reveal a significant chlorophyll front associated with the subtropical front, with high chlorophyll north of the front and low oligotrophic waters south of the front. These observations reveal significant seasonal and interannual migrations of the front northward during the summer months and southward during the winter months (Seki et al., 2002). The southward migration of the subtropical front generally brings these high chlorophyll waters to intersect the northern portions of the NWHI. During some years, these winter migrations of the subtropical front extend southward to include the northern end of the NWHI. Additional evidence suggests decadal scale movements in the southward extent of the subtropical front. During periods when high chlorophyll waters intersect the NWHI, overall productivity of the affected reef ecosystems is expected to be elevated. Changes across many trophic levels of the NWHI ecosystem are believed to be associated with these migrations (Polovina et al., 1995).

OCEAN REMOTE SENSING ANALYSIS: DATA AND METHODS

This oceanographic assessment is based largely on data acquired from satellite and *in situ* sensors to characterize conditions for each of the management areas within the Monument, as well as the larger ecological region. For this report, the study area is defined as: north bounding coordinate – 45ºN; south bound – 15ºN; east bound – 145ºW; and west bound – 175ºE. Spatial patterns in the temperature, temperature fronts and chlorophyll were identified, as well as the variability in those patterns. Time series information was also extracted from the datasets to investigate trends at a variety of time-scales.

The Monument includes 10 special management zones and eco-regions. These management regions are centered on relatively untouched islands, reefs and atolls that are home to thousands of species, some that are found nowhere else on earth. The oldest (approximately 28 million years old) and most northern are Kure Atoll, Midway Island and Pearl and Hermes Atoll. These three ecosystems are subject to similar oceanographic influences and will be analyzed together as the northern grouping. The adjacent, and next most southeasterly grouping – Lisianski Island, Laysan Island, Maro Reef and Gardner Pinnacles – lie along the same latitudinal zone and exhibit similar temperature and chlorophyll climatological profiles, as well as being subjected to similar current regimes. These will be analyzed together as the central group. The most southern and youngest (7-12 million years old) of the atolls are French Frigate Shoals, Mokumanamana Island, and Nihoa Island (Figure 2.7). These three experience milder SSTs, smaller temperature ranges through the year and are less impacted by winter storm waves.

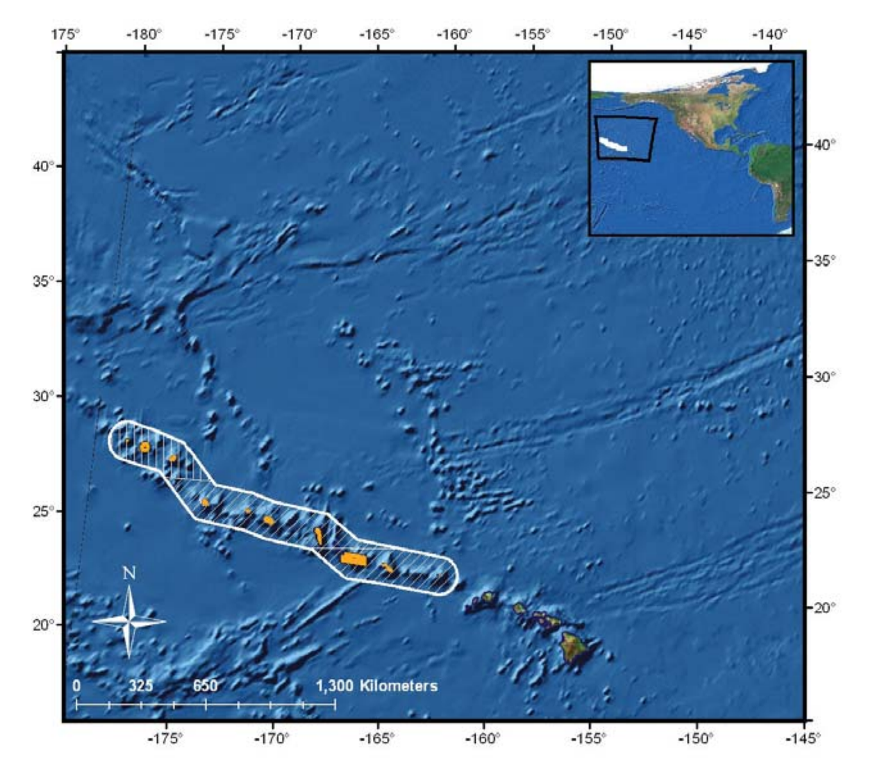

Figure 2.7. Locator map of the study area. Cross-hatched regions represent the northern, central, and southern analysis areas.

The study area encompasses a region much larger than the Monument boundaries so as to allow ecosystem-scale information to be included in management decisions. Much of the oceanographic variety in the region of the Monument happens well away from the atolls themselves. The northern group of atolls is the only which experiences extreme events and changes on a fairly regular basis. Even though the Monument itself is relatively calm compared to the ocean environment around it, the more extreme events of the central pacific influence the migration of fauna in and around the Monument atolls, and thus must be considered.

Data Assembly and Processing

The majority of remote sensing data products were obtained as monthly composites (mean), and subsequently processed into seasonal and interannual monthly means and medians. Seasonal means were calculated using the following constraints: winter (January, February, March); spring (April, May, June); summer (July, August, September); and fall (October, November, December). Production of a consistent time series of imagery in this manner allowed extraction of data from each source within regions of interest, and for regional averages within the bounds of the entire Monument. These time series were extracted for 10 locations in the study region (Figure 2.7, orange polygons), as well as the three regional groupings and the Monument as a whole for preliminary analyses of episodic, seasonal and interannual patterns. Interannual monthly means were then derived from the extracted time series. These data composites over the entire Monument, or for specific locations, were created to summarize trends and to highlight episodic and seasonal events useful for interpreting biogeographic patterns discussed later in this report. Time series images consist of all monthly mean or median data for each month over time. For example, the month of January has an image of mean chlorophyll for each of the years 1998 to 2007. These 10 monthly images are then averaged to obtain an interannual mean of chlorophyll. Monthly and seasonal anomaly images were produced to illustrate the differences between the long-term interannual mean and the monthly image.

Chlorophyll

Chlorophyll products were derived from data obtained from SeaWiFS. SeaWiFS data for research and educational applications have been available through the NASA since its launch in September of 1997 through December 2007. The sensor provides reliable daily observations for the United States at a nominal spatial resolution of 1.1 km for spectral bands encompassing the visible and near-infrared spectrum. The 4 km Global Area Coverage (GAC) product was used because data quality and density of the 1.1 km data was insufficient in the NWHI region (Figure 2.8).

The entire SeaWiFS GAC dataset was processed with SeaDAS version 5, applying the improved algorithms and obtaining georeferenced chlorophyll-a data at 4-km spatial resolution for the central Pacific region. Products were created for the central Pacific region specifically to include the boundaries of the Monument and also encompass the surrounding environment to allow management and scientific inquiry to include the greater ecosystem contextual processes. Estimations of chlorophyll-a in units of µg/L were derived using the standard OC4v4 equation that NASA used for global products from SeaWiFS. NOAA's Center for Coastal Monitoring and Assessment (CCMA) has developed algorithms, implemented by NASA for standard processing, to improve the generation of ocean color data and estimation of chlorophyll from SeaWiFS (Stumpf et al., 2003).

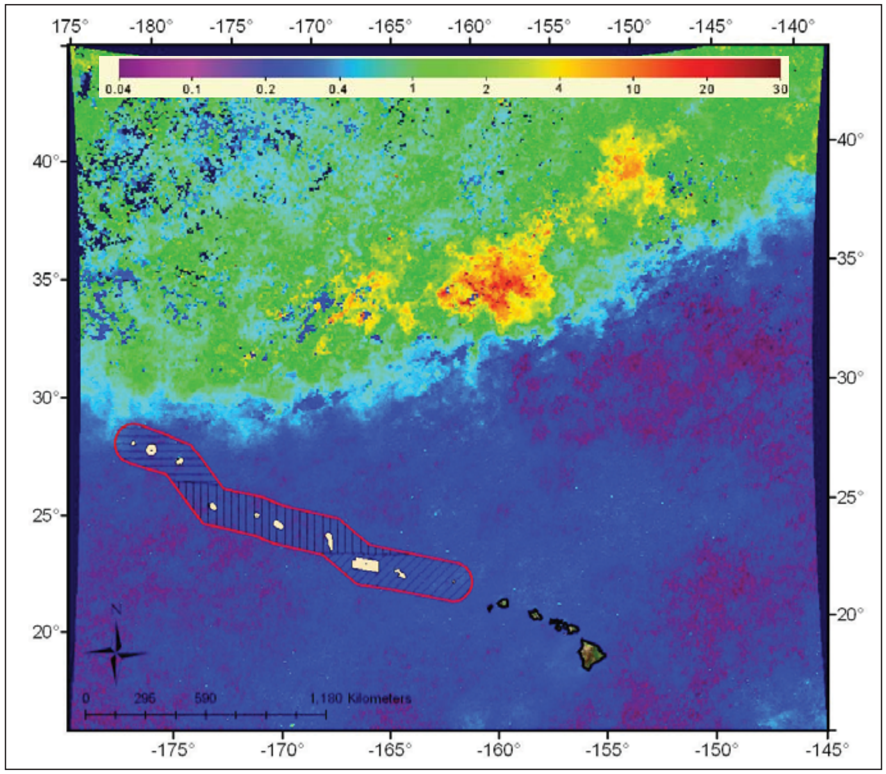

Figure 2.8. Example Global Area Coverage (GAC) chlorophyll distribution throughout the study region (April 2004). Warm tones represent high chlorophyll, while cool tones represent lower estimated chlorophyll concentrations (Units are µg/L).

Chlorophyll-a is the dominant pigment in marine photosynthetic organisms, and is referred to simply as chlorophyll within this report. Time series image sets of chlorophyll were created for the specified regions in Geotiff format. These time series images are useful for determining trends in algal bloom activity and ocean productivity. Final products were projected using the Albers Conical Equal Area (ACEA) projection with the World Geodetic System 1984 (WGS-84) datum. The imagery time series generated from the SeaWiFS data are monthly medians. Seasonal means were created from the appropriate monthly median files resulting in a seasonal image (seasons previously defined), and interannual monthly and seasonal files were generated using all monthly images for a particular month (or season) in the time series as input.

Sea Surface Temperature and Frontal Boundaries

SST data were developed from the NASA Pathfinder Version 5.0 dataset. This dataset derives a climatological grade SST product from Advanced Very High Resolution Radiometer (AVHRR) imagery, which was generated from several NOAA Polar-orbiting Environmental Satellites between 1985 and the present. The Pathfinder dataset was calibrated for inter-comparison of the temperature data across the entire period, facilitating climate and other studies (NASA, 2004; NASA, 2005). Ocean fronts data, regions that delineate the boundary between different water masses, were obtained from the Geostationary Operational Environmental Satellite (GOES).

Fronts were generated from GOES 2000-2006 hourly images (averaged to months) sampled to 4 km (Figure 2.9). Fronts were identified in each image using an algorithm developed by Canny (1986). Front occurrences were tallied at each pixel location for a month, season or year as needed. Climatological means were also created. Data products were mapped and subset to the study area. Geotiffs were created using the ACEA projection with the WGS-84 datum (Figure 2.9).

Spatial resolution of the Pathfinder data varies slightly with latitude, with a horizontal resolution of approximately 4 km at 35 degrees of latitude. Pathfinder is distributed along a 0.04 degree grid in Cartesian coordinates. The original global 4 km data were subset to the study area bounds. Geotiffs were created of the monthly mean time series (1985-2006) using the ACEA projection with the WGS-84 datum. SST image datasets were created from monthly means for the region; units are degrees Celsius (ºC).

Ocean Currents

The calculation of SSH is based on a reference ellipsoid. This reference ellipsoid is a raw approximation of Earth's surface, a sphere flattened at the poles. This position is determined relative to an arbitrary reference surface, an ellipsoid. The satellite altitude above the reference ellipsoid (distance S) is available to within 3 cm. The SSH, is the range at a given instance from the sea surface to a reference ellipsoid. Since the sea depth is not known accurately everywhere, this reference provides accurate, homogeneous measurements. The sea level is simply the difference between the satellite height and the altimetric range.

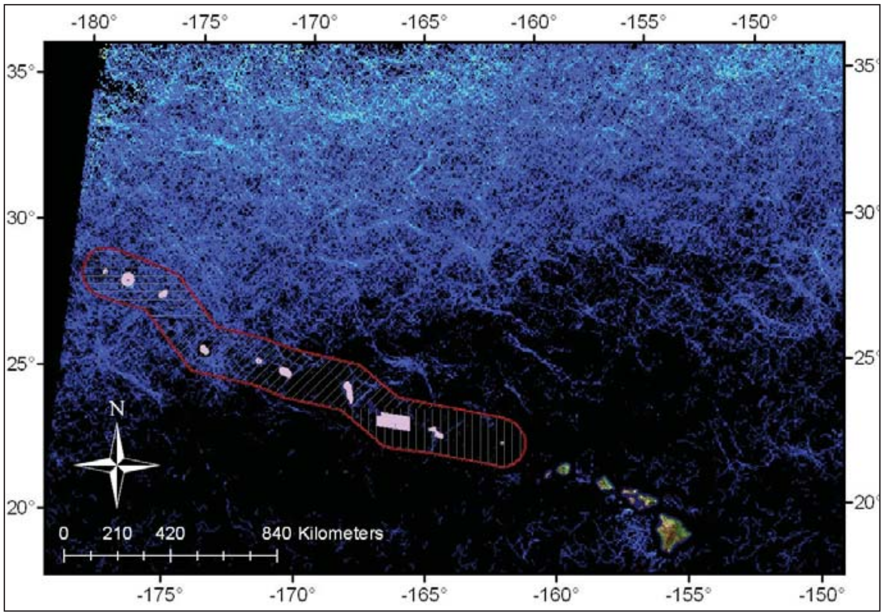

Figure 2.9. Example average sea surface frontal boundaries for the region (April, 2005). Dense clustering of boundaries, and lighter tones indicate elevated frontal boundary detection. Note higher frontal activity in the northern and western reaches of the Monument.

Merged sea surface height anomaly (SSHA) data from altimetry were obtained from Archiving, Validation and Interpretation of Satellite Data in Oceanography (AVISO) delayed time products of SSH generated from merged Topex/Poseidon (T/P), Jason-1/2, ERS-1/2 and ENVISAT missions. Merged SSHA data from altimetry were obtained from AVISO delayed time products of SSH generated from merged Topex/Poseidon (T/P), Jason-1/2, ERS-1/2 and ENVISAT missions. Weekly (seven-day) and monthly averaged data were used. Monthly estimates of vertical SSH from mean sea level were obtained following a simple bin averaging technique. A calendar of monthly averaged SSHA data to dissect climatological patterns of space-time variability for the region of interest is shown.

Post processing involved conversion from Network Common Data Format (NetCDF) format to raw binary image format, binning of weekly SSHA data, georeferencing and tiff generation of by-products. The binning procedure followed a simple arithmetic averaging technique to compute a monthly estimate of vertical SSH from mean sea level. Map projection is a 1/4° geographic (lat/long) projection grid, where number of values for X (found in file) = 1,080 and number of values for Y (found in file) = 720. Final georeferenced products were converted to 32 bit Geotiffs (v6). 8 bit Geotiffs were also created for reference. The time period for SSHA data analyzed here range from October 1992 to present.

Winds

NOAA's National Centers for Environmental Prediction (NCEP) generates global wind data termed "reanalysis winds" which are processed using a state of the art analysis system, and are used primarily for long-term climate studies. The data were produced at a 2.5 degree spatial resolution. NCEP uses all available atmospheric data to model winds every six hours, and is available from January 1, 1948 through the present. Reanalysis winds are distributed in NetCDF, and have a time component, latitude, longitude, zonal component (u) and a meridional component (v).

From the u and v wind components, direction (in degrees) and magnitude (in speed; m/s) can easily be derived. The data are available for 17 different pressure levels. To estimate the winds closest to the atmosphere-ocean interface we chose the highest pressure level (1,000 millibars). Using the six hour observations, NCEP calculates daily, monthly, and annual average and standard deviation reanalysis wind products. NOAA's CCMA has created direction and speed images created as 32-bit Geotiffs in geophysical units primarily for qualitative assessment purposes and an 8-bit scaled Geotiff version primarily designed for quantitative assessments. Monthly, seasonal and annual means for the study region have been created in this fashion.

The monthly data from NASA's Quick Scatterometer (QuikSCAT) was obtained and processed form from the French Institute for Exploring the Sea (IFREMER). Scatterometers, such as QuikSCAT, measure the roughness of the surface of the ocean, which in turn may be used as a proxy to estimate wind speed and direction. Scatterometer data are not available near or adjacent to land. The QuikSCAT NetCDF data files were generated from monthly data composites that covered the period ranging from August 1999 though February 2007. Seasonal and yearly climatological files were generated through the combination of monthly data composites that covered the period January 2000 though December 2006. The data were spatially subset to the study area at a spatial resolution of 0.5 degrees per pixel. Each file contained the following parameters: wind stress curl (Pa/m), wind speed divergence (m/s), wind speed (m/s), zonal wind speed (m/s), meridional wind speed (m/s), wind stress (Pa), meridional wind stress (Pa) and zonal wind stress (Pa; IFREMER, 2002). The resulting data files for each parameter were converted to 8-bit and 32-bit Geotiff format, in the same manner as the reanalysis wind products.

OCEAN REMOTE SENSING ANALYSIS: RESULTS

Sea Surface Temperature

Latitude is a primary driver in oceanographic conditions of the Monument and SST is highly correlated with latitude. This is evident in the stratification of SST within the Monument moving from north to south. SST analysis suggests that the 10 management regions can be segregated into three latitudinal subgroups. Mean SST highs in August and September are similar for all of the regions, around 27ºC, but lows in February and March are varied and highlight the latitudinal differences (Figure 2.10).

The northern atoll group (Kure, Pearl and Hermes and Midway) has a wide range of temperatures throughout the year, typically from around 20ºC in February to 27ºC during the summer; however, temperatures have reached as low as 16ºC and as high as 29ºC. This range is one of the widest temperature ranges for any coral reef system on the planet (Friedlander et al., 2005). In addition, the northern islands are unexpectedly warmer in the summer than the most southern atolls of Nihoa, Mokumanamana and French Frigate Shoals. This north-south temperature stratification results in a latitudinal partitioning of flora and fauna causing endemic species and species composition changes within the Monument (Polovina et al., 1995; Friedlander et al., 2005).

Average monthly SST images clearly show the seasonal variation and north-south temperature gradient in the NWHI (Figure 2.11). The southern region experiences warmer temperatures compared to those in the north, but less variability throughout the year, while the northern atolls have much more variability within and between years (Figures 2.4 and 2.11). The southernmost island grouping (French Frigate Shoal, Mokumanamana Island, and Nihoa island) experience an environment with a restricted range in temperature when compared to islands to the north and west; approximately 23ºC in the winter to 27ºC in the summer. Summer SSTs for this group are generally lower than or the same as the northern atoll group. This is possibly due to weaker winds in the north, caused by proximity to the North Pacific high pressure ridge, resulting in less mixing with subsurface waters (Hoeke et al., 2006).

Pattern and periodicity in SSTs within the Monument are remarkably stable from 1985-2006 (Figure 2.12). Anomalies are rarely more than a degree from the long-term mean and typically occur during the winter months (Figure 2.12). Wintertime negative temperature anomalies occurred in June 1987, May 1992, December 1996, February 1997 and June 1997, while positive anomalies occurred during the early spring in 1999, 2000 and 2001 (Figure 2.12). These observed anomalous variations in SST are likely associated with the interactions and state of the PDO and ENSO and trend strongly towards the phase of the PDO, either warm or cold. There is less observed variability during the summer months; however, prolonged positive anomalies of 1ºC during the warmest months are likely indicators of coral bleaching (Kenyon et al., 2006a; Kenyon and Brainard, 2006). Similar time-series analysis has been performed for data extracts from each of the 10 islands, atolls and special management areas. Results are provided in Appendix I.

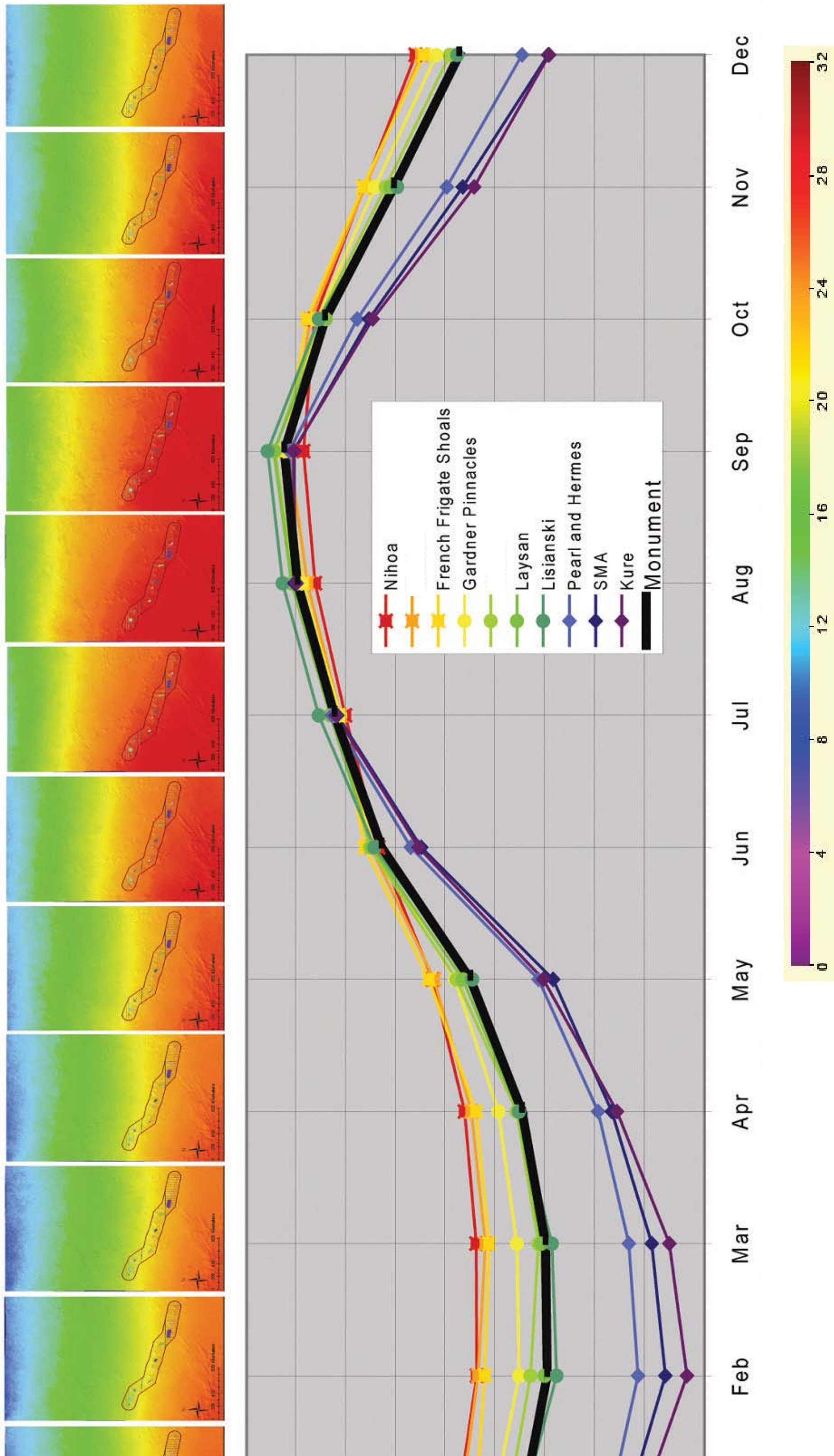

Figure 2.10. Long-term average monthly SST derived from NASA Pathfinder AVHRR. SST imagery for climatological monthly mean in Monument region. Time series ranges from 1985-2006.

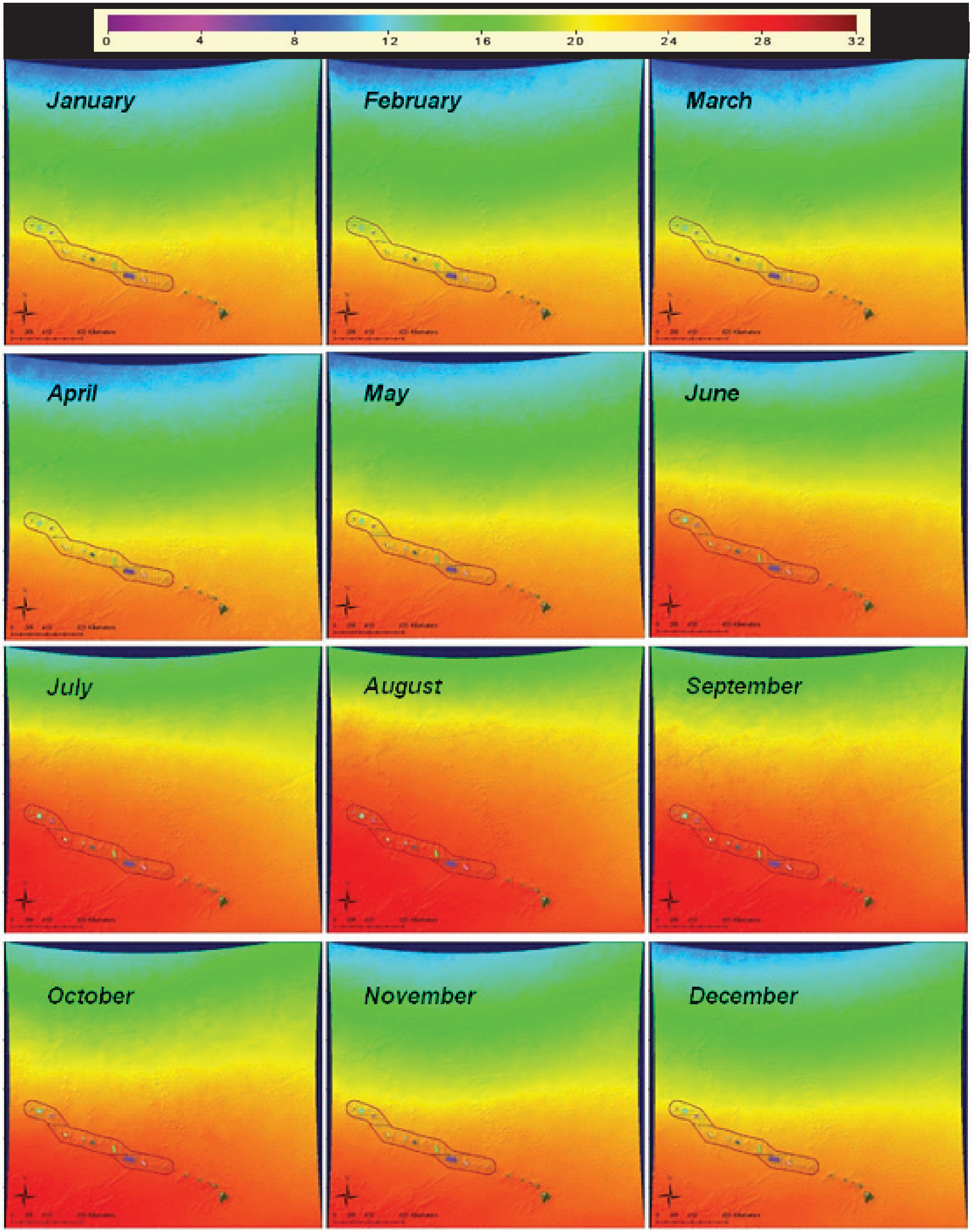

Figure 2.11. Monthly mean climatological SST, 1985-2006. Color bar is in degrees Celsius. Warm waters encompass the entire island chain in summer months but cooler waters intrude on the northern end of the Monument from November through May.

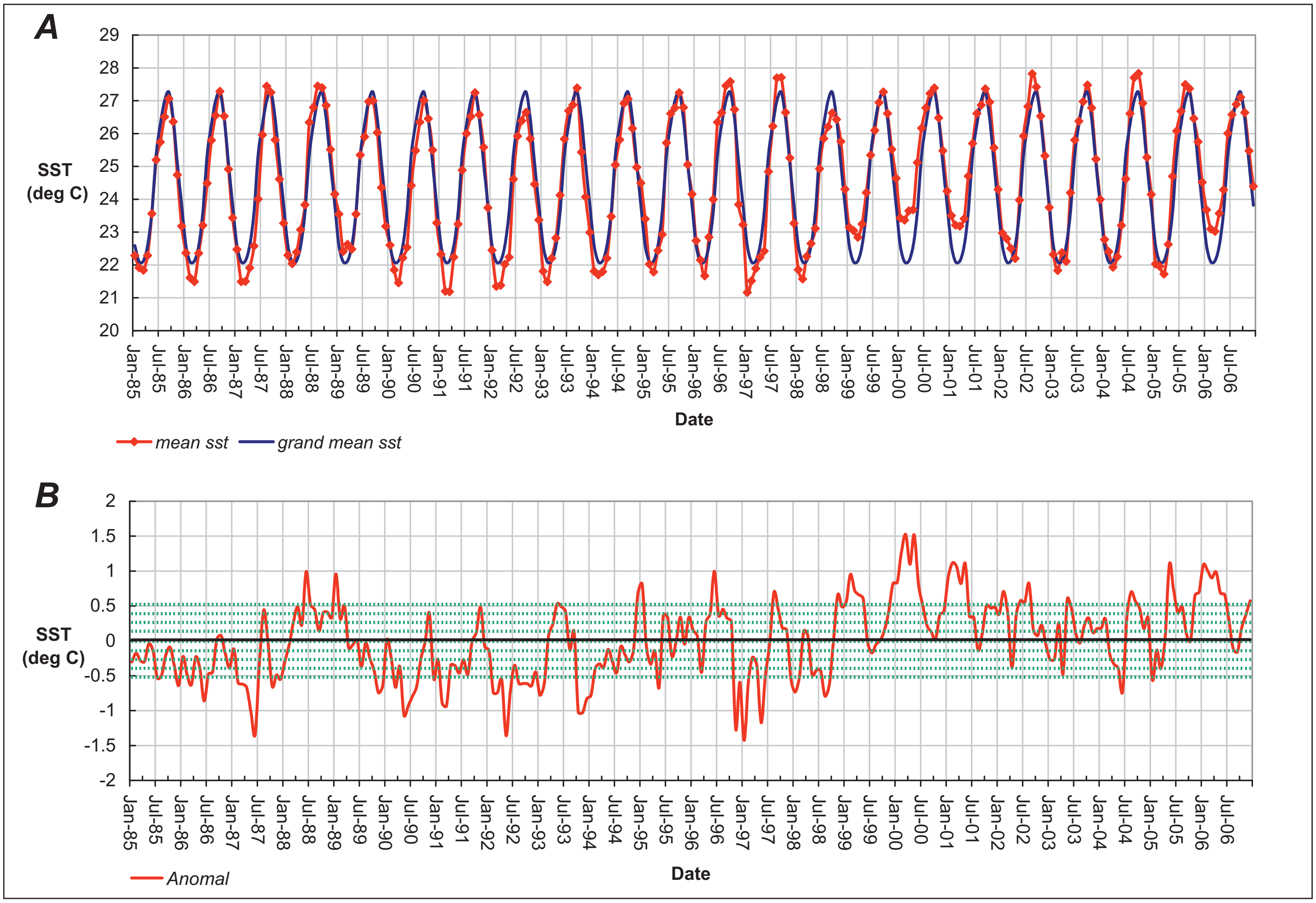

Figure 2.12. Panel A shows SST derived from NASA Pathfinder AVHRR imagery. Data from the entire Monument have been averaged to highlight temporal patterns from 1985 through 2006. Grand mean indicates the "climatological" average. Panel B shows temperature anomalies for the same period of record. Green bar indicates the range of one standard deviation of the anomaly time series. Peaks that fall above or below this range can be considered departures from "expected" anomalies.

NOAA led Pacific Reef Assessment and Monitoring Program expeditions to the NWHI documented the first recorded major bleaching events in the region. The NWHI were impacted by mass coral bleaching during late summer 2002 and again in 2004 principally due to a distinct region of higher than normal temperatures pervasive in the northern reaches of the Monument (Figure 2.13; Abey et al., 2003; Kenyon et al., 2006). No records of mass coral bleaching in the NWHI existed before this time. It was previously thought that the NWHI were less susceptible to bleaching due to the high latitude location whereas coral bleaching was documented in the MHI back in 1996 (Jokiel and Brown, 2004). During both events, bleaching was most severe at the three northern-most atolls (Pearl and Hermes, Midway and Kure), with lesser incidences of bleaching at Lisianski Island and farther south in the NWHI. SST data derived from both remotely sensed satellite observations as well as *in situ* buoys from the NOAA's Coral Reef Early Warning System suggest that protracted, elevated SST was a likely explanation for the bleaching response. This period of elevated SST coincided with a prolonged period of light wind speed, suggesting increased stratification due to decreased wave mixing of the upper ocean (Hoeke et al., 2006).

The time series analysis of SSTs data also suggests that two bleaching events may have occurred undetected in the summers of 1987 and 1991 (Figure 2.14). On these occasions, the northern atolls experienced temperature anomalies of 1ºC or greater during the highest mean temperature months of August and September. Similar or larger positive anomalies have occurred in other regions and times but likely did not lead to coral bleaching because these events did not occur during peak temperature months.

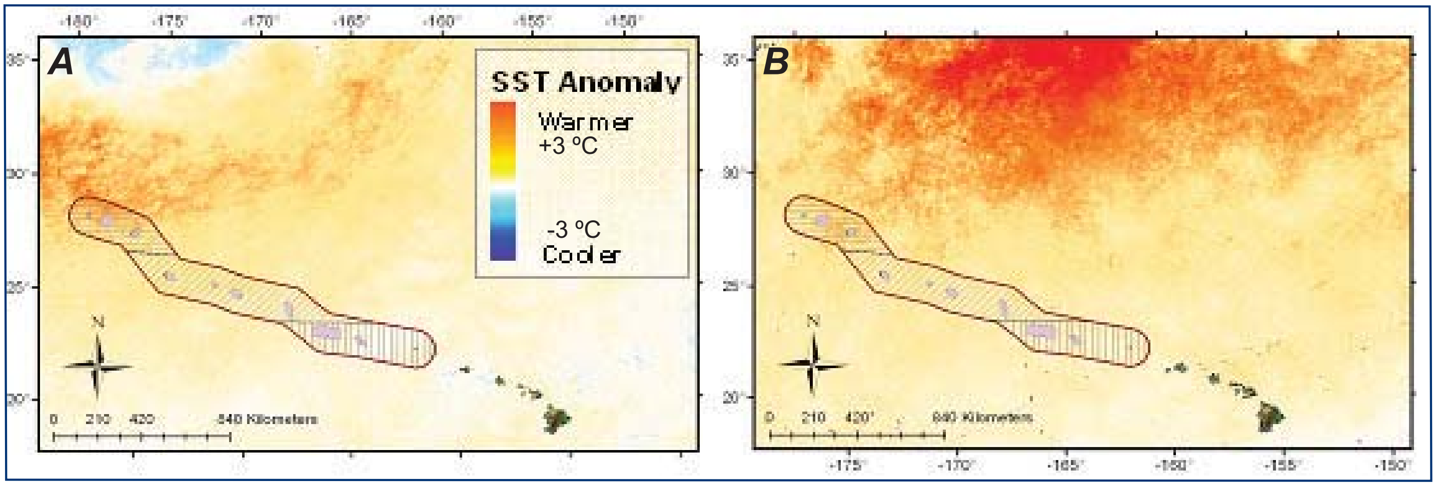

Figure 2.13. SST Anomaly images for August 2002 (A) and September 2004 (B). These periods of anomalously high SSTs in the northern atolls have been associated with coral bleaching. Source: NOAA GOES Imager.

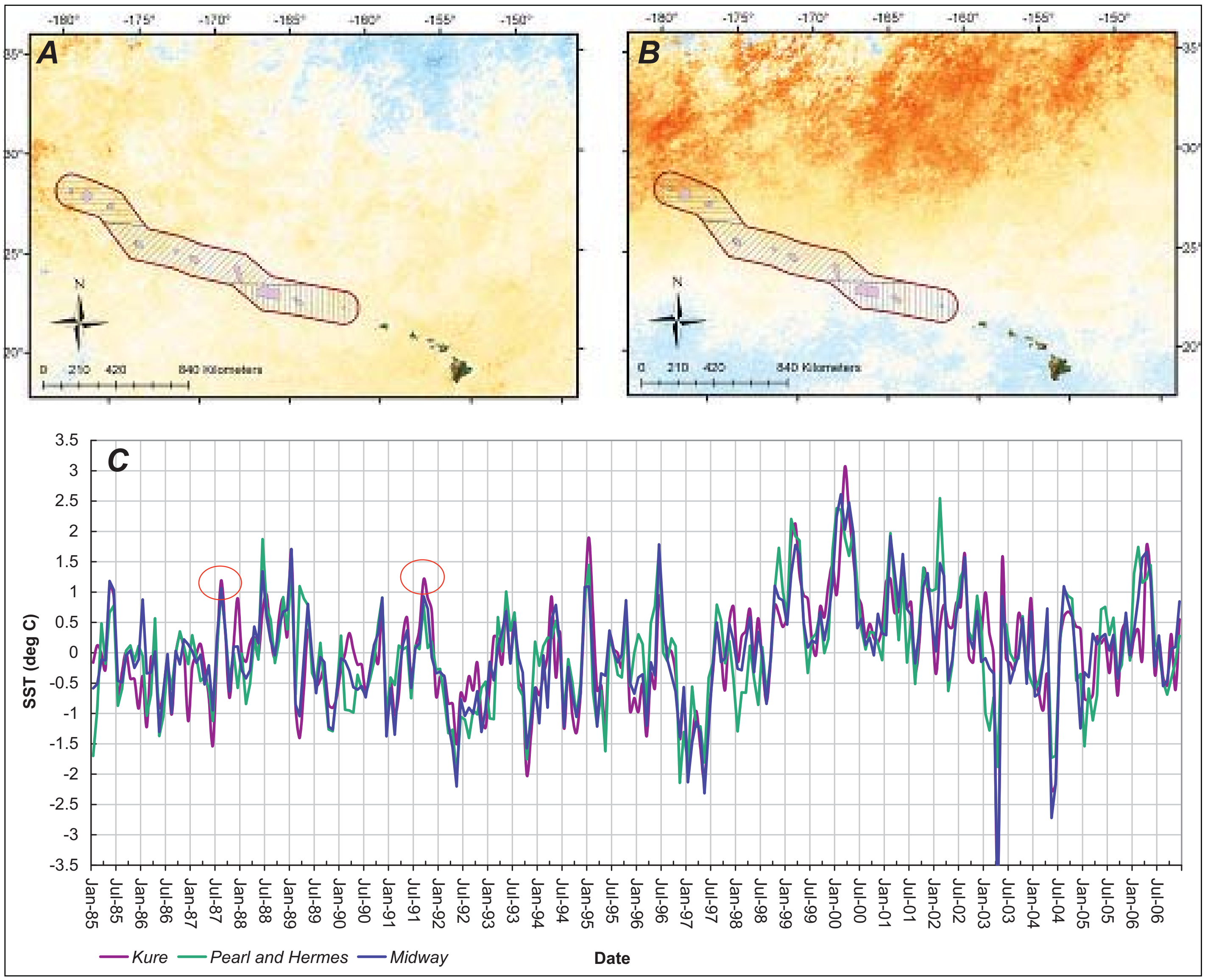

Figure 2.14. SST Anomaly images for September 1987 (A) and September 1991 (B). Distinct SST peaks in the northern atolls can be seen in the time series data (C).

Sea Surface Temperature Fronts

Bottom topography, ocean current confluence, variable wind stress and heat-water exchange across the sea surface produces patterns of vertical circulation, fronts or eddy-like motions that can affect biological distributions (Kazmin and Rienecker, 1996; Polovina, et al., 2001; Nakamura and Kazmin, 2003). Fronts are created by a variety of physical processes and have a wide range of biological consequences. A frontal system denotes areas of water mass convergence and usually produces zones of downwelling and upwelling flow. These vertical displacements have considerable ecological effects because environmental gradients, such as light, pressure, temperature, salinity, oxygen, nutrients, etc., are steepest in the vertical axis of the water column.

Vertical motion in fronts is often highly localized and can be easily identified with remote sensing techniques (Ullman and Cornillon, 1999). Areas with frontal activity tend to be areas of high biological activity (Polovina et al., 2001; Nakamura and Kazmin, 2003). The vigorous mixing of the water column at water mass confluence stimulates phytoplankton photosynthesis and sustains concentrations along the frontal zone (Savidge, 1976; Savidge and Foster, 1978). In response, zooplankton tend to concentrate along the fronts and are preyed upon by higher trophic groups. Marine birds, marine mammals and fish often aggregate at frontal areas as well. Tracking and catch studies have shown that key apex predators, swordfish, albacore tuna and loggerhead turtles, use these fronts for forage habitat on long distance migrations through the North Pacific (Bigelow et al., 1999; Laurs et al., 1984; Polovina, et al., 2001). Additionally, it has been shown that biological diversity is positively correlated with thermal fronts (Kazmin and Rienecker, 1996)

SST fronts are an important marine ecological feature for the overall eco-region of the Monument and the dynamic environment created by the fronts support many species that reside near or in the Monument. Large, persistent front generating regions are important for species transiting through the Monument during migration. However, front concentration within the Monument is relatively low, reaching highest levels in spring and primarily in the northern end of the Monument where the subarctic and subtropical gyres interact. Consistent with SST observations, SST frontal data indicate a seasonal patterned and latitudinal division within the Monument. Figure 2.15 illustrates the north-south movement of frontal concentration throughout the year. The northern region of the Monument experiences an active frontal season from December through April, usually with a peak in March. Even during the peak frontal probability period the southern region experiences few fronts. In mid-summer the frontal activity zone retreats far enough north that even the most northern atolls may not experience any significant fronts.

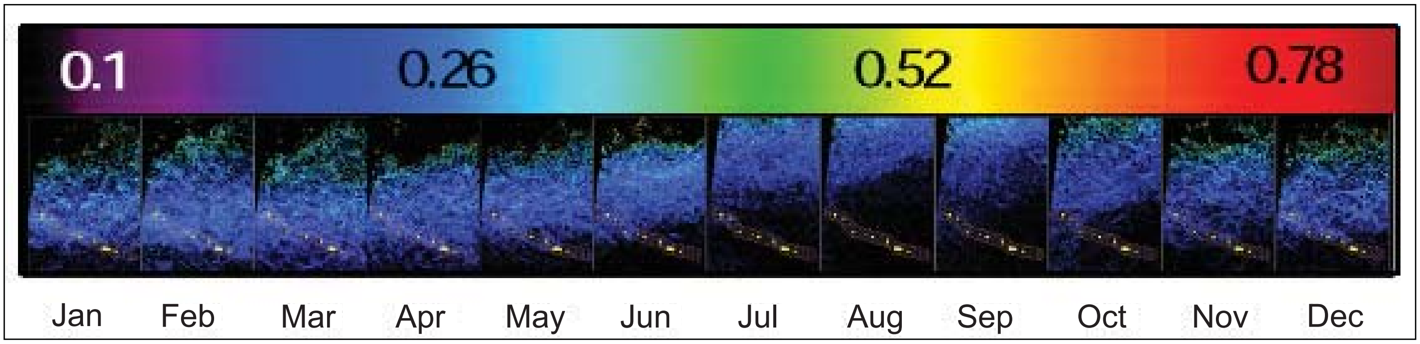

Figure 2.15. Average monthly sea surface frontal boundaries for the region. Dense clustering of boundaries, and lighter tones indicate elevated frontal boundary detection. Note higher frontal activity in the northern and western reaches of the Monument. Color strip denotes calculated frontal probability.

These pelagic habitats are poorly understood and warrant additional studies to improve the knowledge base for ecosystem management. It is possible with remotely sensed data to track these frontal zones over large, difficult to access regions through time. The interaction of these productive zones with the biota of the Monument may hold clues to long term sustainability of the Monument reef systems.

Chlorophyll

Chlorophyll concentrations are relatively low throughout the Monument, exhibiting oligotrophic characteristics common in open ocean environments. Even at these low levels, seasonal and latitudinal patterns are evident in both the chlorophyll images and the time series charts. The images shown in Figure 2.16 illustrates the temporal distribution of chlorophyll. This distribution is determined by the location of the convergence zones of the subarctic and subtropical gyres. A major area of productivity associated with this convergence area, referred to as the transition zone chlorophyll front (TZCF), contributes significantly to the variable productivity of the Monument region.

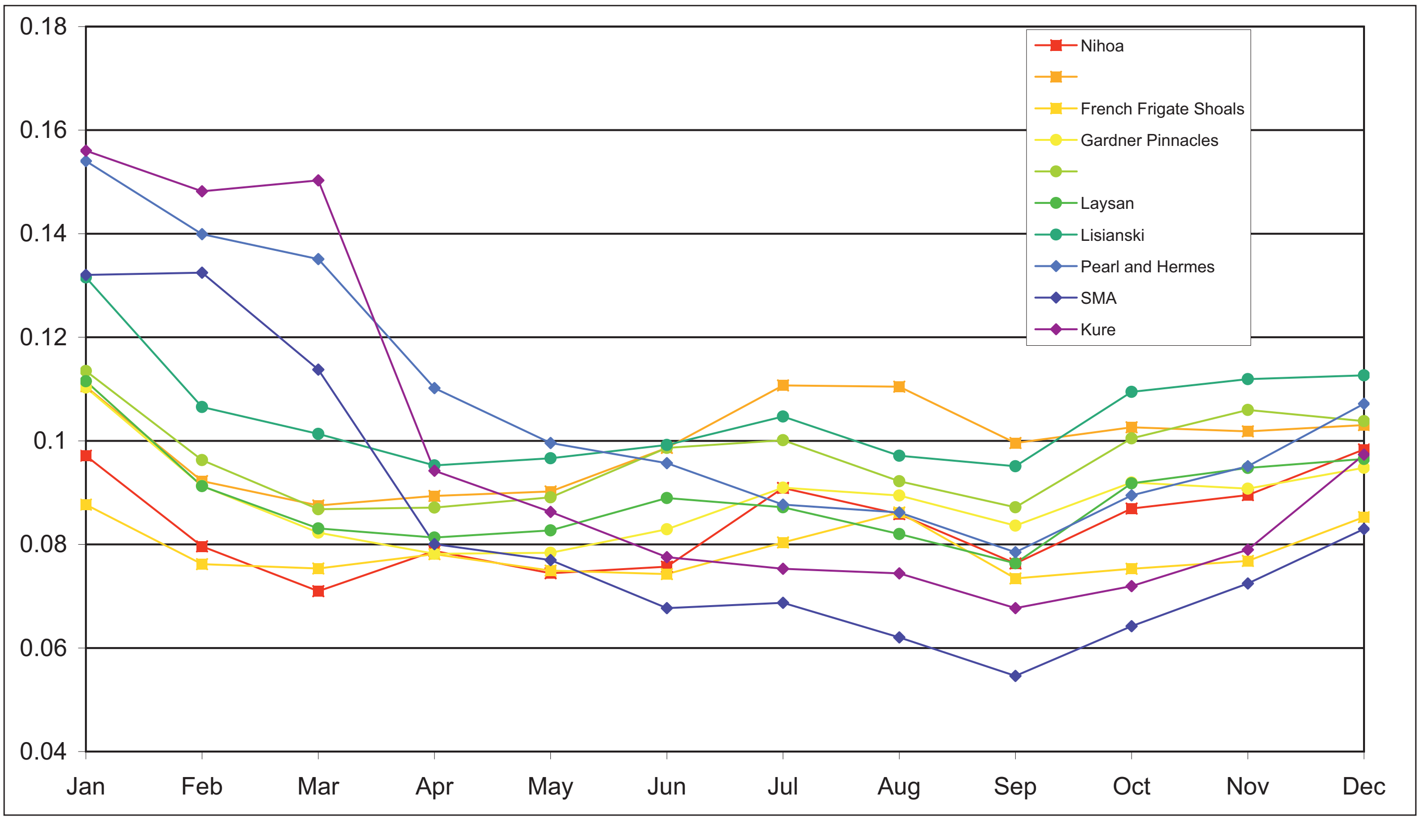

Figure 2.16. Average monthly chlorophyll concentration (mg/m^3) values for the study region.

The TZCF is a high productivity zone in the open ocean used by many species as an important feeding and migration zone. The TZCF has been identified as a chlorophyll concentration of approximately 0.2 µg/L or greater as measured from satellite (Polovina, 2005). The TZCF only rarely transits far enough south during its winter southerly shift to interact directly with the northern regions of the Monument. Even in these instances chlorophyll concentrations within the Monument generally do not reach as high as 0.2 µg/L. However, both permanent and seasonal residents of the Monument do make use of this productive zone and more southern tracks of the TZCF have been correlated with higher fish catches in the Hawaiian Islands (Polovina et al., 2001). Coral reefs are also impacted by these occasional pulses of higher chlorophyll through population increases of the coral eating sea star, *Acanthaster planci* commonly known as the crown-of-thorns sea star (Hoeke et al., 2006). These periodic increases in productivity within the Monument likely have meaningful consequences to management of the atolls and reefs of the Monument.

Mean chlorophyll concentrations have cyclical temporal variability. Higher chlorophyll concentrations move south into the Monument boundaries during the winter months and retreat far north in the summer. The northern region experiences the largest variability in mean concentration from high season to low season ranging from highs of nearly 0.18 µg/L to lows below 0.06 µg/L. The central and southern regions exhibit a more constant environment with chlorophyll concentrations ranging between 0.07 and 0.11 µg/L. In addition to seasonal changes, the northern regions also exhibit high interannual variability in chlorophyll concentrations. The northern atolls experienced very low concentrations of chlorophyll in 1999, 2000 and 2001, but also relatively high concentration years in 1998, 2003, 2004 and 2005 (Figure 2.17). Note that even the highest mean monthly chlorophyll concentration is below the threshold of 0.2 µg/L used to identify the biologically active TZCF. Time-series analysis has been performed for chlorophyll data extracts from each of the analysis regions, and results are provided in Appendix II.

While these values are low relative to coastal continental chlorophyll concentrations, these chlorophyll blooms offer sustenance to support a diverse community around the atolls of the Monument. The southern atoll group exhibits little variance through time and can be characterized as having generally low chlorophyll concentrations, usually between 0.06 and 0.09 µg/L. The central region exhibits slightly higher variability and a broader range in chlorophyll concentrations when compared to the south, likely owing to its position as a transition zone between the subarctic north and the subtropical south.

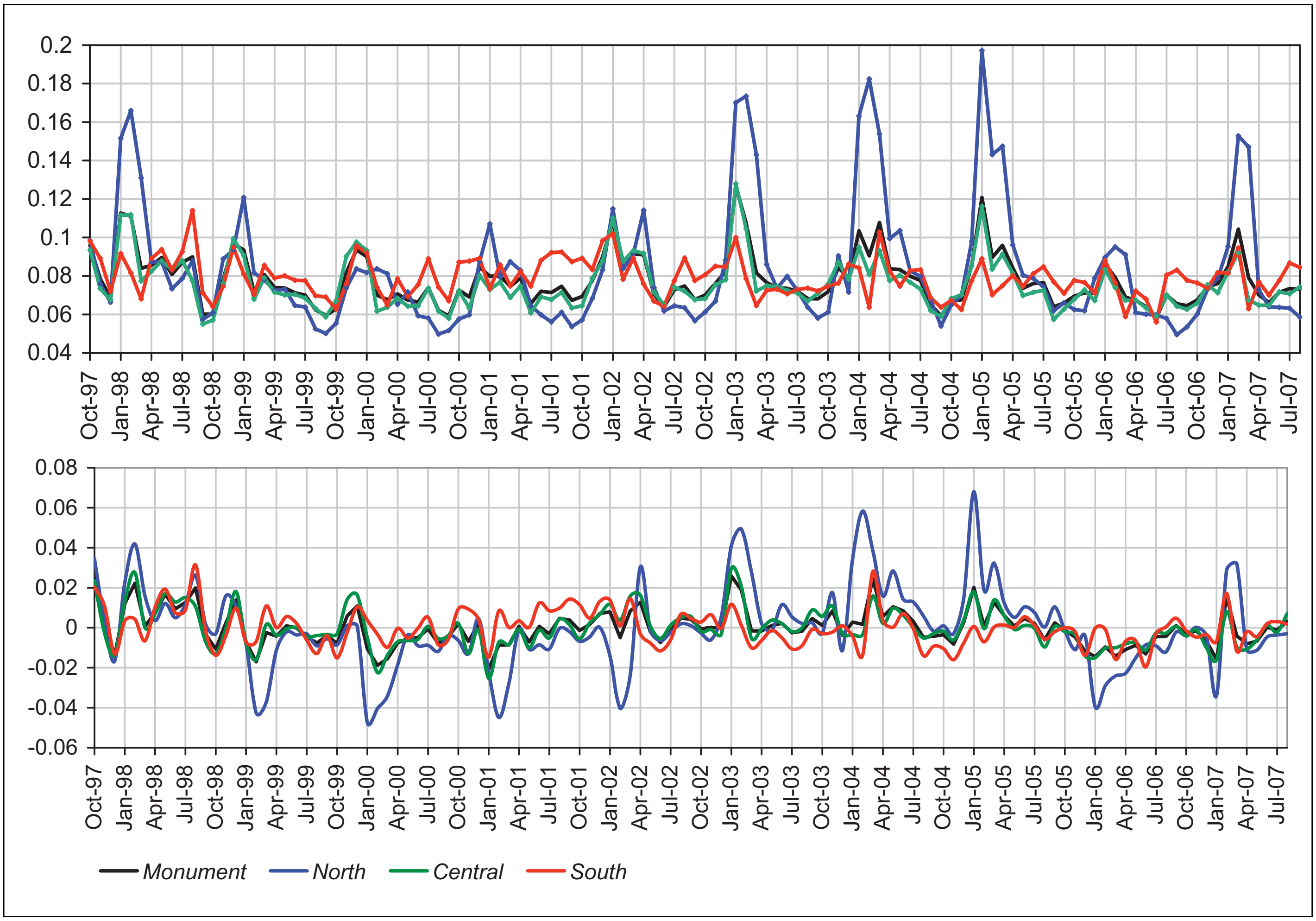

Figure 2.17. Time-series for chlorophyll (top) and chlorophyll (mg/m^3) anomaly (bottom) in each analysis region of the Papahanaumokuakea Marine National Monument (1997-2006). Source: SeaWiFS.

Trends in chlorophyll concentration anomalies can be correlated with the PDO and ENSO via the multivariate ENSO index (MEI). Chlorophyll concentrates in the more northern atolls are positively correlated with the PDO index (ρ=+ 0.404) where as the southern atolls are negatively correlated (ρ=-0.02). The rank correlation compares the relative size and direction of the indicators. For example, in the northern regions from 1998-2002, relatively strong cool phase PDO index values (negative) are positively correlated with periods of relatively low chlorophyll concentration anomalies (Figure 2.18). This correlation is expected as a cool phase PDO is typically indicated by higher SSTs in the north central Pacific (Mantua et al., 1997), and warmer SSTs are associated with lower levels of chlorophyll production. An inverse relationship between chlorophyll concentrations and the PDO index in the southern atolls is explained by the typically cooler tropical waters in the eastern Pacific during cool phase PDO and the association of higher chlorophyll counts and cooler waters. Additionally, PDO effects are primarily seen in the more northern latitudes (Mantua et al., 1997), so an increasing strong relationship with increasing latitude is not entirely surprising.

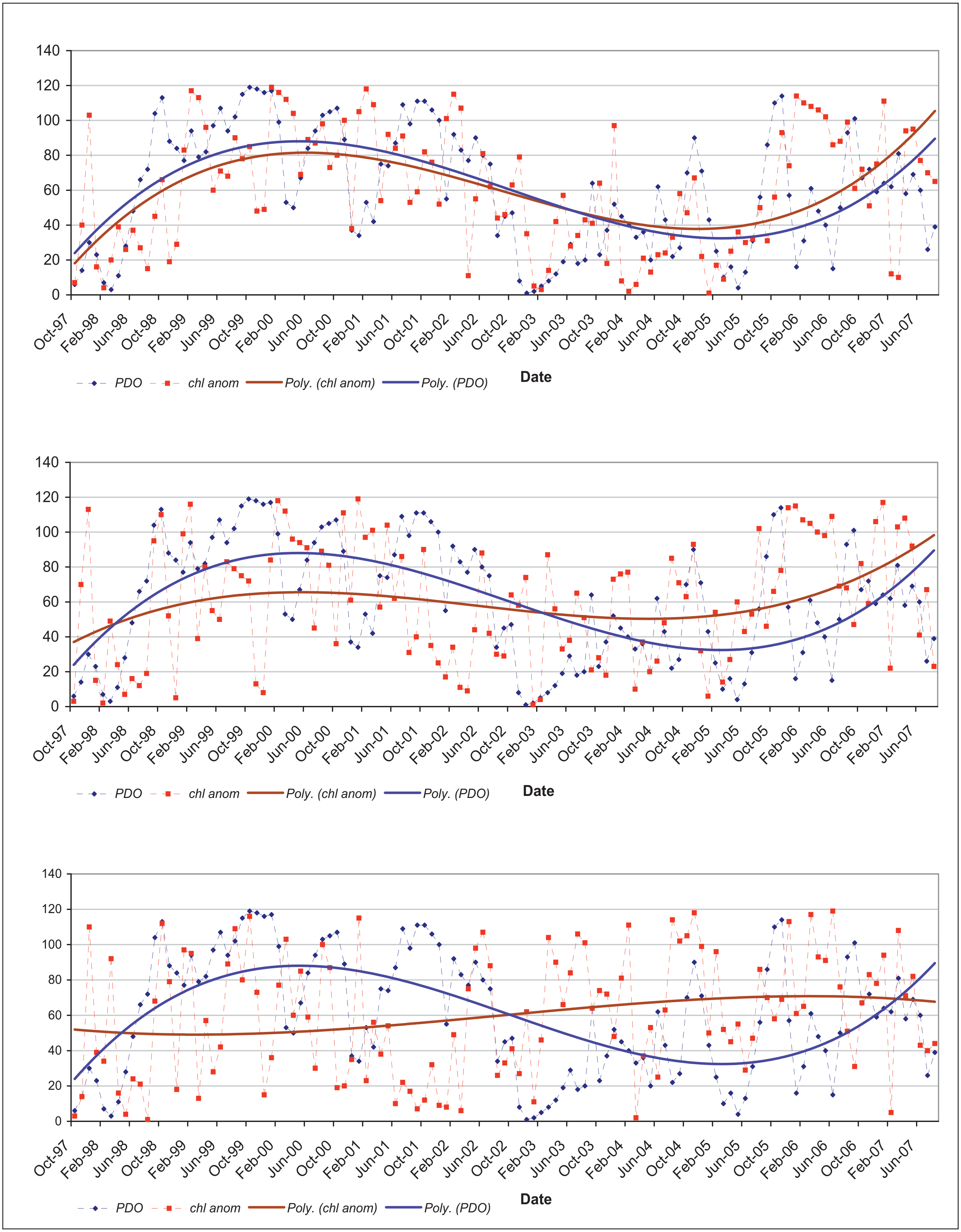

Figure 2.18. Plots of rank-ordered chlorophyll anomaly and PDO Index 1997-2007 values for the northern (top), central (middle) and southern (bottom) regions of the Monument. Lines represent non-linear trends through the time-series to highlight the degree and nature of correspondence. Poly is a 3rd order polynomial fit through each time-series (trend).

Six El Niño events occurred during the time series analyzed here, including: 1987, late 1991- early 1992, late 1997-early 1998, late 2002-early 2003, late 2004-early 2005 and late 2006 (National Weather Service, 2007). The 1997-1998 was possibly the most intense in the 20th century; however, the northern region of the NWHI were more strongly influenced by the weaker events of 2003, 2004 and 2005. This is possibly due to interactions between PDO and ENSO. The El Niño events are evident in the SST time series throughout the Monument but are particularly apparent in the chlorophyll time series of the northern atolls. The 1997-1998, 2003, 2004 and 2005 El Niños led to much higher chlorophyll concentrations than normal in the northern half of the Monument. During El Niño events, the Aleutian Low pressure system is more intense and extends south into the Monument region, resulting in stronger winds, more mixing and cooler SSTs (Bromirski et al., 2005). La Niña phases of ENSO show opposite characteristics in the Monument region leading to warmer waters and lower chlorophyll concentrations. La Niña events occurred in 1988, early 1989, and late 1998-2000. The La Nina events produced slight decreases in chlorophyll, but not of the magnitude of increase seen in the El Niño years.

Wind

Winds of the NWHI are generally dominated by the Trades, a persistent system that blows from the northeast to the southwest. These winds move from the Americas to Asia between the equator and 30oN, and are remarkably consistent throughout the year. Meridional variability is relatively weak and is dominated by Coriolis Forces which set up the North Pacific Gyre. Meridional winds are defined as the directional component along the local meridian, and are positive if from the south, and negative if from the north. Likewise, the zonal wind component is positive if it blows from the west and negative if from the east (i.e., Westerlies). An analysis of wind data (1985-present) revealed strong NWHI zonal variability in the NWHI, and three distinct components in the region.

The southerly portion of all monthly wind climatologies – from 15ºN to approximately 30ºN – is dominated by the trade winds which are associated with warmer air and the Pacific High Pressure System (Figure 2.19). North of the trade wind zone is a transitional area extending from approximately 30ºN to 40ºN of weak variable winds known as the North Pacific Doldrums, which ancient mariners referred to as the “Horse Latitudes”. In the northern portion of the study area (above 40°N), winds prevail out of the west southwest, which is associated with cooler air and dominated by the Aleutian Low pressure system. The location of the three respective areas migrates north and south seasonally, and is a major forcing function of regional oceanographic conditions. In addition to the analysis of monthly winds described above, average annual winds were calculated and analyzed for the study area. Most years exhibited only modest changes in interannual variability. The one notable exception was the intense El Niño event of 1997. Figure 2.20 shows the annual mean wind vectors from 1996, 1997 and 1998, sequentially. The Trade Winds in the annual mean of 1997 a near full directional reversal. In 1996 and 1998 the Trade Winds were out of the east northeast, as expected. In 1997; however, the winds were strongly blowing out of the south southwest. Also notable is that the general circular pattern of the winds, which typically form a gyre in the North Pacific, were absent. Throughout the analyzed region winds were out of the southwest which is a drastic difference from all other calendar years analyzed (1985-2007). 1997 also showed remarkable zonal variability along 30ºN. West of -170º the magnitude of the winds were much less than they were to the east.

Circulation around the high pressure is clockwise in the northern hemisphere and counterclockwise in the southern hemisphere. The high pressure in the center is due to the westerly winds on the northern side of the gyre and easterly trade winds on the southern side of the gyre. These cause frictional surface currents towards the latitude at the center of the gyre. The buildup of water in the center of the gyre creates equatorward flow in the upper 1,000 to 2,000 m of the ocean, through rather complex dynamics. This equatorward flow is returned poleward in an intensified western boundary current. The North Pacific Gyre comprises most of the northern Pacific Ocean, and occupies an area of approximately 34 million km^2. The Gyre has a clockwise circular pattern and comprises four prevailing ocean currents: the North Pacific Current to the north, the California Current to the east, the North Equatorial Current to the south, and the Kuroshio Current to the west.

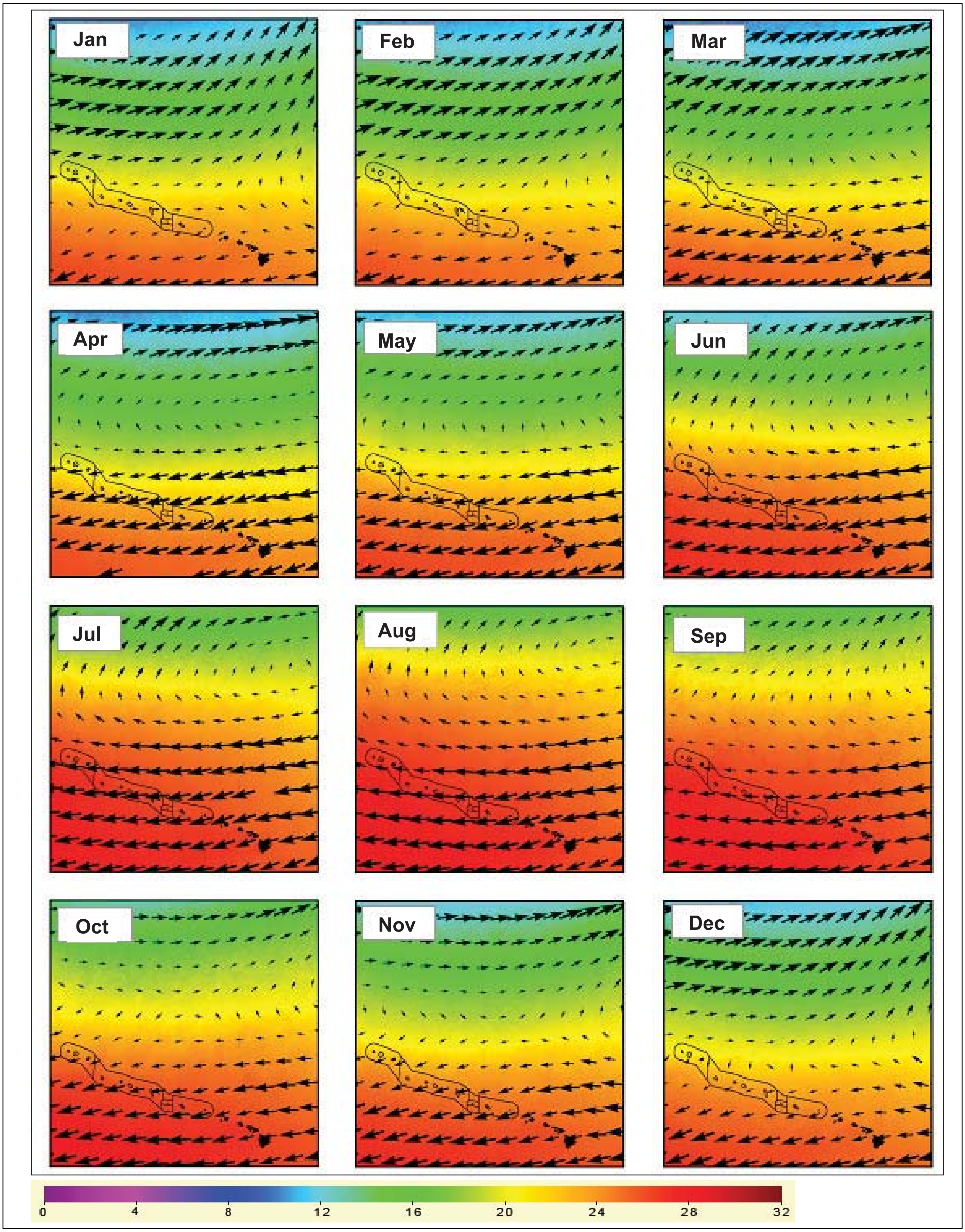

Figure 2.19. Long-term averaged monthly climatological wind data from 1948 through 2007 from the NCEP Reanalysis winds. Wind field data are superimposed on a false-color image of average monthly SSTs (warm tones=warm water, cool tones=cool water). Arrow size denotes relative wind strength. Source: AVHRR climatology.

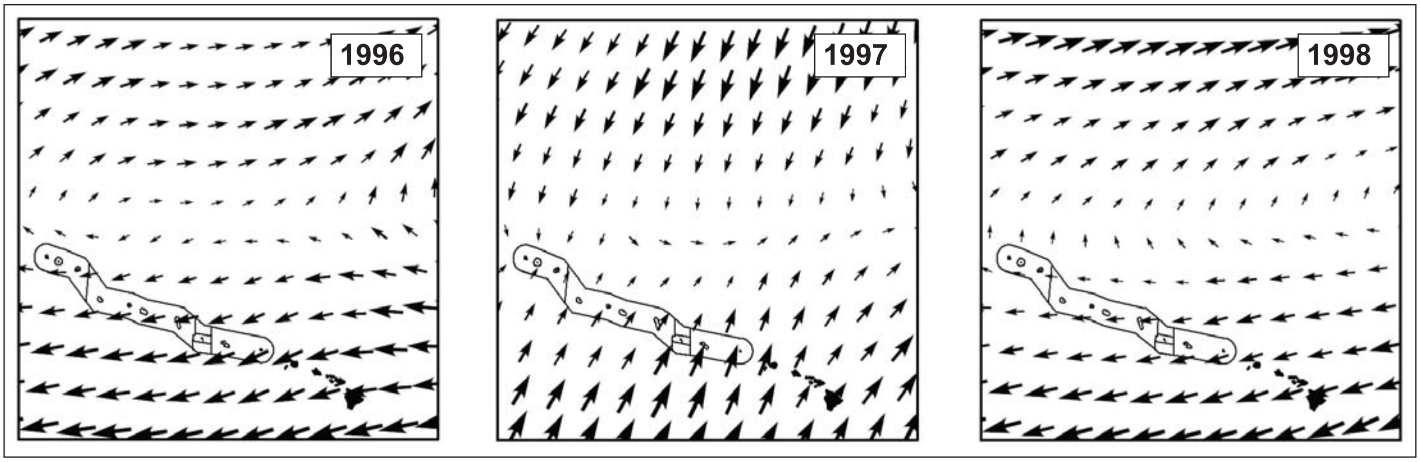

Figure 2.20. Three examples of annual means (1996, 1997 and 1998) from the NCEP Reanalysis winds. The El Niño event from 1997 shows relatively drastic variability from the preceding and subsequent years. Arrow size denotes relative wind strength.

Sea Surface Height and Currents

The height of the sea surface is determined by the mass of water at a given location and by the water's density (a function of temperature, salinity and pressure). Space based altimeters such as the Jason and Topex/Poseidon missions measures changes in SSH due to both of these factors - redistribution of mass and changes in density. On seasonal to interannual time-scales, density changes are the largest contributor to sea level variability. In the tropics they are the dominant one (Gilson et al., 1998).

Ocean currents can increase SSH by up to a meter higher over the surrounding area. Currents can therefore be mapped by measuring height variations. A view of the global ocean circulation shows currents circulating around elevations and depressions in SSH. Currents flows around positive SSH in a clockwise direction in the Northern Hemisphere, and in a counterclockwise direction around negative SSH (the opposite occurs in the Southern Hemisphere). Figure 2.21 shows an example AVISO derived SSHA image for the study region during December 2005. Warm tones indicate regions of surface height elevation, while cool tones highlight surface depressions. Current vectors derived from SSHA are superimposed on the image to show modeled surface currents (geostrophic flow). As described, note the counterclockwise rotation around the blue tones.

Numerous studies have summarized the positive association between SSH maximums and SST maximum in open ocean environments (Jones et al., 1998; Wilson and Coles, 2005; Fu 2004). Given the setting of the Monument in the middle of the Pacific Ocean, it is therefore not surprising that SSHA patterns correlate with SST seasonal patterns. The difference between the measurements is that SSH are more a measure of the heat (energy) that is stored in the ocean below while SST is a surface measurement that tells us about interactions with the atmosphere on a more immediate time scale (JPL). The ocean energy below the surface reflected in the SSHA influences surface events over much longer periods and areas.

Localized and episodic SSHA events can be attributed more readily to wind events (Di Lorenzo et al. 2008; http://www.ig.utexas.edu/research/projects/od_sst/) but larger regional SSHA patterns are clearly tied to SST. The direct influence of SSHA on the atolls of the Monument can be found in generation of winds and a current related to transient local eddies and fronts (Seki et al., 2002). Mesoscale SSHAs can be used to identify areas of convergence that can indicate upwelling and productive ocean zones concentrating and attracting species throughout the food web (Seki et al., 2002). These mesoscale features are embedded in larger scale frontal zones that scan large quadrants of the Pacific Ocean and change over periods of months and years. The PDO is a long period ocean feature reflected in SSHA. The PDO waxes and wanes between cool and warm phases approximately every five to 20 years. In the cool phase, higher than normal SSH caused by warm water form a horseshoe pattern that connects the north, west and southern Pacific, with cool water in the middle (JPL). The NWHI lie along the typical boundary between cool and warm waters during a cool phase PDO.

SSHAs in the Monument do have a seasonal signal with higher anomalies occurring in late summer and lows in the spring (Figure 2.22). The regional differences observed in the other oceanographic factors are not as pronounced with SSHA. The northern regions do experience a less pronounced swing in anomalies from high season to low season.

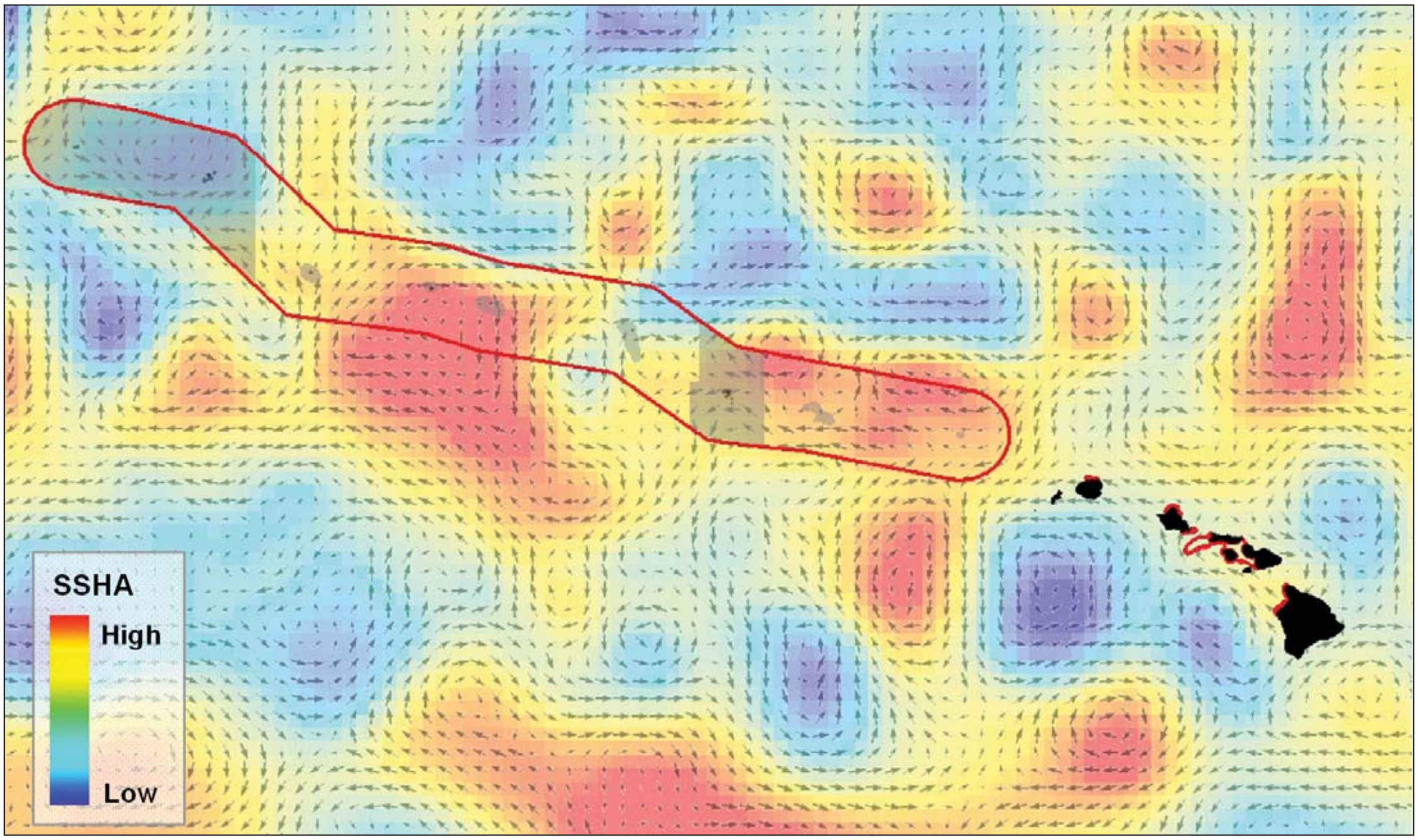

Figure 2.21. Example sea surface height anomaly image and associated surface currents in the study region (December 2005). Red tones indicate "peaks", while blue tones indicate "valleys", and arrows indicate direction of flow. Muted polygons delineate Monument "Special Protection Areas".

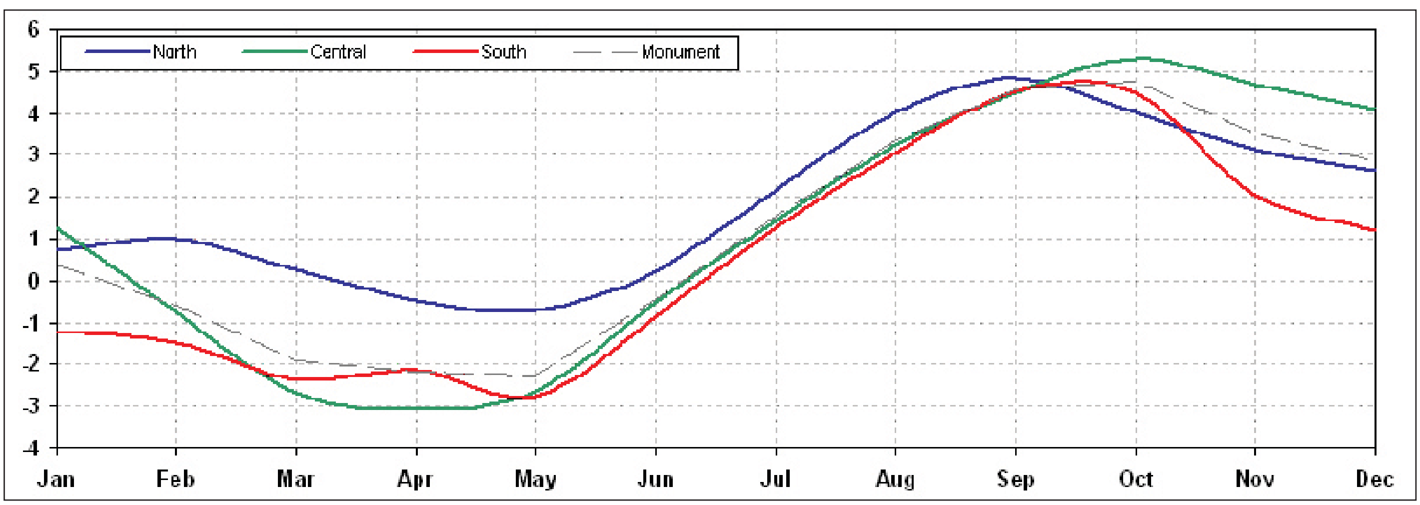

Figure 2.22. Average monthly sea surface height anomaly (cm) for each region in the Monument.

EXISTING DATA GAPS

Overall there is a need for basic information on spatial and temporal patterns of water movement, quality and characteristics within the NWHI at a range of scales. Moving forward it is important for resource managers to have a unified hydrodynamic model to describe connectivity, identify seasonal areas of oceanographic productivity, detect change in the pattern and scales of movement, dispersal and recruitment of living resources at various life stages, identify and document variability in larval and nutrients sources, understand debris dispersal and establish management units within the NWHI. Specific opportunities include research to improve the understanding of:

- carbon, nitrogen and phosphorus in the ecosystem and the transfer to higher trophic levels;
- community changes that will result from alterations to reef structure by major ocean/atmosphere events;
- discerning anthropogenic impacts from natural variability of the physical ocean environment;
- PDO/ENSO events and effects;
- geomorphological and sedimentalogical processes affecting reefs and terrestrial areas;
- dispersion patterns of key pollutants; and
- physical and biological effects of extreme events on the ecosystem.

CONCLUSIONS

The Monument is a unique open ocean ecological observatory, relatively free from the activities of humans and so large it encompass multiple overlapping and interacting marine ecosystems. The Monument's position near the shifting boundary of the oligotrophic North Pacific Central Gyre and the productive waters of the North Pacific Subpolar Gyre makes it an ecosystem that is influenced directly by climate systems that vary greatly in time, over years and decades, and space, over hundreds of kilometers. The atolls and islands are subject to typical yearly seasonal patterns as well as the larger climactic cycles of the PDO and the ENSO.

The ecosystems of the Monument are linked by these circulation patterns but are also stratified by their distance from the frontal zone where the gyres meet. There are three latitudinal groups within the Monument bounds. The northern group, Kure, Midway and Pearl and Hermes; the central group, Lisianski, Laysan, Maro Reef and Gardener Pinnacles; and the southern group, French Frigate Shoals, Mokumanamana and Nihoa. These groups exhibit similarities in all the factors that were examined. The environmental factors examined in this report are all directly impacted by the changes in the basin wide circulation system. These linkages happen over monthly, seasonal, annual and longer term climactic time intervals. Examination of chlorophyll-a, SST, SST fronts, and SSHA over climatological and monthly periods make it clear that these factors are linked.

In addition, these factors correlate with patterns and changes in climactic scale events such as the PDO and ENSO. These large-scale oceanographic forcing mechanisms change the characteristics of water temperature and productivity across the Pacific, and have a significant effect on the habitat range and movements of pelagic species in the NWHI. Tuna are often concentrated near islands and seamounts that create oceanographic divergence and convergence zones, which in turn tend to concentrate forage species (PMNM, 2008). Swordfish and numerous other pelagic species tend to concentrate along food-rich temperature fronts between cold upwelled water and warmer oceanic water masses (Polovina et al., 2001). These frontal zones also have been determined to function as migratory pathways for loggerhead sea turtles (Polovina et al., 2001, 2004).

Hundreds of thousands of seabirds breed in the Monument and are primarily pelagic feeders. The fish and squid they consume are generally associated with schools of larger predatory fish described above. While both the predatory fish and the birds are capable of foraging throughout their pelagic ranges (which encompass the entire Monument and tropical Pacific Ocean), the birds are most successful at feeding their young when they can find schools of predatory fish within easy commuting range of the breeding colonies (Ashmole, 1963; Feare, 1976; Flint, 1991).

Recent analyses of SeaWiFS remotely-sensed ocean color data shows an expansion of low productivity ocean water worldwide (Polovina et al., 2008). This expansion of low chlorophyll water has reached the Hawaiian Archipelago and has implications for the productivity of the entire ecosystem. These oligotrophic areas are expected to continue to expand with future global warming forcing (Polovina et al., 2008).

While there is well documented small-scale (i.e., local) variation in population structures (Ashmole and Ashmole, 1967; Boehlert, 1993; Johannes, 1981), the large-scale patterns in oceanography described in this chapter provide a dominant force in modulating these populations. Finer-scale, stochastic processes also operate within this climate driven construct. It is important to note that these processes cannot easily be resolved using remote sensing technologies (e.g., wind wakes, wake eddies, etc.), yet are what likely produce pelagic "habitat" conditions that attract individuals and sub-populations to a given region, island, atoll or pinnacle. The following chapters featured in this document will provide a more detailed view of the abundance, distribution and temporal "behavior" of biological populations inhabiting the NWHI.

APPENDIX I. SEA SURFACE TEMPERATURE (AND RELATED) TIME SERIES PLOTS

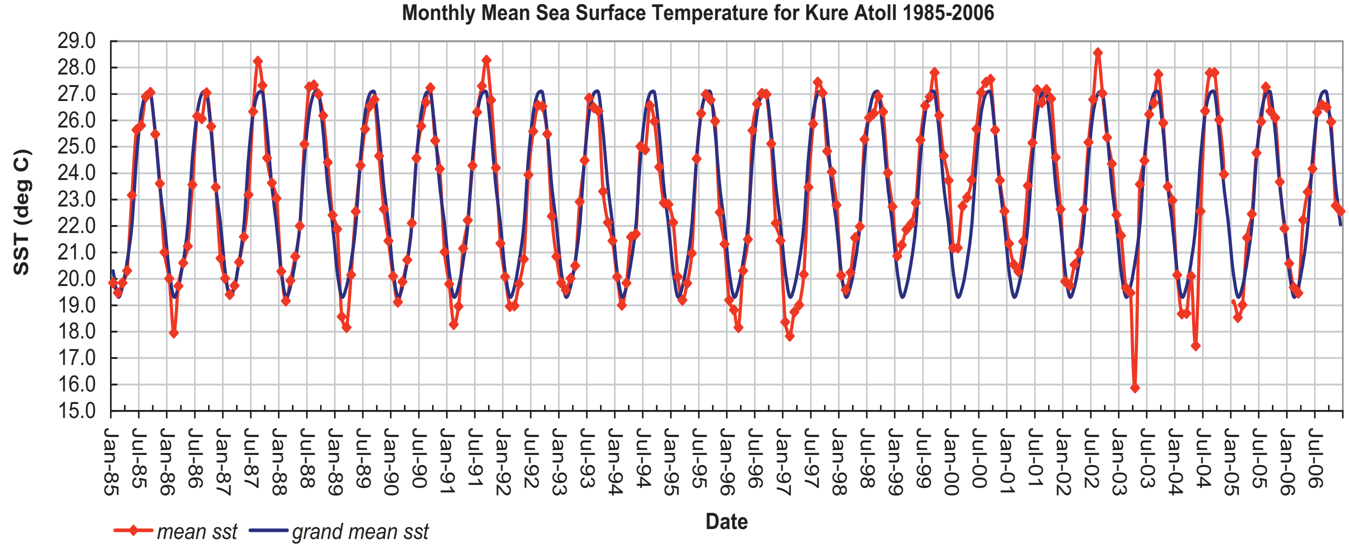

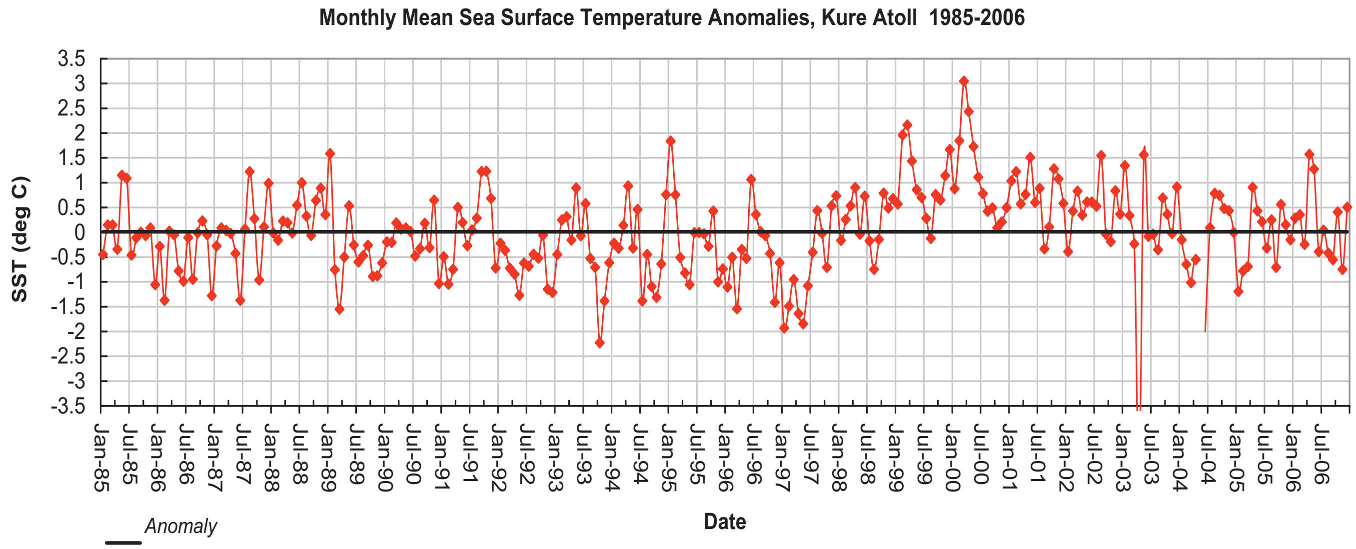

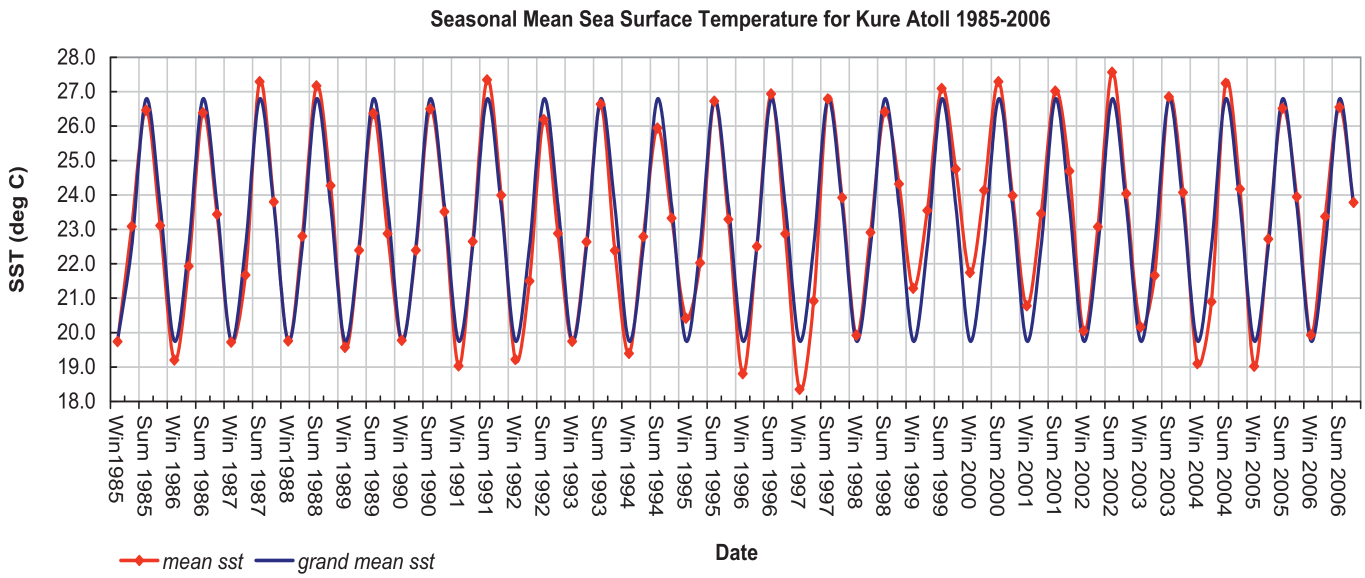

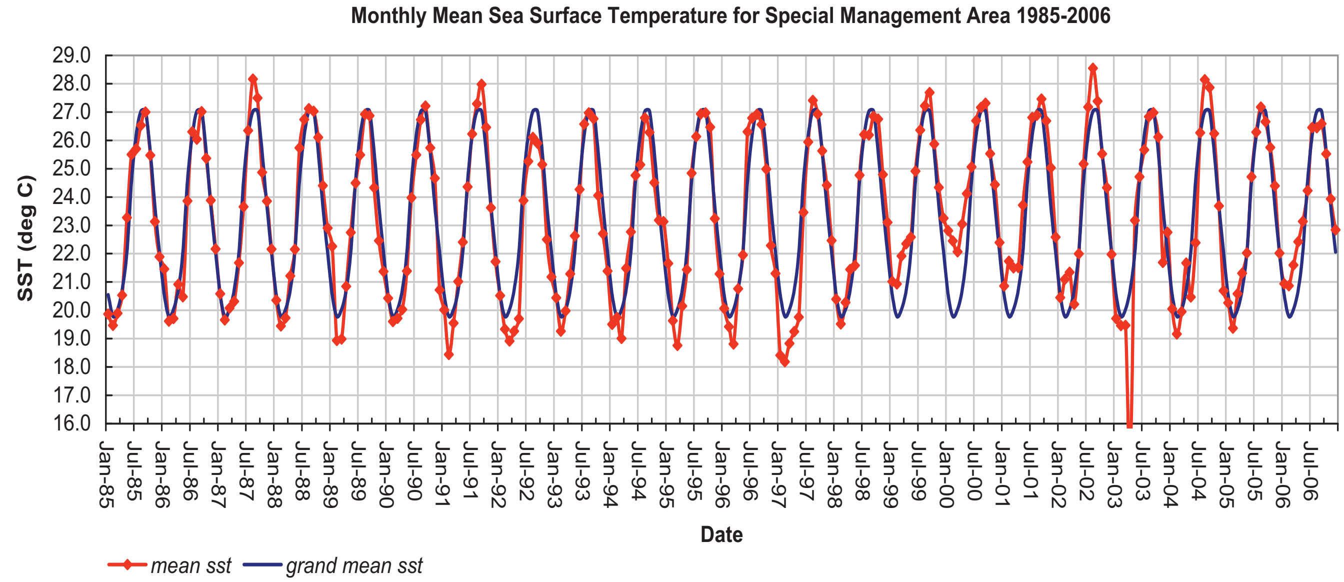
Monthly Mean Sea Surface Temperature for Special Management Area 1985-2006
SST (deg C)
Date
mean sst
grand mean sst

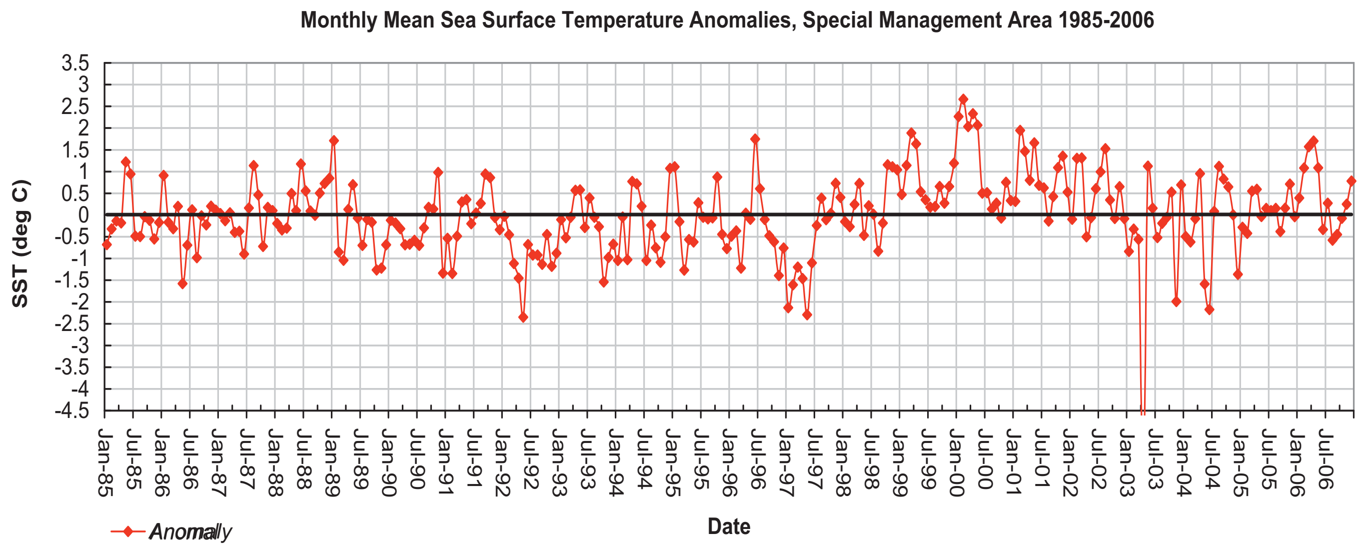
Monthly Mean Sea Surface Temperature Anomalies, Special Management Area 1985-2006
SST (deg C)
Date
Anomally

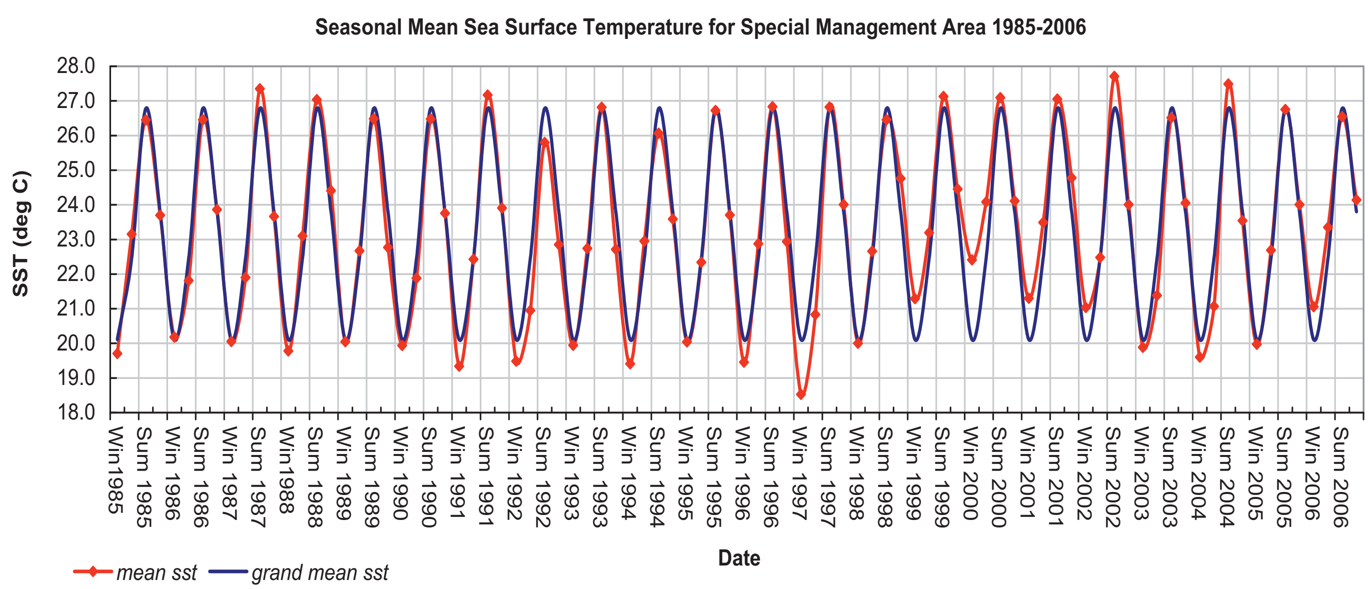
Seasonal Mean Sea Surface Temperature for Special Management Area 1985-2006
SST (deg C)
Date
mean sst
grand mean sst

Monthly Mean Sea Surface Temperature for Pearl and Hermes 1985-2006

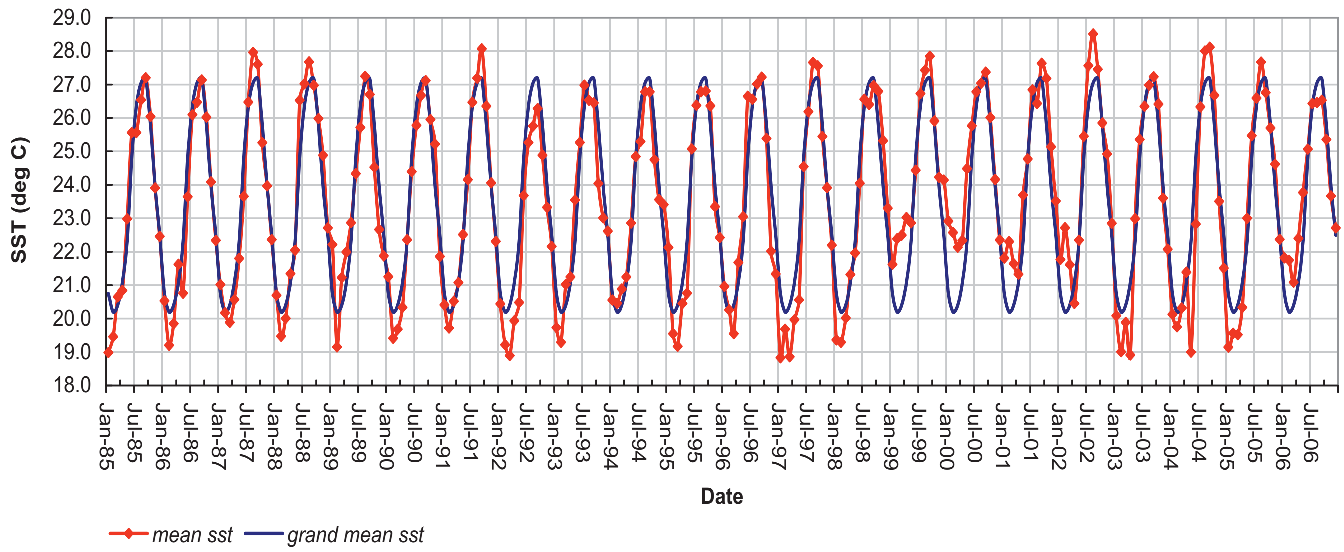

Monthly Mean Sea Surface Temperature Anomalies, Pearl and Hermes 1985-2006

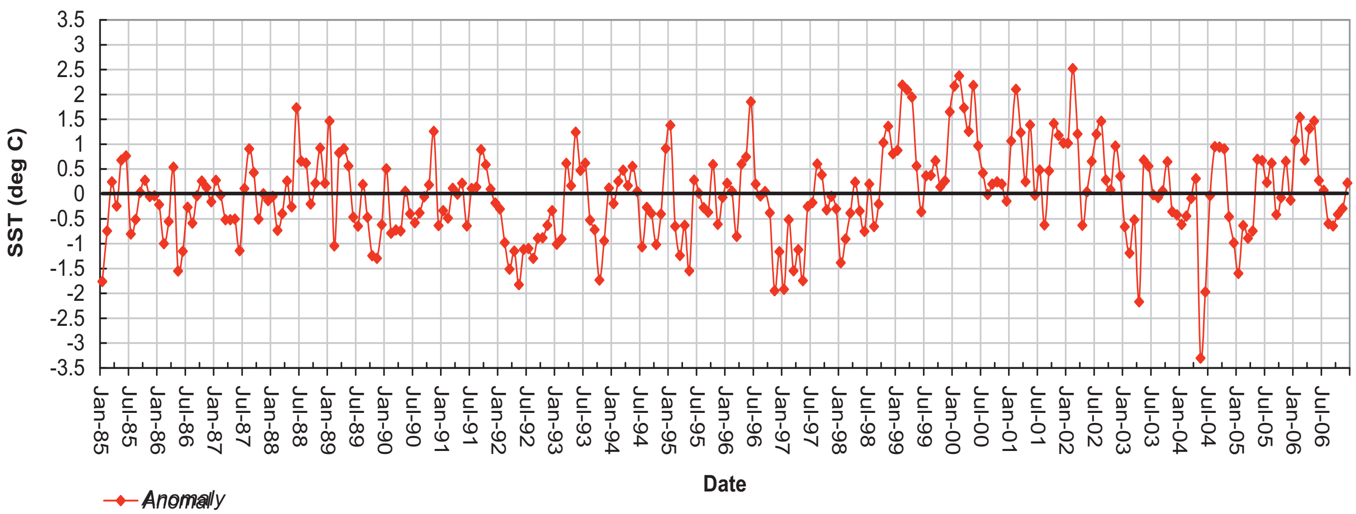

Seasonal Mean Sea Surface Temperature for Pearl and Hermes 1985-2006

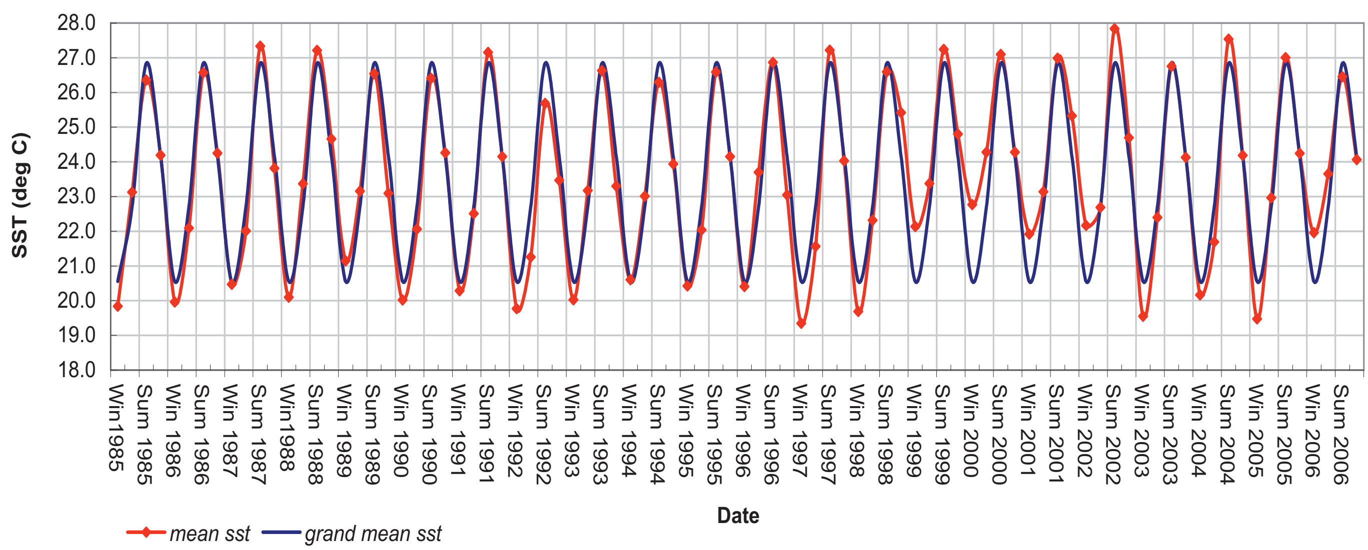

Monthly Mean Sea Surface Temperature for Lisianski Island 1985-2006

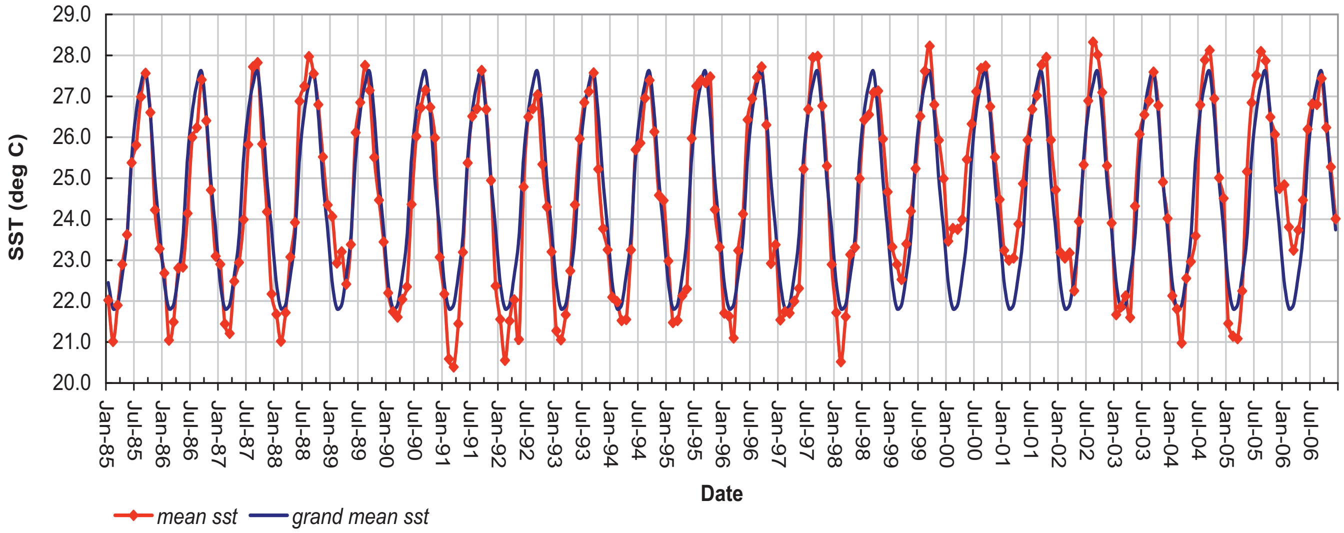

Monthly Mean Sea Surface Temperature Anomalies, Lisianski Island 1985-2006

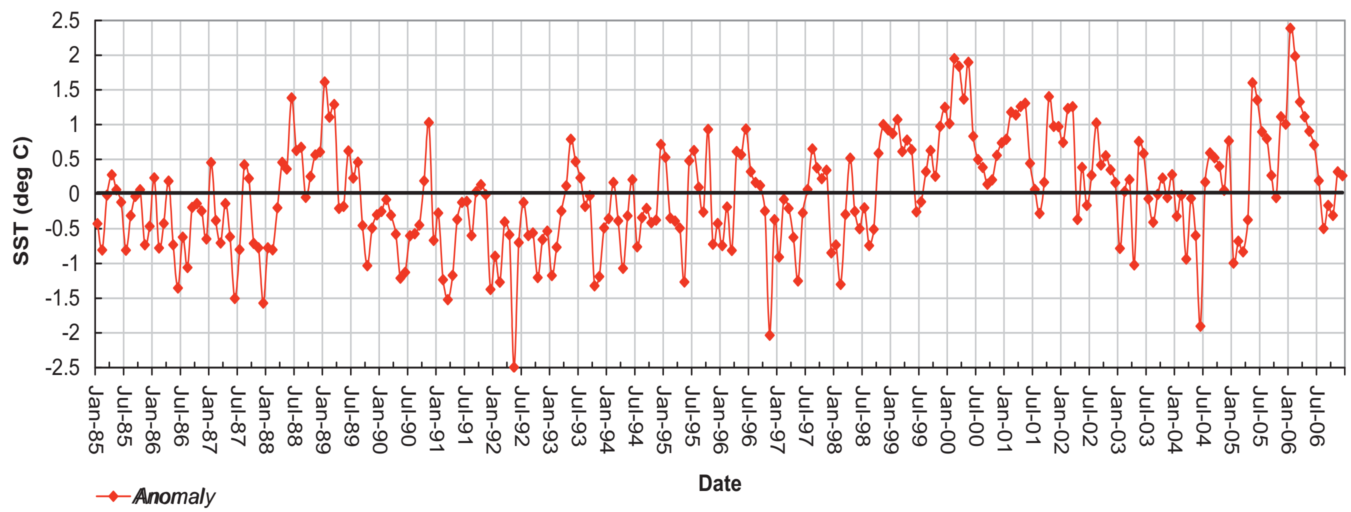

Seasonal Mean Sea Surface Temperature for Lisianski 1985-2006

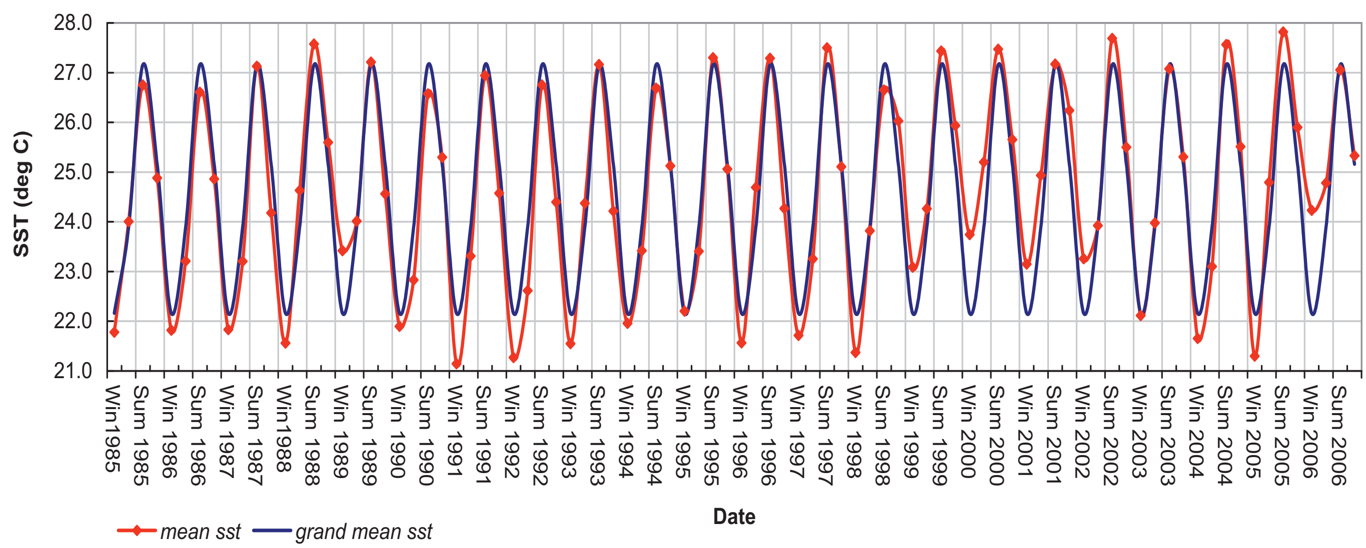

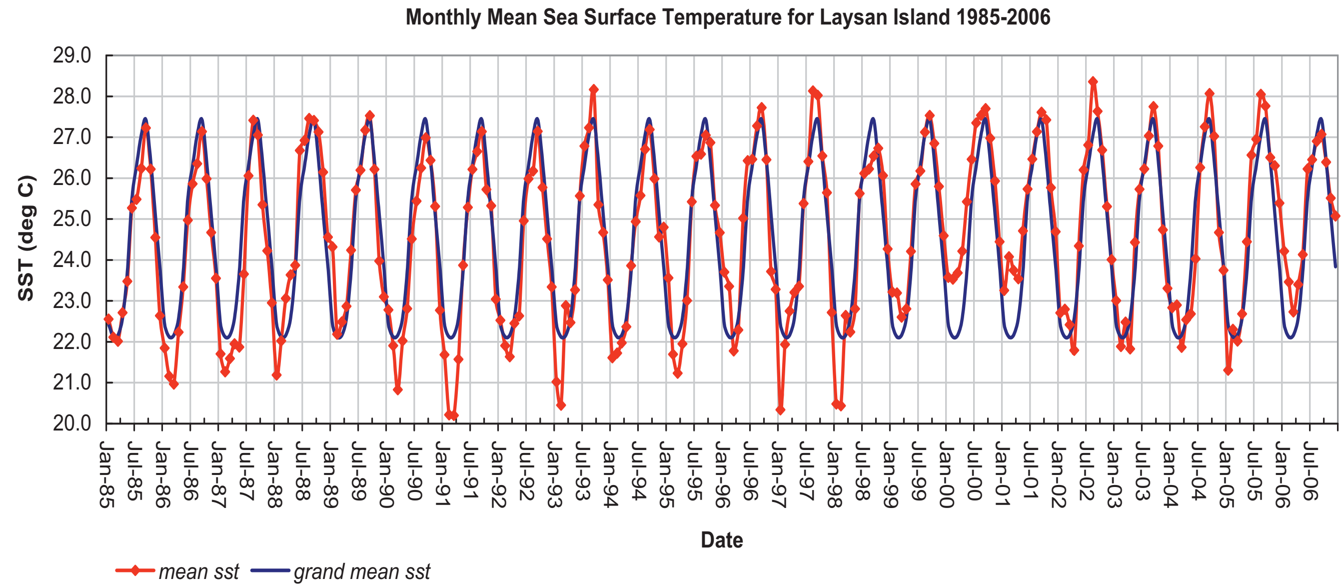
Monthly Mean Sea Surface Temperature for Laysan Island 1985-2006
SST (deg C)
Date
mean sst
grand mean sst

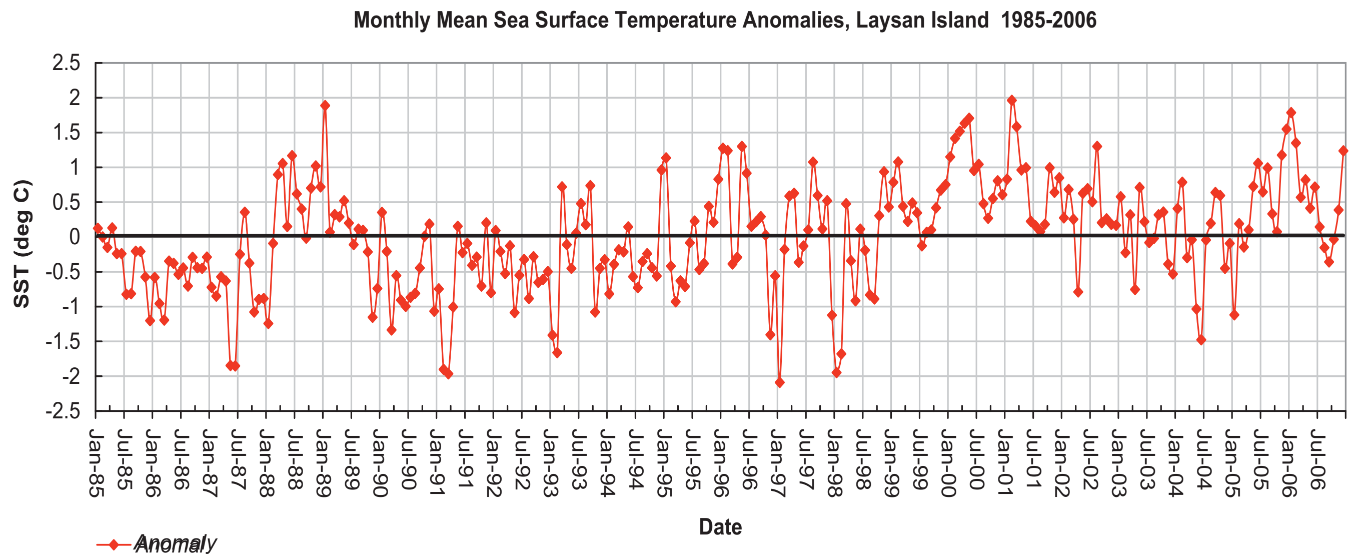
Monthly Mean Sea Surface Temperature Anomalies, Laysan Island 1985-2006
SST (deg C)
Date
Anomaly

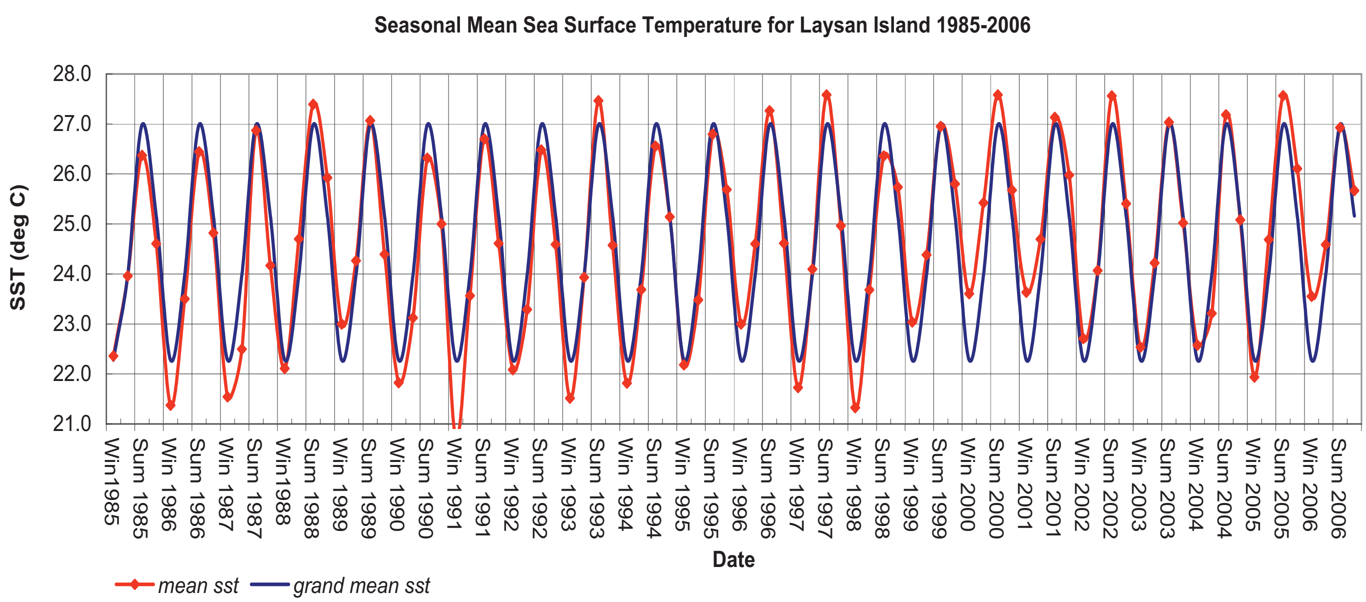
Seasonal Mean Sea Surface Temperature for Laysan Island 1985-2006
SST (deg C)
Date
mean sst
grand mean sst

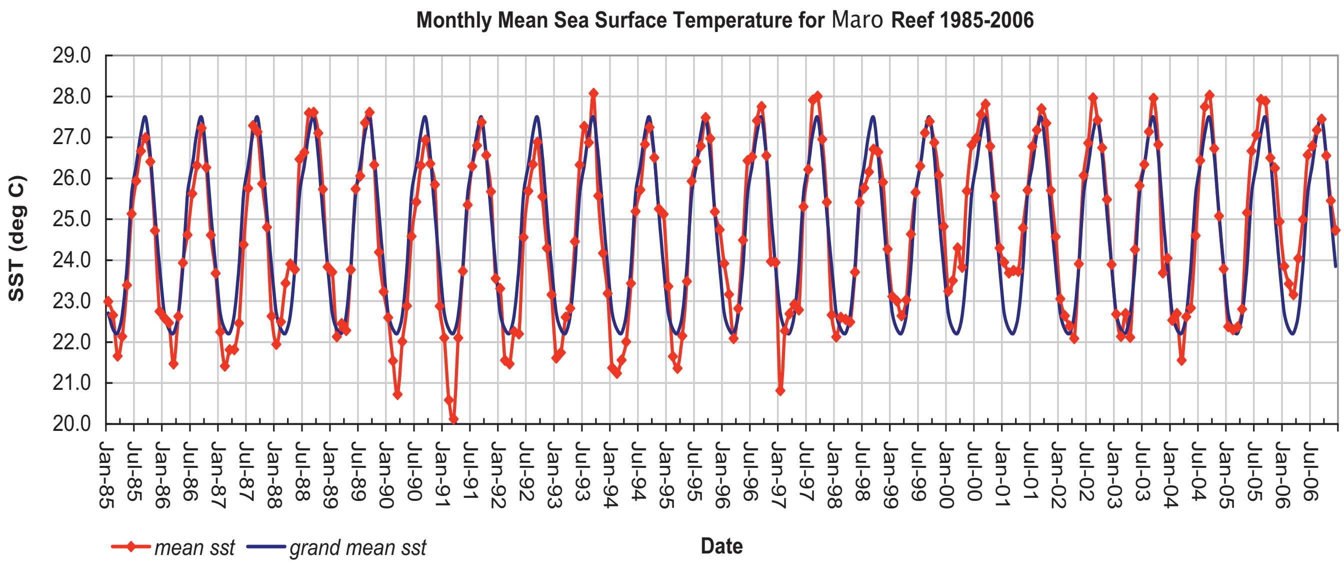
Monthly Mean Sea Surface Temperature for Maro Reef 1985-2006
SST (deg C)
Date
mean sst
grand mean sst

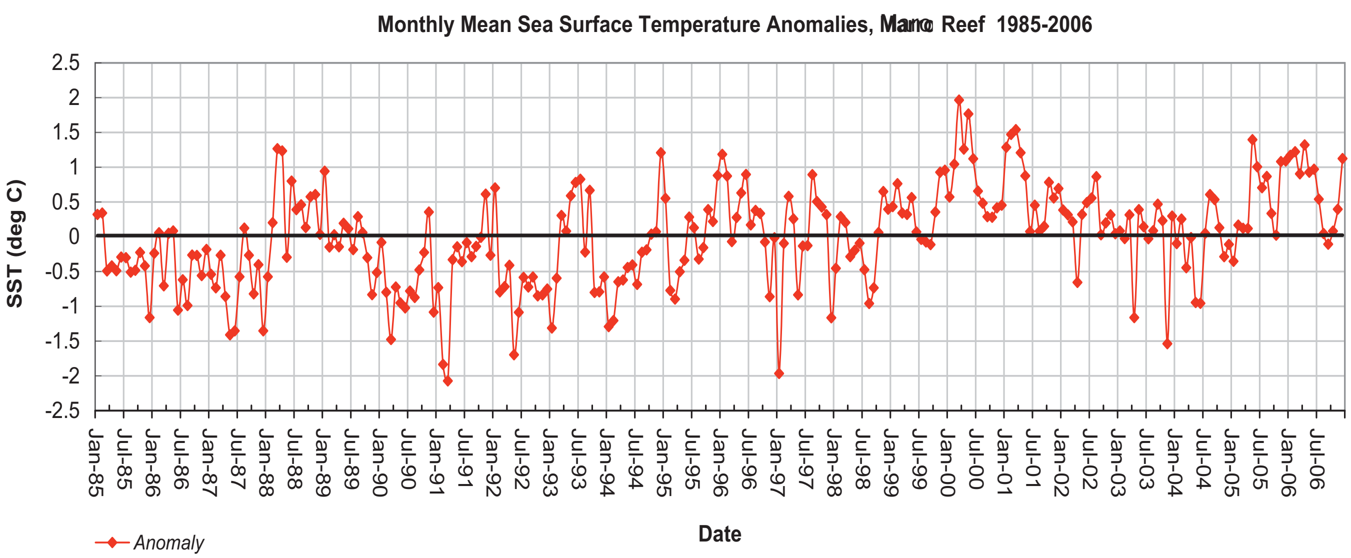
Monthly Mean Sea Surface Temperature Anomalies, Maro Reef 1985-2006
SST (deg C)
Date
Anomaly

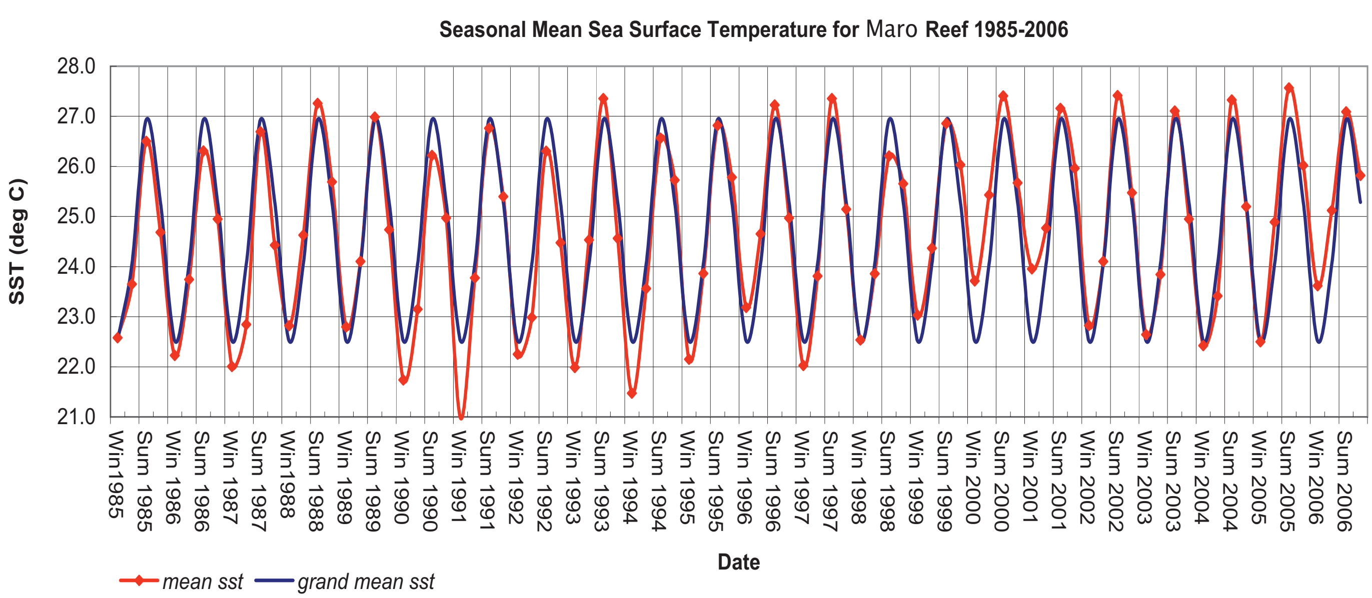
Seasonal Mean Sea Surface Temperature for Maro Reef 1985-2006
SST (deg C)
Date
mean sst
grand mean sst

Monthly Mean Sea Surface Temperature for Gardner Pinnacles 1985-2006

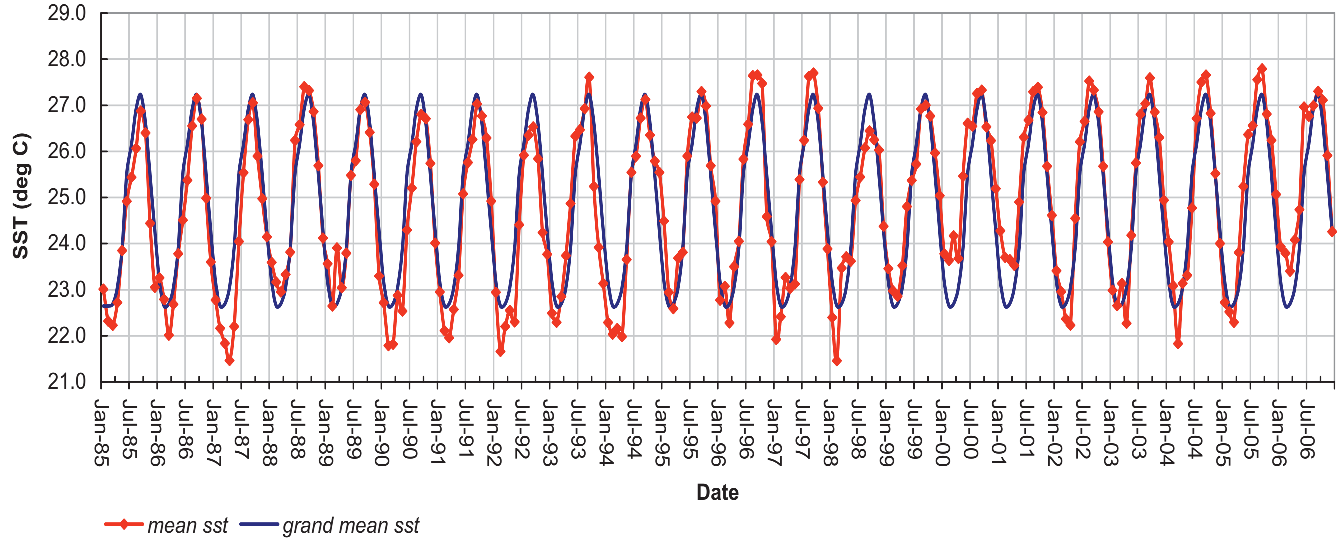

Monthly Mean Sea Surface Temperature Anomalies, Gardner Pinnacles 1985-2006

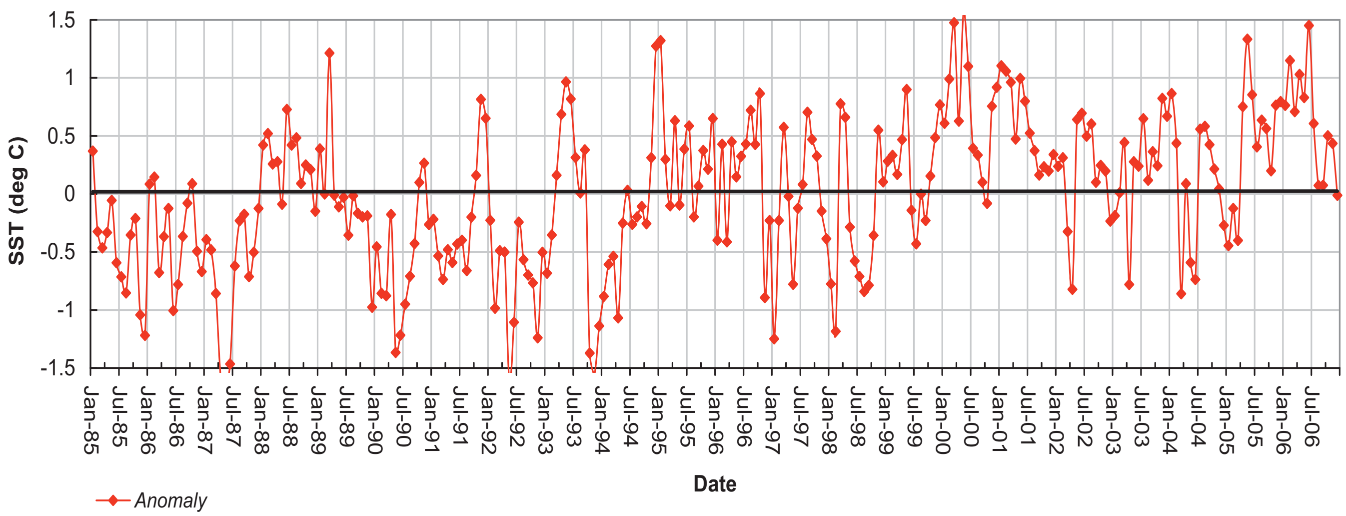

Seasonal Mean Sea Surface Temperature for Gardner Pinnacles 1985-2006

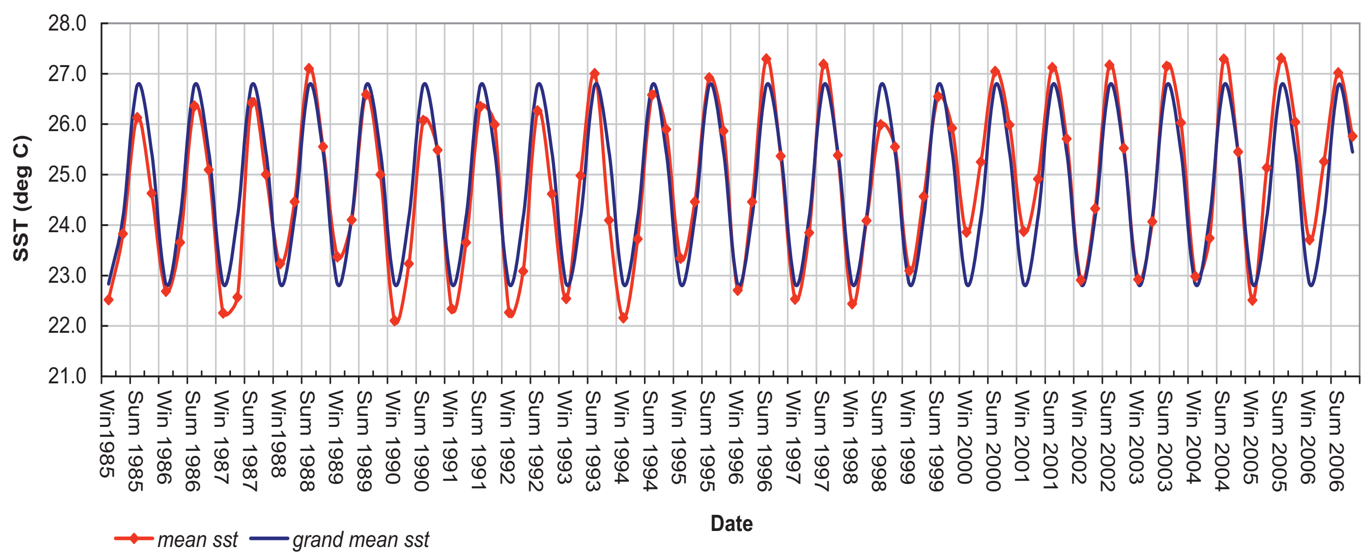

Mean Sea Surface Temperature for French Frigate Shoals NMS 1985-2006

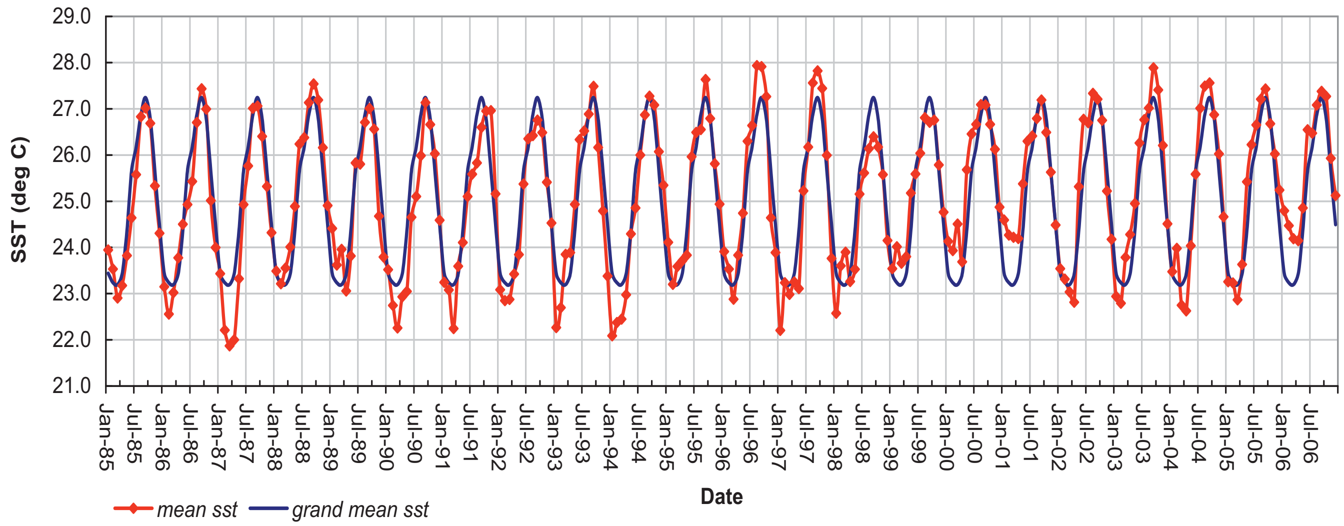

Mean Sea Surface Temperature Anomalies, French Frigate Shoals 1985-2006

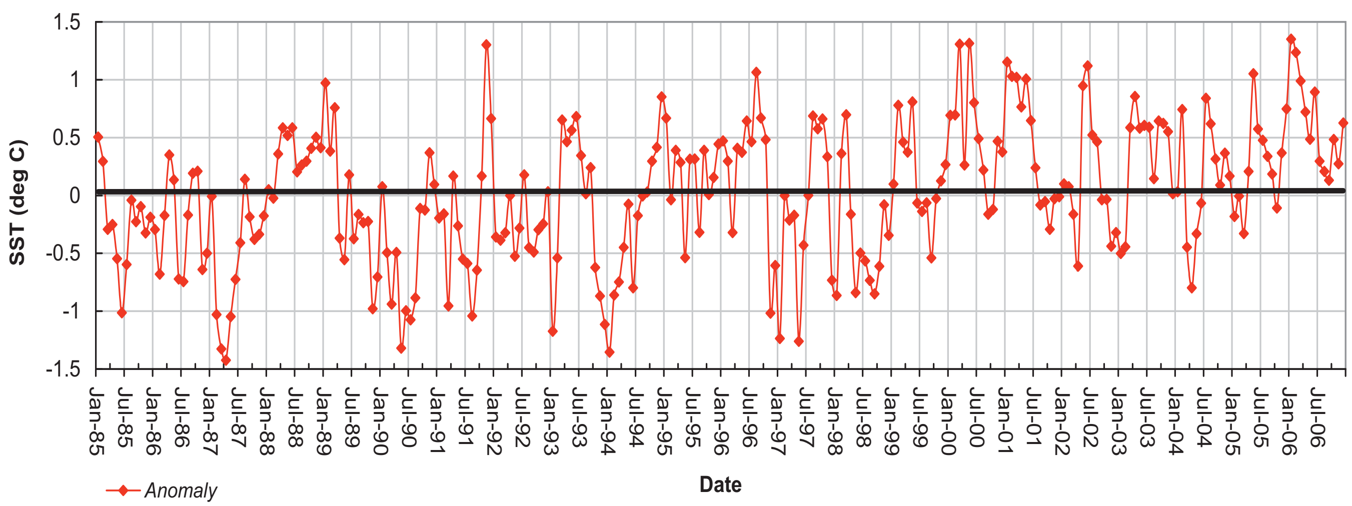

Seasonal Mean Sea Surface Temperature for French Frigate Shoals 1985-2006

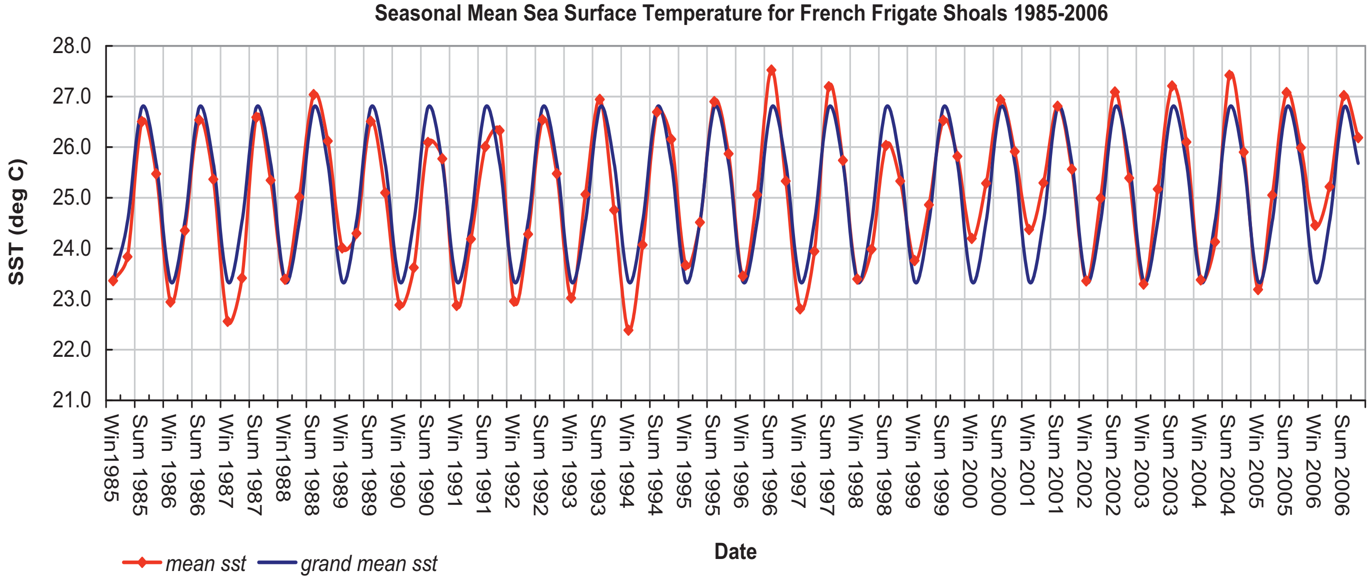

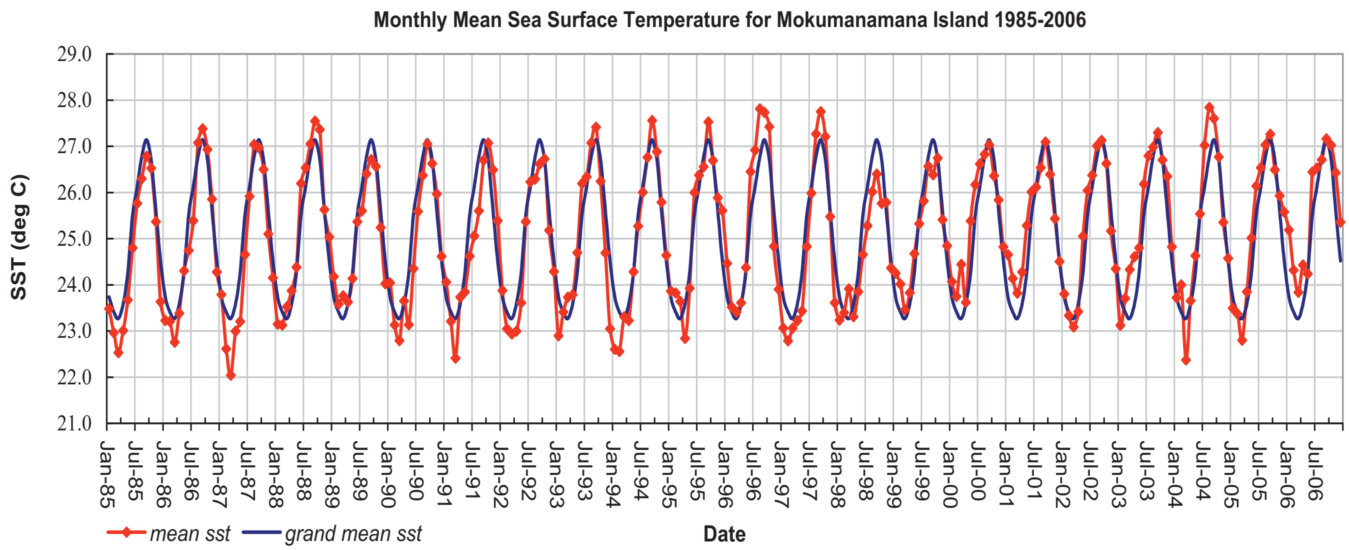
Monthly Mean Sea Surface Temperature for Mokumanamana Island 1985-2006
SST (deg C)
Date
mean sst
grand mean sst

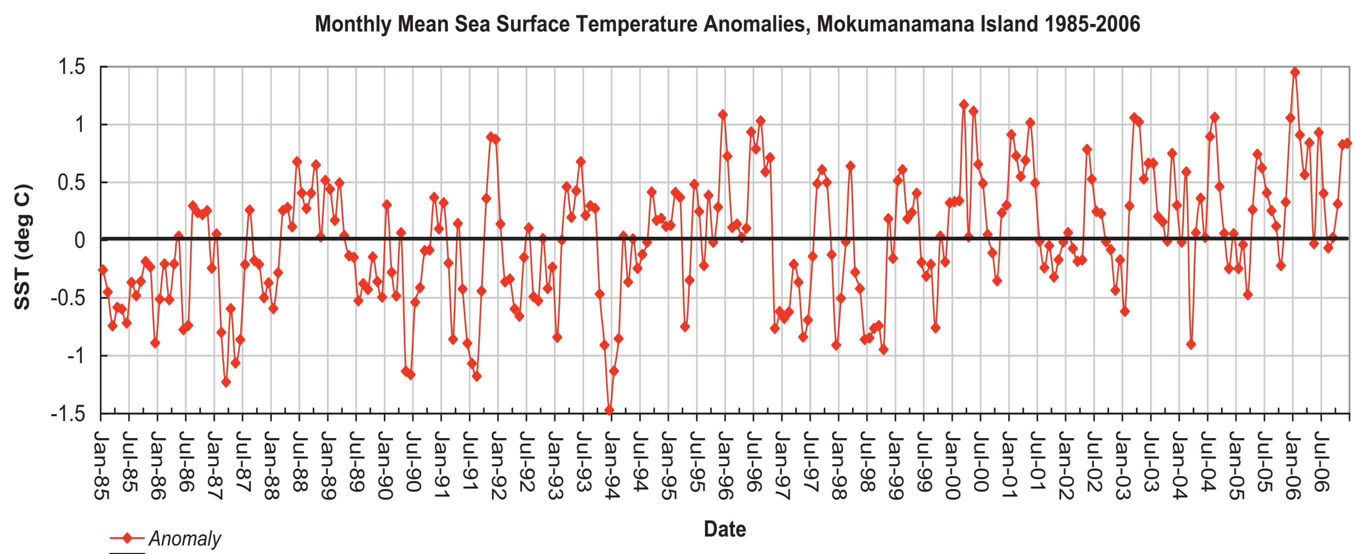
Monthly Mean Sea Surface Temperature Anomalies, Mokumanamana Island 1985-2006
SST (deg C)
Date
Anomaly

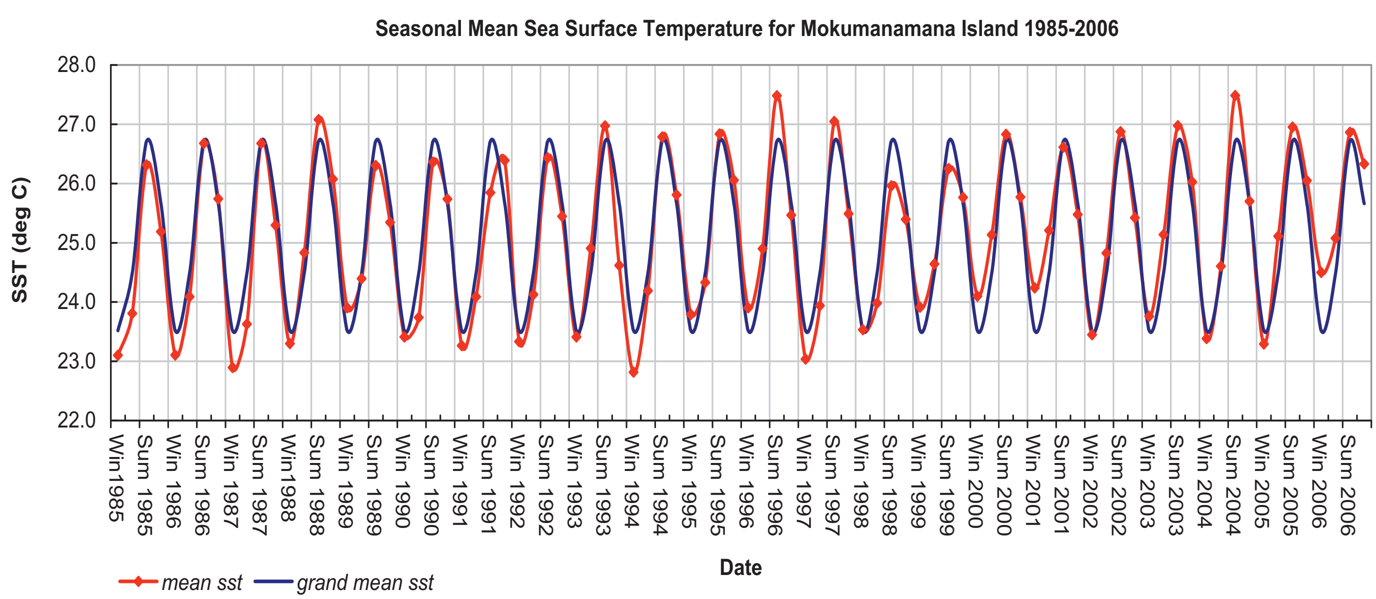
Seasonal Mean Sea Surface Temperature for Mokumanamana Island 1985-2006
SST (deg C)
Date
mean sst
grand mean sst

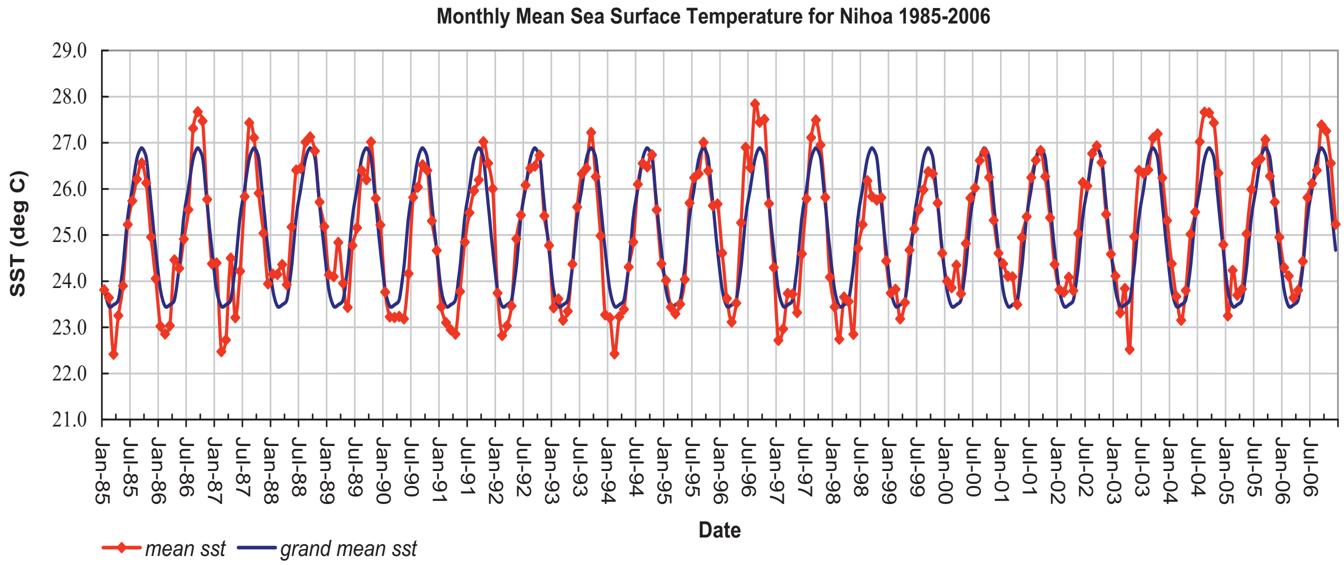
Monthly Mean Sea Surface Temperature for Nihoa 1985-2006
SST (deg C)
Date
mean sst
grand mean sst

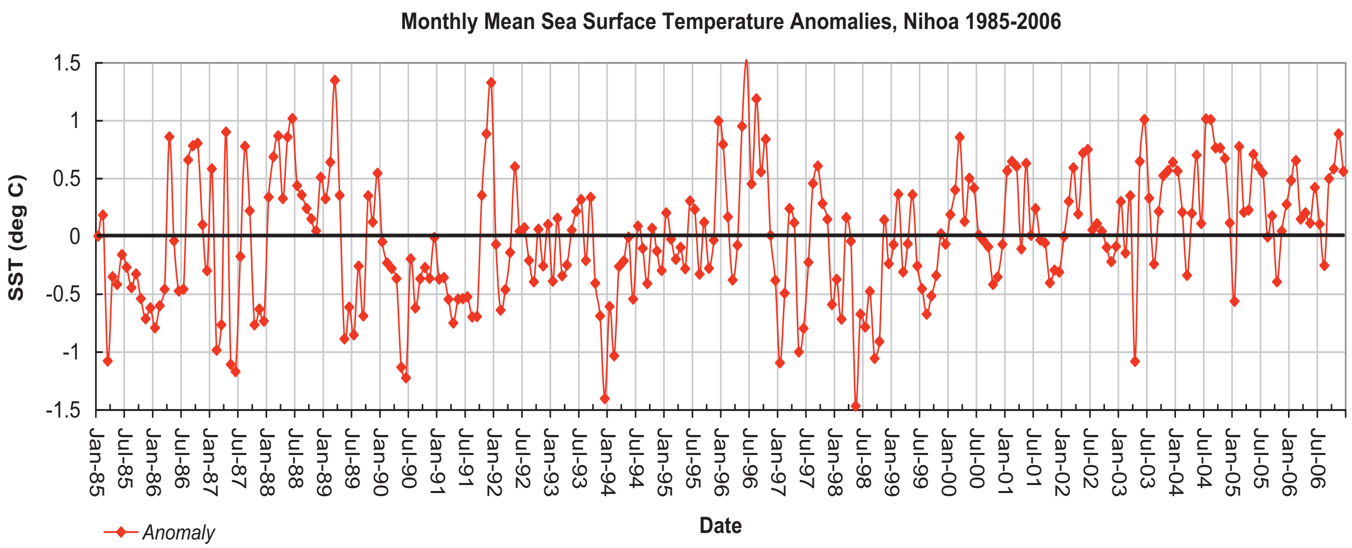
Monthly Mean Sea Surface Temperature Anomalies, Nihoa 1985-2006
SST (deg C)
Date
Anomaly

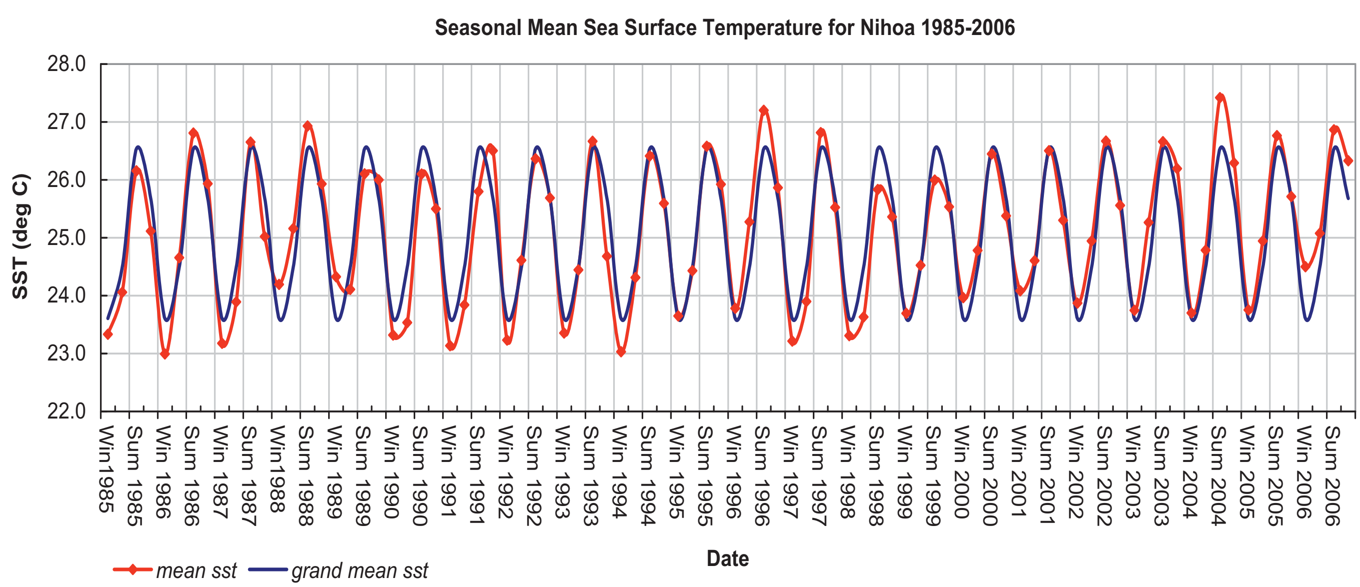
Seasonal Mean Sea Surface Temperature for Nihoa 1985-2006
SST (deg C)
Date
mean sst
grand mean sst

APPENDIX II. CHLOROPHYLL (AND RELATED) TIME SERIES PLOTS

Monthly Median Chlorophyll for Kure 1997-2007

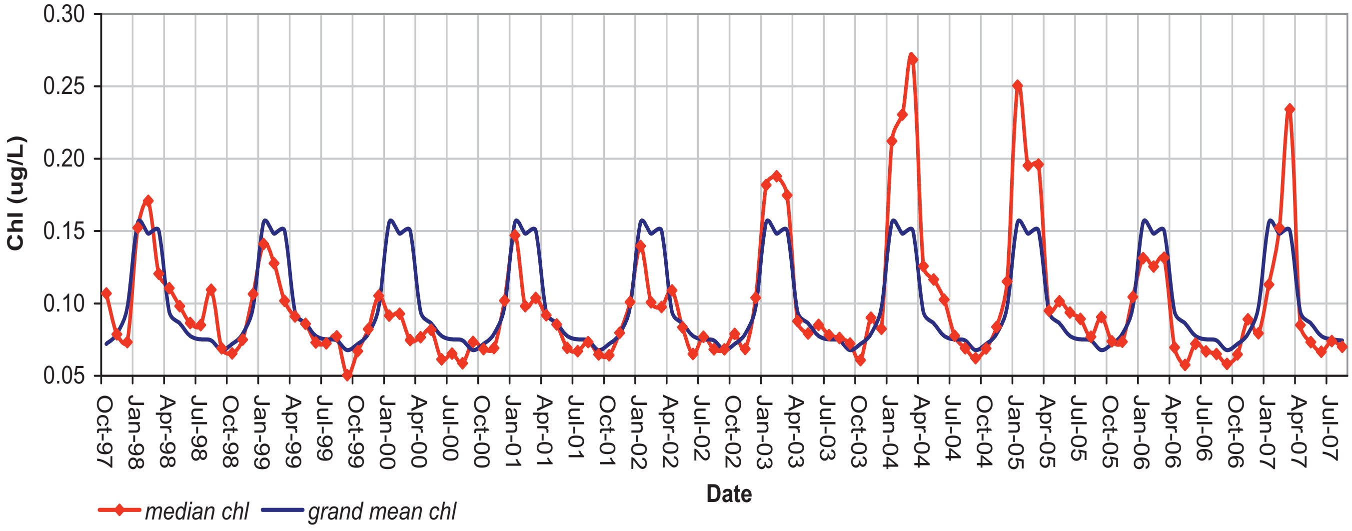

Monthly Median Chlorophyll Anomaly, Kure 1997-2007

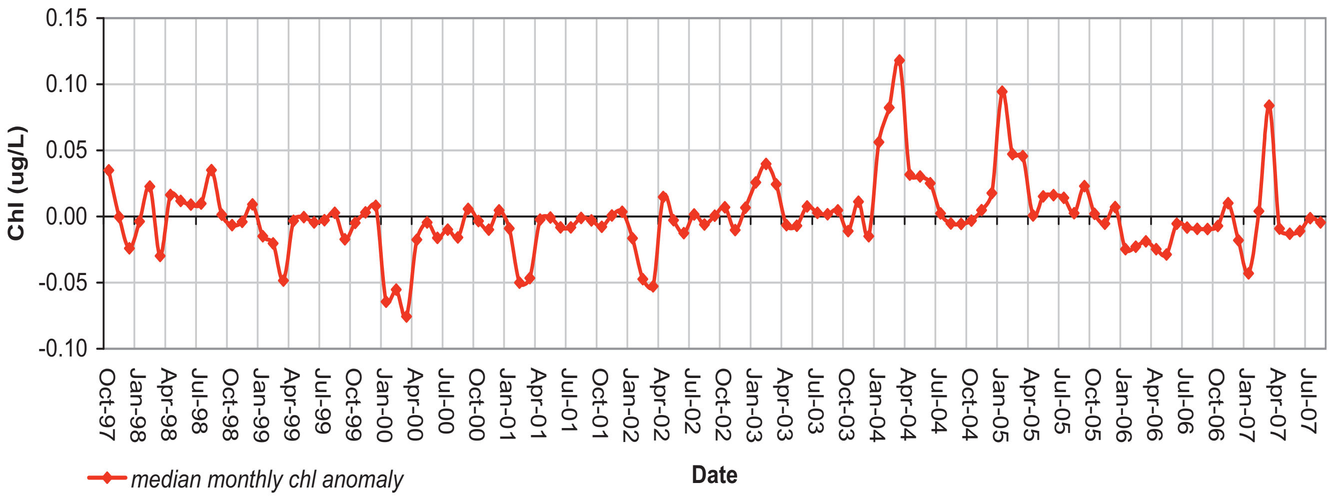

Mean Seasonal Chlorophyll for Kure 1997-2007

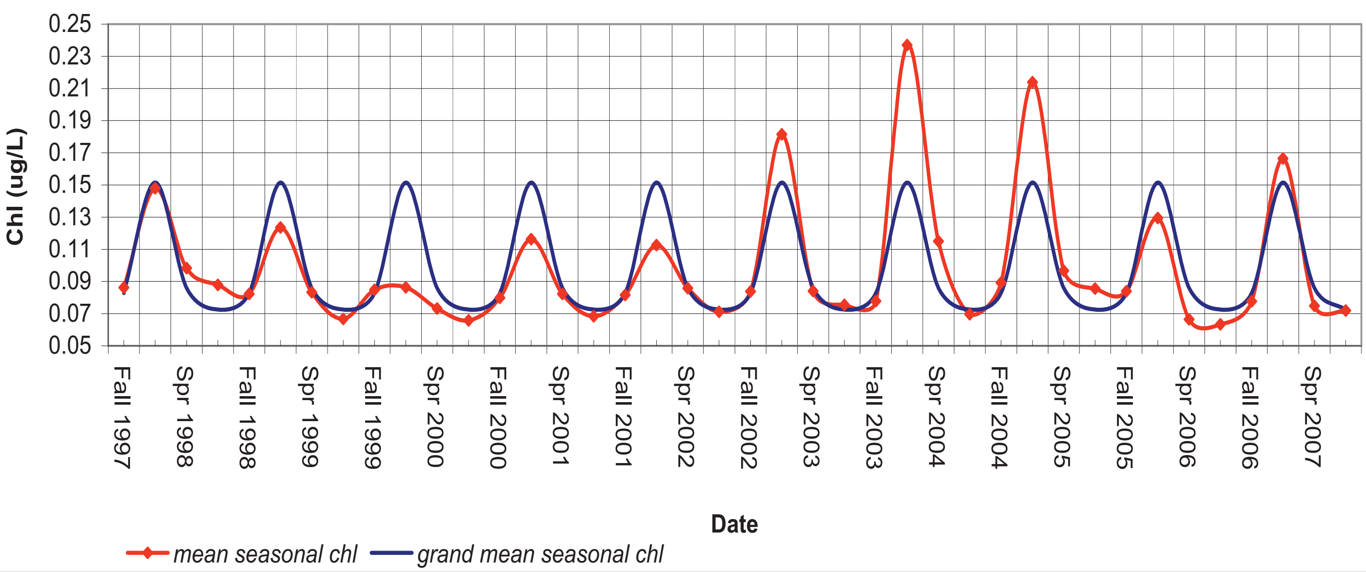

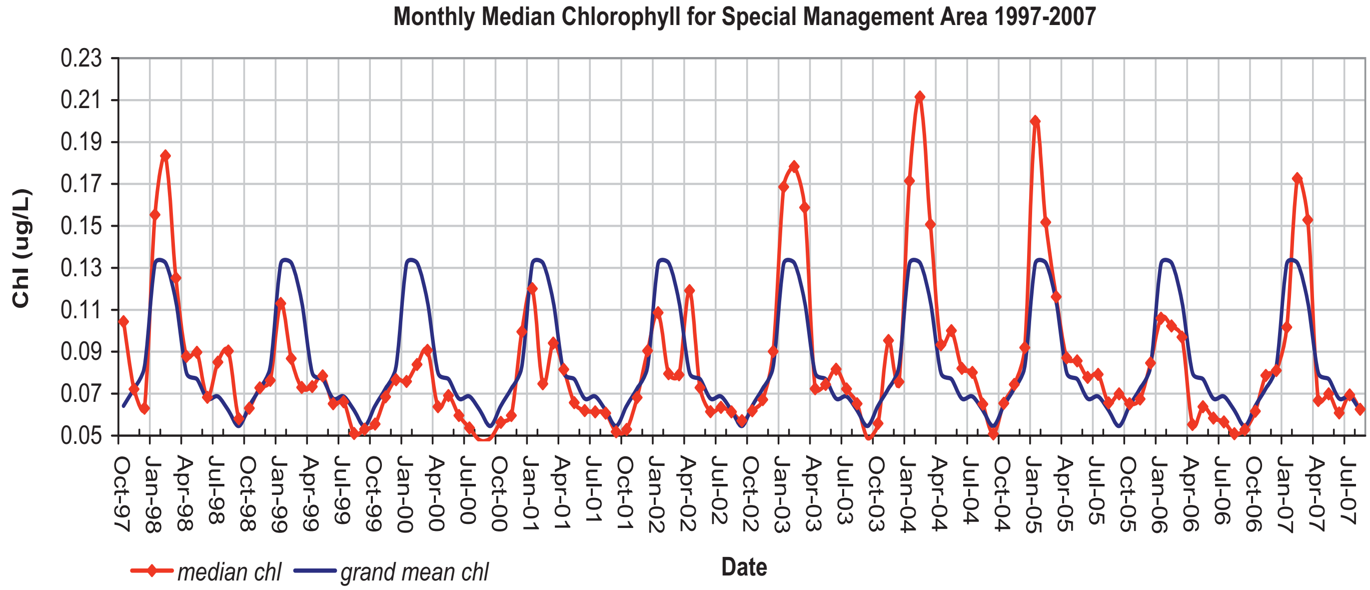
Monthly Median Chlorophyll for Special Management Area 1997-2007
Chl (ug/L)
0.23
0.21
0.19
0.17
0.15
0.13
0.11
0.09
0.07
0.05
Oct-97
Jan-98
Apr-98
Jul-98
Oct-98
Jan-99
Apr-99
Jul-99
Oct-99
Jan-00
Apr-00
Jul-00
Oct-00
Jan-01
Apr-01
Jul-01
Oct-01
Jan-02
Apr-02
Jul-02
Oct-02
Jan-03
Apr-03
Jul-03
Oct-03
Jan-04
Apr-04
Jul-04
Oct-04
Jan-05
Apr-05
Jul-05
Oct-05
Jan-06
Apr-06
Jul-06
Oct-06
Jan-07
Apr-07
Jul-07
Date
median chl
grand mean chl

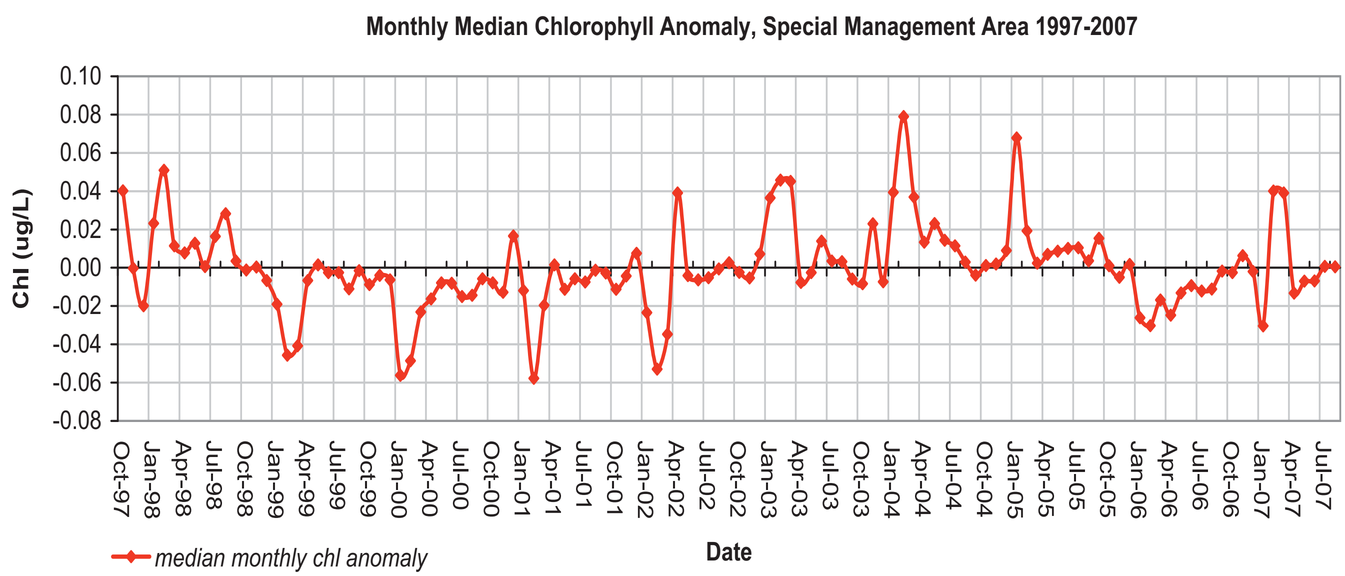
Monthly Median Chlorophyll Anomaly, Special Management Area 1997-2007
Chl (ug/L)
0.10
0.08
0.06
0.04
0.02
0.00
-0.02
-0.04
-0.06
-0.08
Oct-97
Jan-98
Apr-98
Jul-98
Oct-98
Jan-99
Apr-99
Jul-99
Oct-99
Jan-00
Apr-00
Jul-00
Oct-00
Jan-01
Apr-01
Jul-01
Oct-01
Jan-02
Apr-02
Jul-02
Oct-02
Jan-03
Apr-03
Jul-03
Oct-03
Jan-04
Apr-04
Jul-04
Oct-04
Jan-05
Apr-05
Jul-05
Oct-05
Jan-06
Apr-06
Jul-06
Oct-06
Jan-07
Apr-07
Jul-07
Date
median monthly chl anomaly

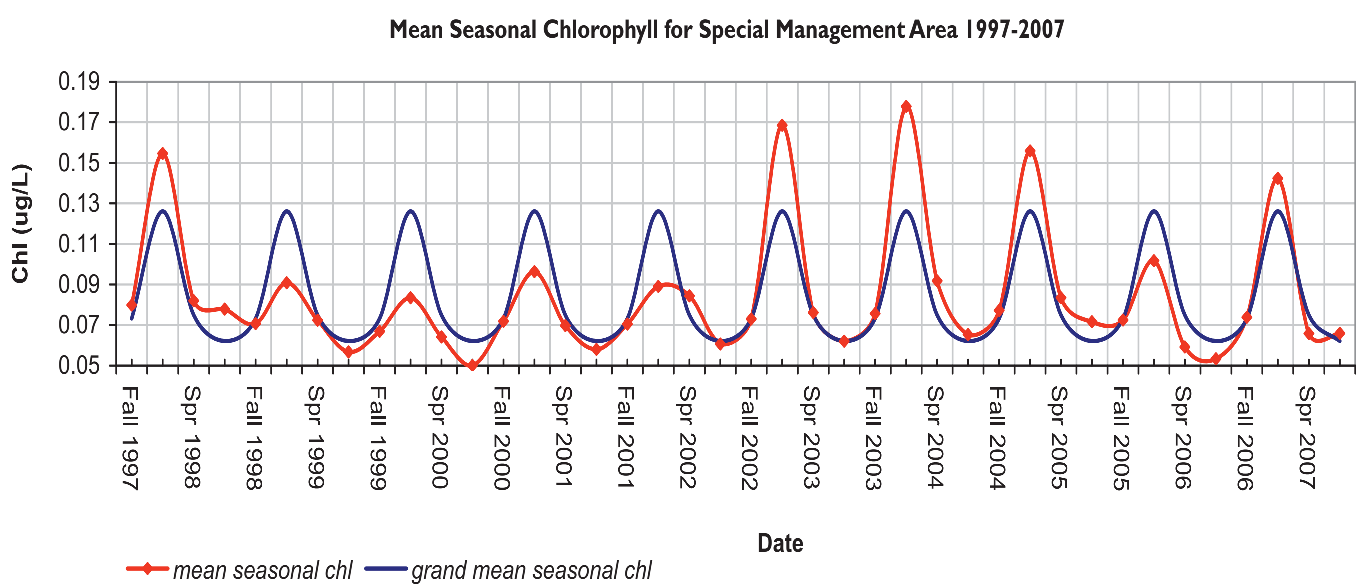
Mean Seasonal Chlorophyll for Special Management Area 1997-2007
Chl (ug/L)
0.19
0.17
0.15
0.13
0.11
0.09
0.07
0.05
Fall 1997
Spr 1998
Fall 1998
Spr 1999
Fall 1999
Spr 2000
Fall 2000
Spr 2001
Fall 2001
Spr 2002
Fall 2002
Spr 2003
Fall 2003
Spr 2004
Fall 2004
Spr 2005
Fall 2005
Spr 2006
Fall 2006
Spr 2007
Date
mean seasonal chl
grand mean seasonal chl

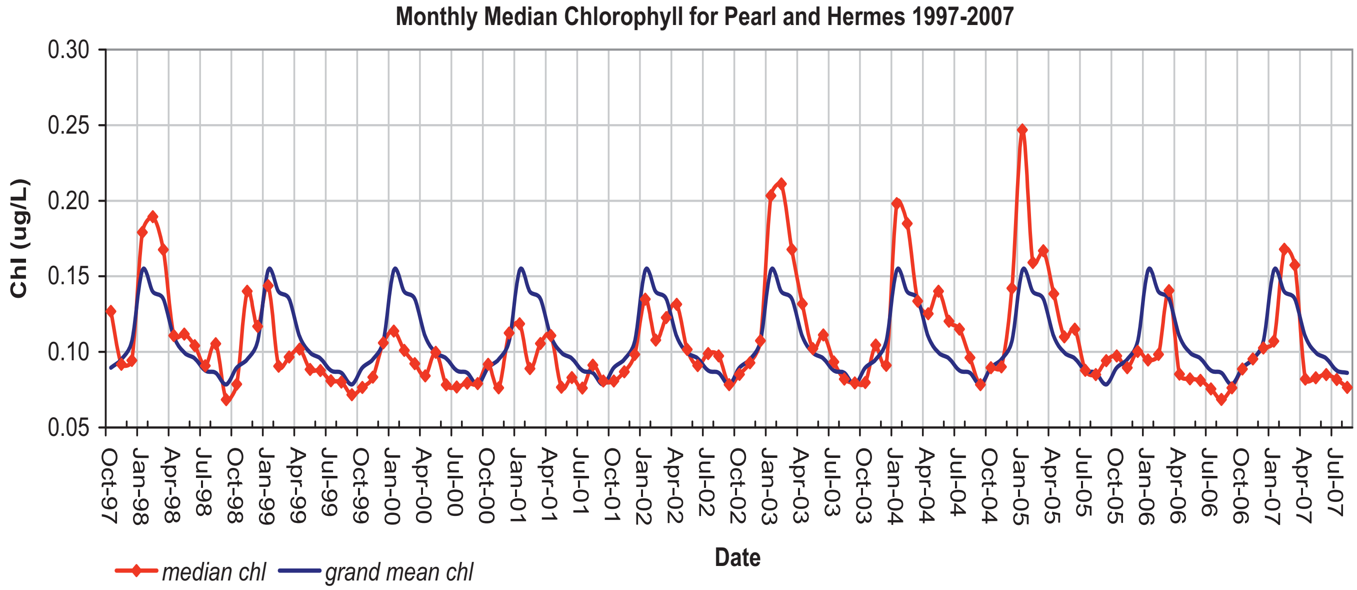
Monthly Median Chlorophyll for Pearl and Hermes 1997-2007
0.30
0.25
0.20
0.15
0.10
0.05
Chl (ug/L)
Oct-97 Jan-98 Apr-98 Jul-98 Oct-98 Jan-99 Apr-99 Jul-99 Oct-99 Jan-00 Apr-00 Jul-00 Oct-00 Jan-01 Apr-01 Jul-01 Oct-01 Jan-02 Apr-02 Jul-02 Oct-02 Jan-03 Apr-03 Jul-03 Oct-03 Jan-04 Apr-04 Jul-04 Oct-04 Jan-05 Apr-05 Jul-05 Oct-05 Jan-06 Apr-06 Jul-06 Oct-06 Jan-07 Apr-07 Jul-07
Date
median chl
grand mean chl

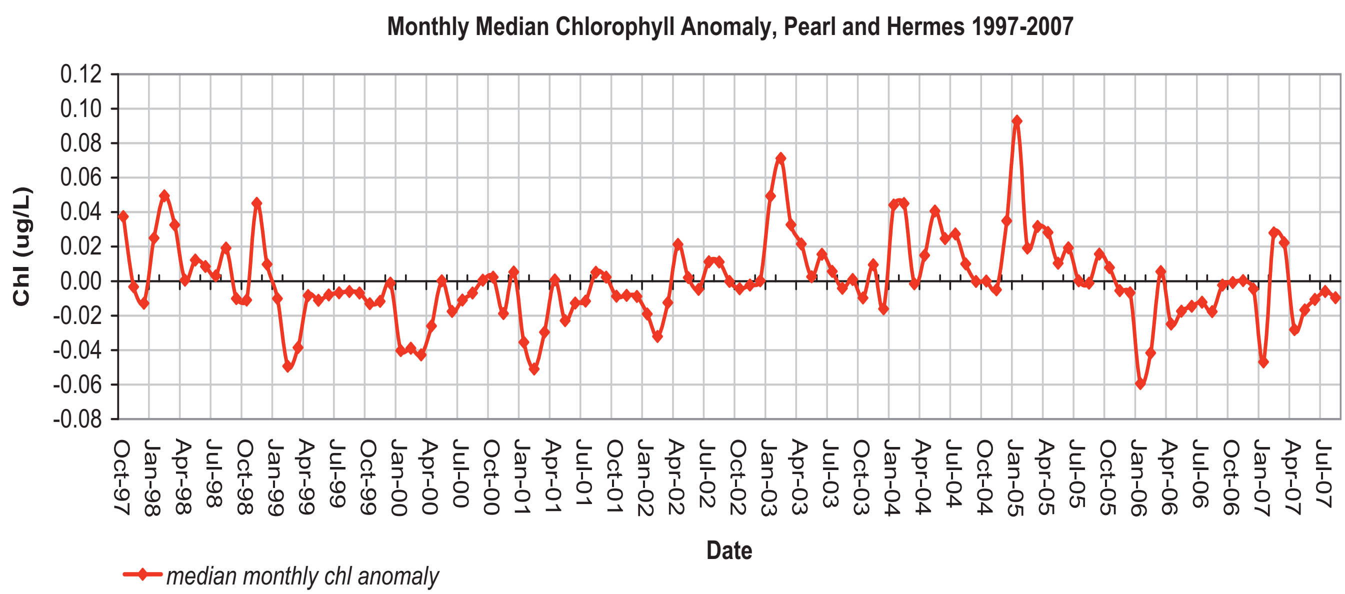
Monthly Median Chlorophyll Anomaly, Pearl and Hermes 1997-2007
0.12
0.10
0.08
0.06
0.04
0.02
0.00
-0.02
-0.04
-0.06
-0.08
Chl (ug/L)
Oct-97 Jan-98 Apr-98 Jul-98 Oct-98 Jan-99 Apr-99 Jul-99 Oct-99 Jan-00 Apr-00 Jul-00 Oct-00 Jan-01 Apr-01 Jul-01 Oct-01 Jan-02 Apr-02 Jul-02 Oct-02 Jan-03 Apr-03 Jul-03 Oct-03 Jan-04 Apr-04 Jul-04 Oct-04 Jan-05 Apr-05 Jul-05 Oct-05 Jan-06 Apr-06 Jul-06 Oct-06 Jan-07 Apr-07 Jul-07
Date
median monthly chl anomaly

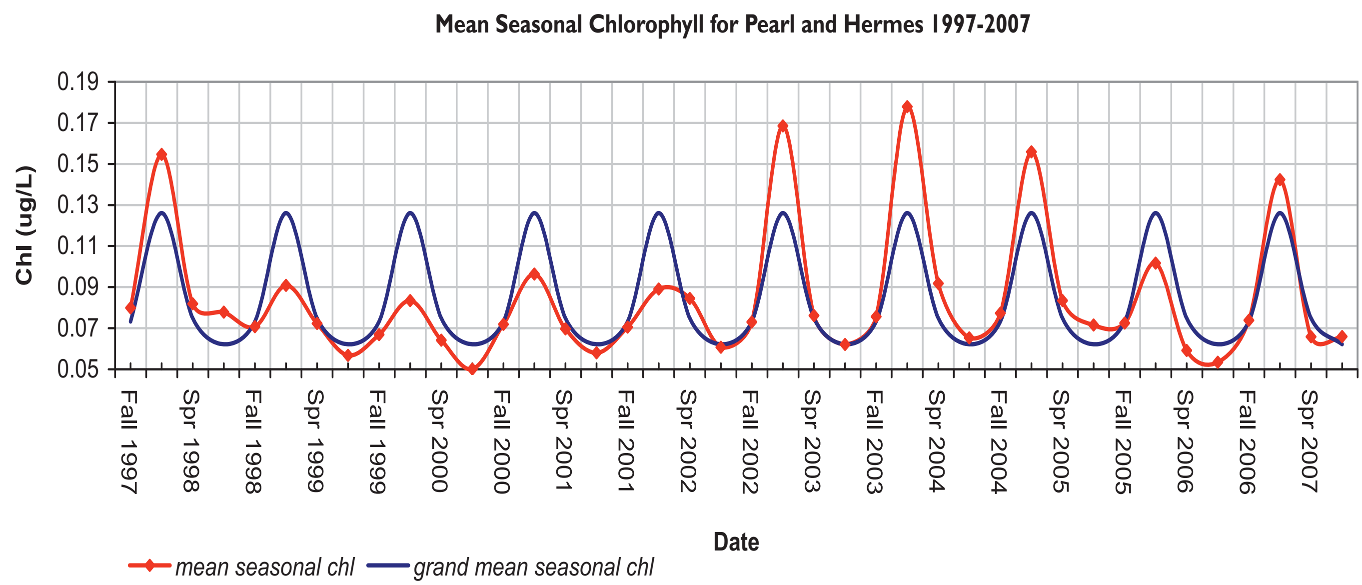
Mean Seasonal Chlorophyll for Pearl and Hermes 1997-2007
0.19
0.17
0.15
0.13
0.11
0.09
0.07
0.05
Chl (ug/L)
Fall 1997 Spr 1998 Fall 1998 Spr 1999 Fall 1999 Spr 2000 Fall 2000 Spr 2001 Fall 2001 Spr 2002 Fall 2002 Spr 2003 Fall 2003 Spr 2004 Fall 2004 Spr 2005 Fall 2005 Spr 2006 Fall 2006 Spr 2007
Date
mean seasonal chl
grand mean seasonal chl

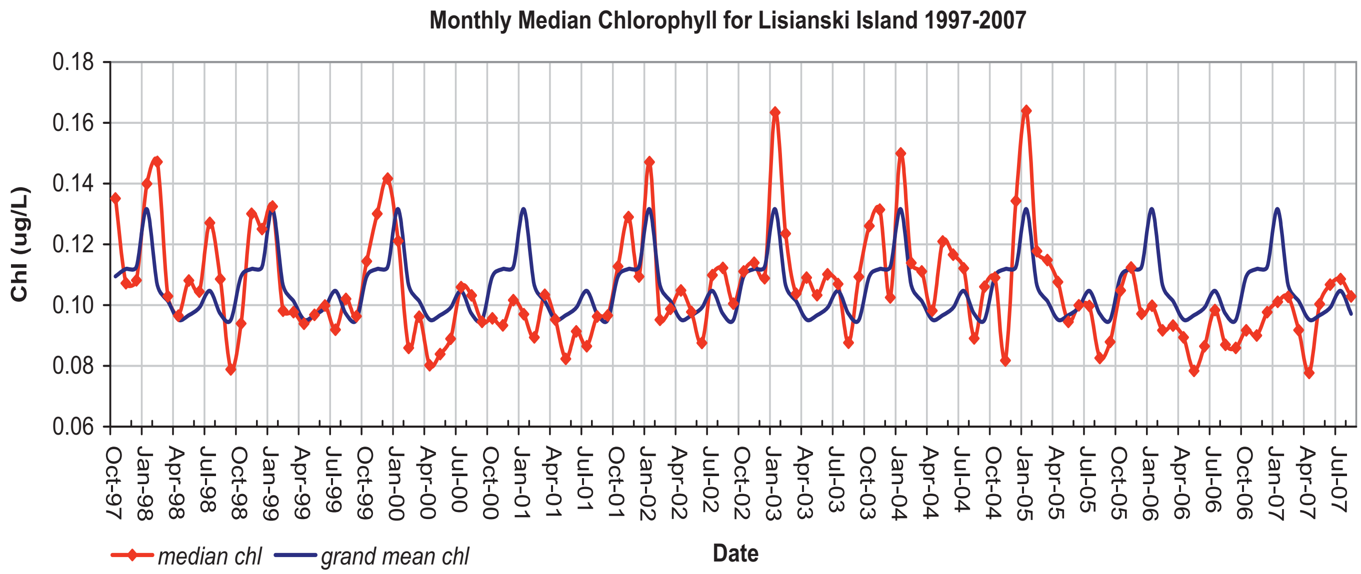
Monthly Median Chlorophyll for Lisianski Island 1997-2007
Chl (ug/L)
Date
median chl
grand mean chl

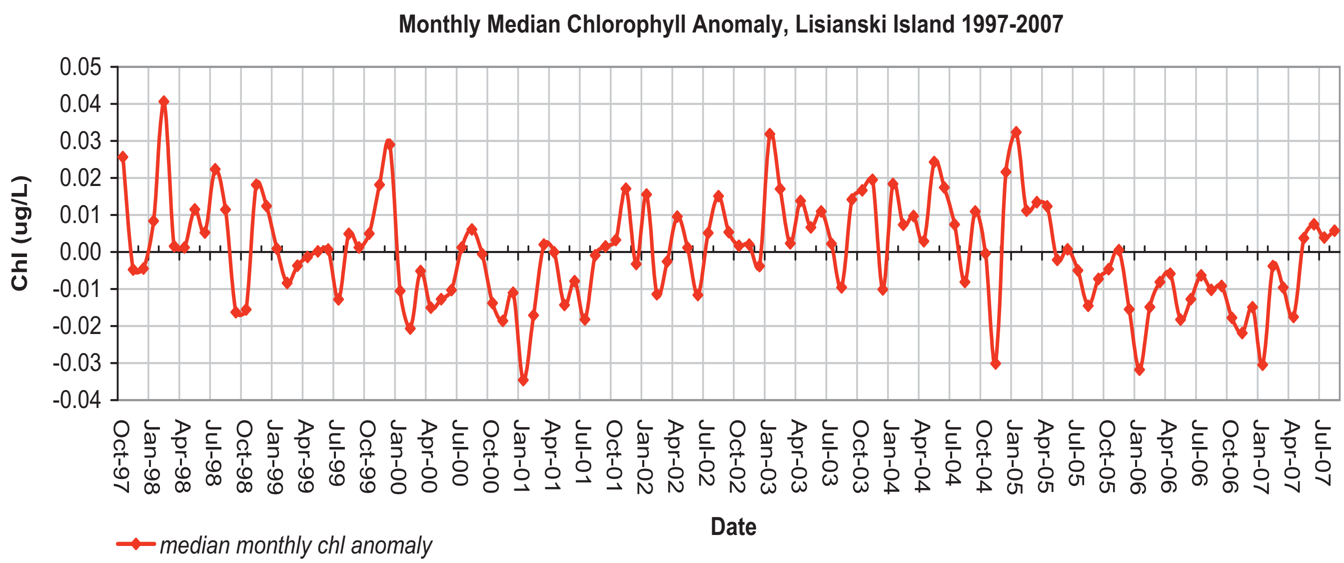
Monthly Median Chlorophyll Anomaly, Lisianski Island 1997-2007
Chl (ug/L)
Date
median monthly chl anomaly

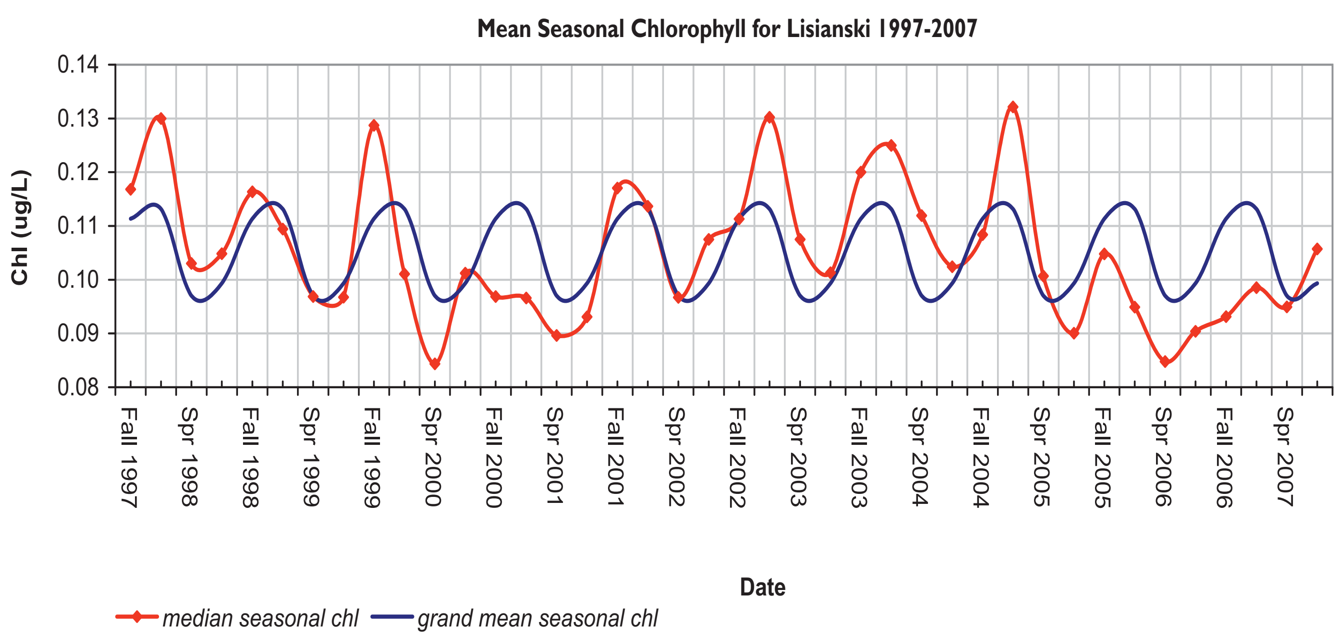
Mean Seasonal Chlorophyll for Lisianski 1997-2007
Chl (ug/L)
Date
median seasonal chl
grand mean seasonal chl

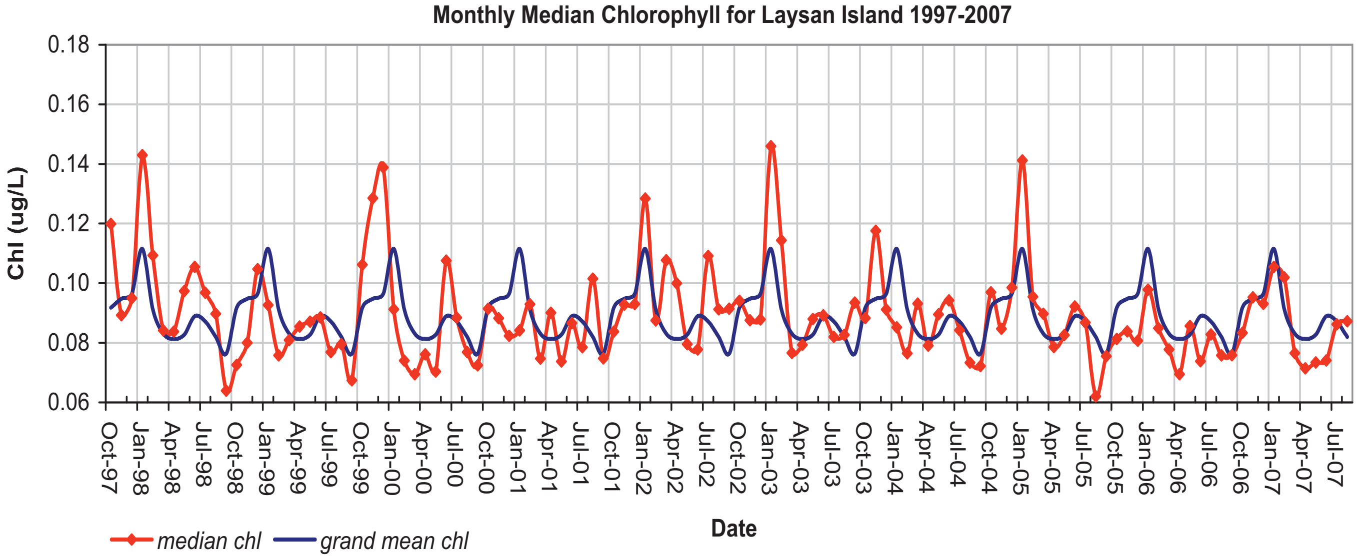
Monthly Median Chlorophyll for Laysan Island 1997-2007
Chl (ug/L)
Date
median chl
grand mean chl

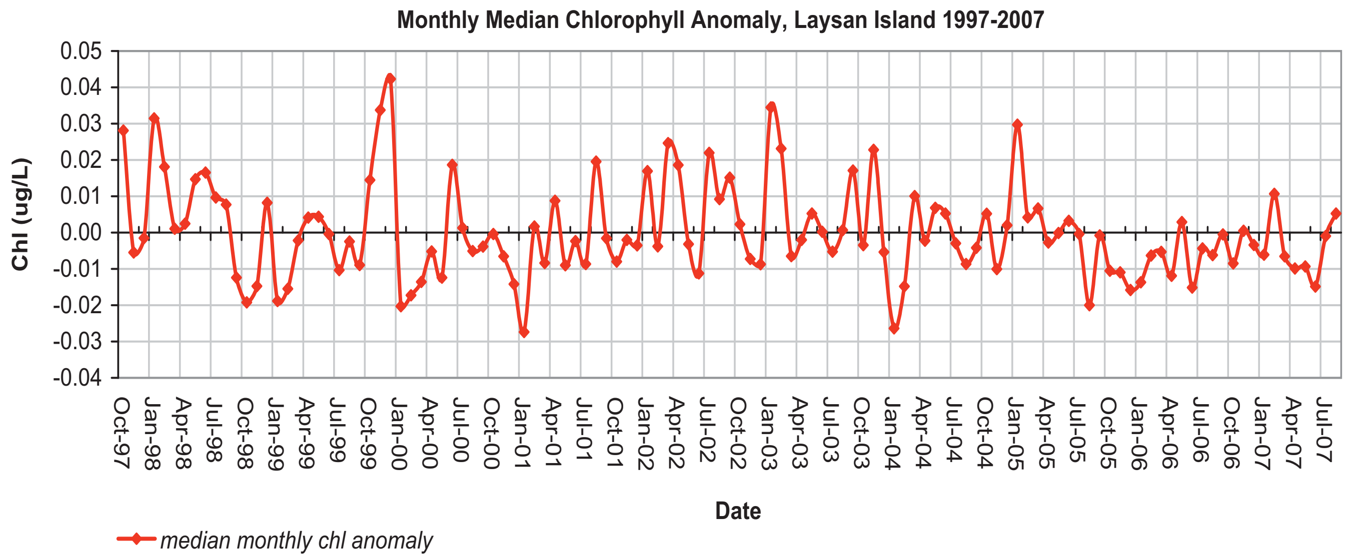
Monthly Median Chlorophyll Anomaly, Laysan Island 1997-2007
Chl (ug/L)
Date
median monthly chl anomaly

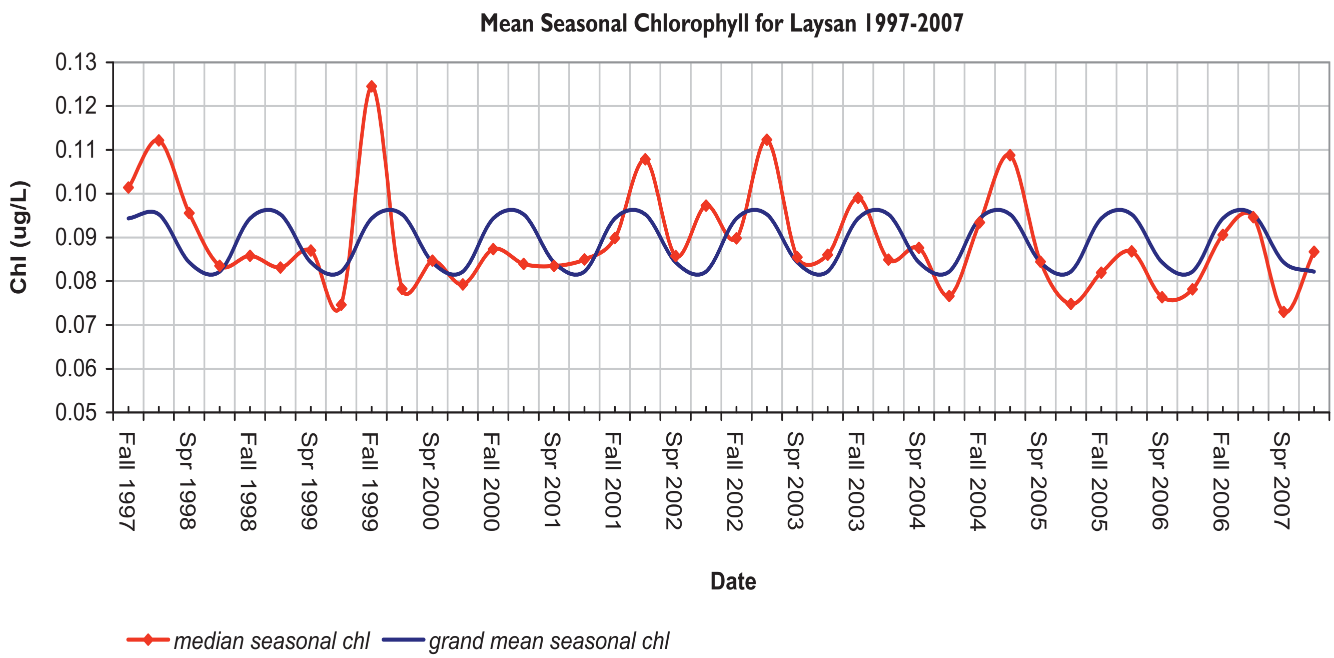
Mean Seasonal Chlorophyll for Laysan 1997-2007
Chl (ug/L)
Date
median seasonal chl
grand mean seasonal chl

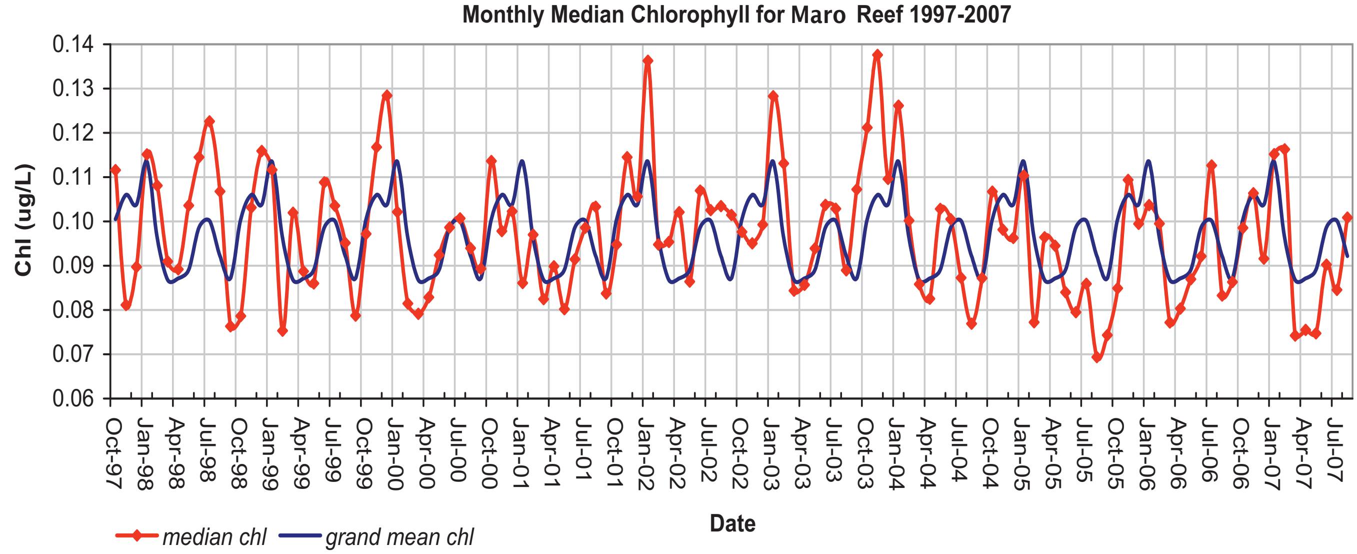
Monthly Median Chlorophyll for Maro Reef 1997-2007
Chl (ug/L)
0.14
0.13
0.12
0.11
0.10
0.09
0.08
0.07
0.06
Oct-97
Jan-98
Apr-98
Jul-98
Oct-98
Jan-99
Apr-99
Jul-99
Oct-99
Jan-00
Apr-00
Jul-00
Oct-00
Jan-01
Apr-01
Jul-01
Oct-01
Jan-02
Apr-02
Jul-02
Oct-02
Jan-03
Apr-03
Jul-03
Oct-03
Jan-04
Apr-04
Jul-04
Oct-04
Jan-05
Apr-05
Jul-05
Oct-05
Jan-06
Apr-06
Jul-06
Oct-06
Jan-07
Apr-07
Jul-07
Date
median chl
grand mean chl

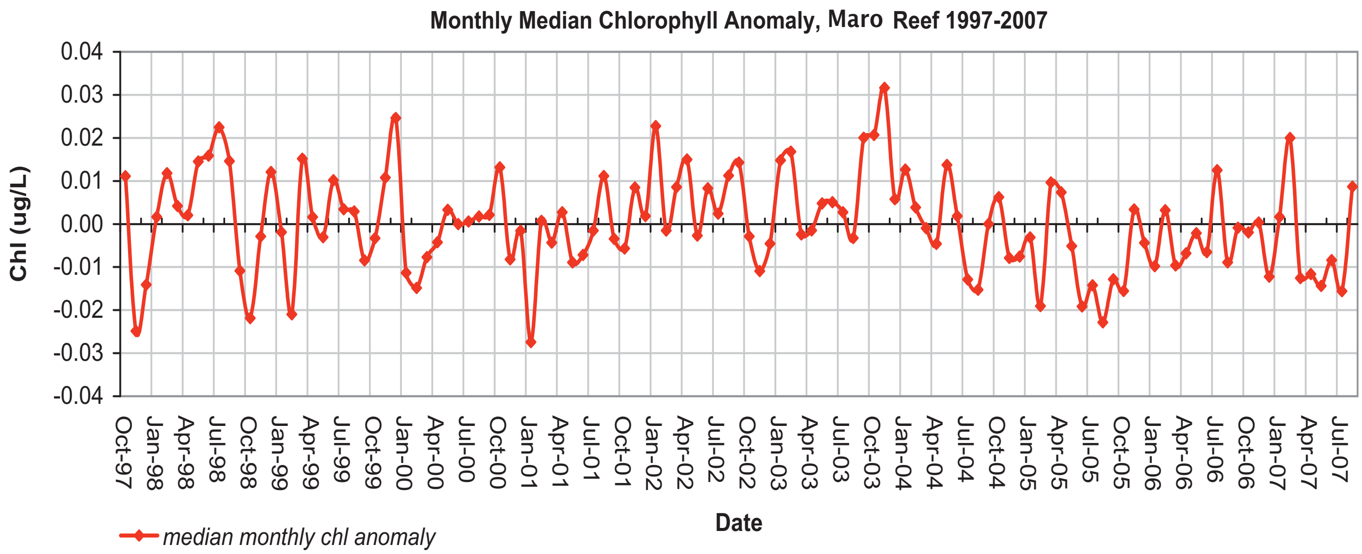
Monthly Median Chlorophyll Anomaly, Maro Reef 1997-2007
Chl (ug/L)
0.04
0.03
0.02
0.01
0.00
-0.01
-0.02
-0.03
-0.04
Oct-97
Jan-98
Apr-98
Jul-98
Oct-98
Jan-99
Apr-99
Jul-99
Oct-99
Jan-00
Apr-00
Jul-00
Oct-00
Jan-01
Apr-01
Jul-01
Oct-01
Jan-02
Apr-02
Jul-02
Oct-02
Jan-03
Apr-03
Jul-03
Oct-03
Jan-04
Apr-04
Jul-04
Oct-04
Jan-05
Apr-05
Jul-05
Oct-05
Jan-06
Apr-06
Jul-06
Oct-06
Jan-07
Apr-07
Jul-07
Date
median monthly chl anomaly

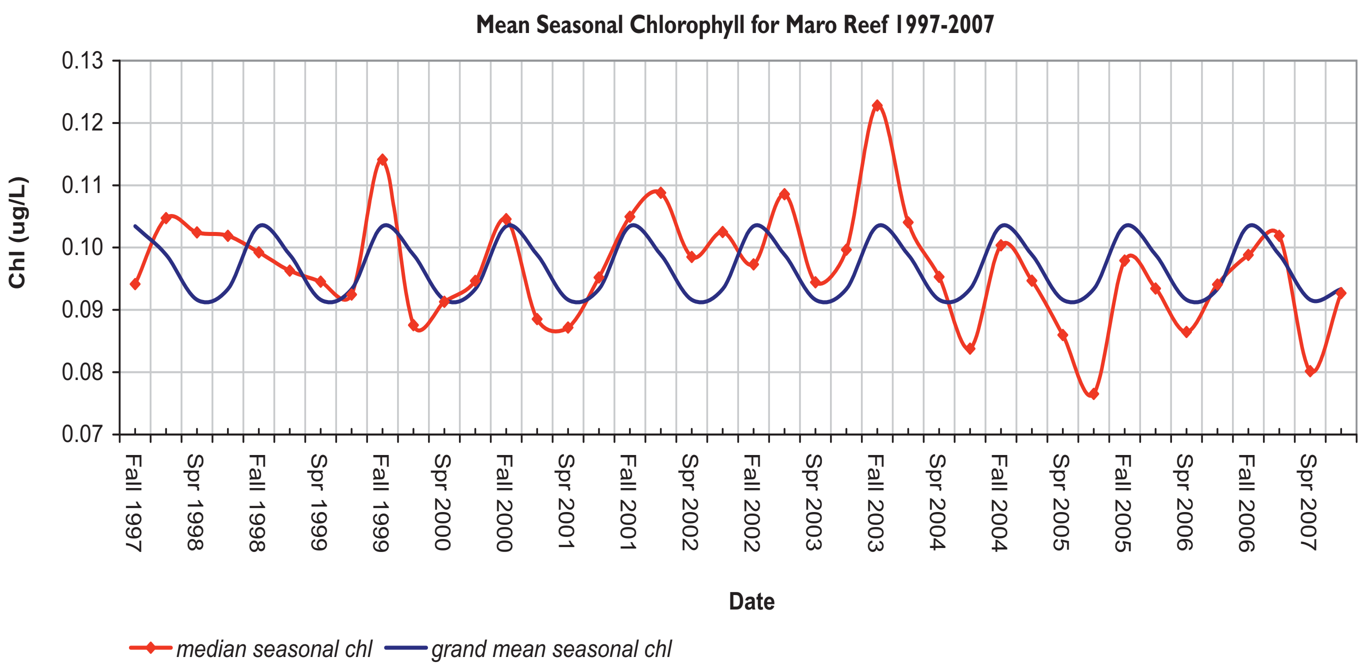
Mean Seasonal Chlorophyll for Maro Reef 1997-2007
Chl (ug/L)
0.13
0.12
0.11
0.10
0.09
0.08
0.07
Fall 1997
Spr 1998
Fall 1998
Spr 1999
Fall 1999
Spr 2000
Fall 2000
Spr 2001
Fall 2001
Spr 2002
Fall 2002
Spr 2003
Fall 2003
Spr 2004
Fall 2004
Spr 2005
Fall 2005
Spr 2006
Fall 2006
Spr 2007
Date
median seasonal chl
grand mean seasonal chl

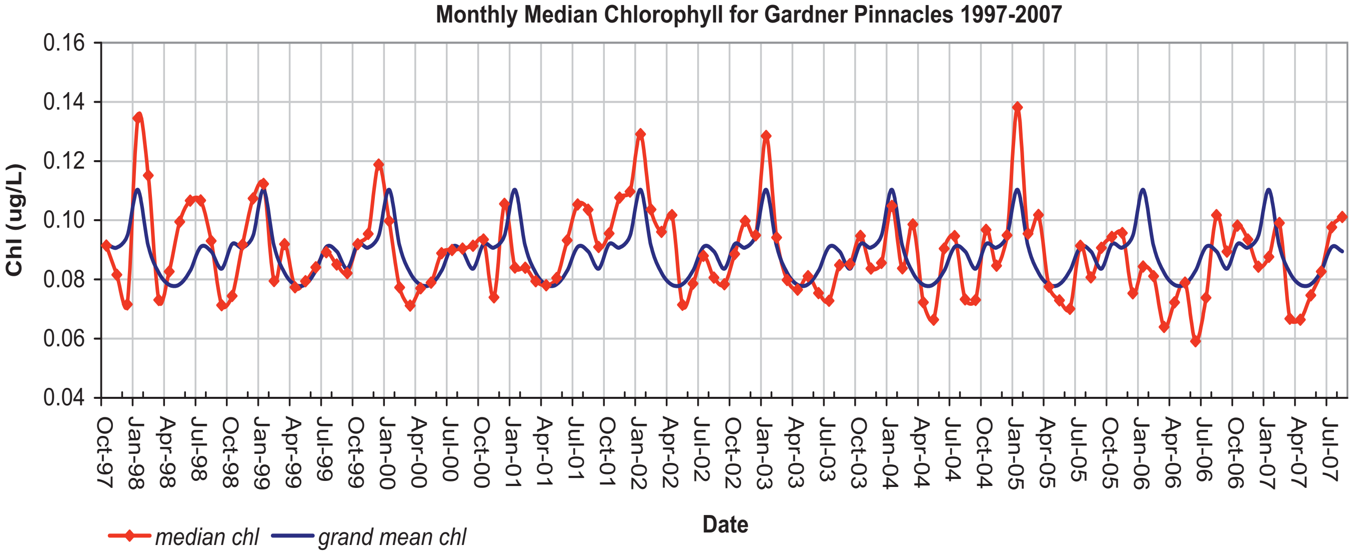
Monthly Median Chlorophyll for Gardner Pinnacles 1997-2007
Chl (ug/L)
Date
median chl
grand mean chl

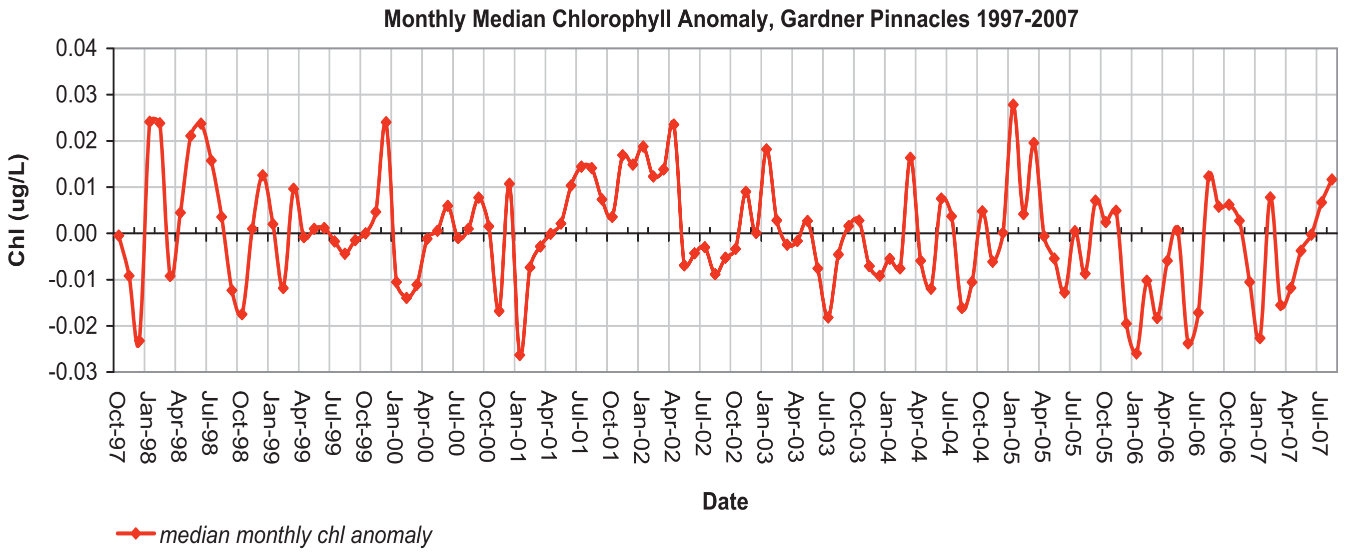
Monthly Median Chlorophyll Anomaly, Gardner Pinnacles 1997-2007
Chl (ug/L)
Date
median monthly chl anomaly

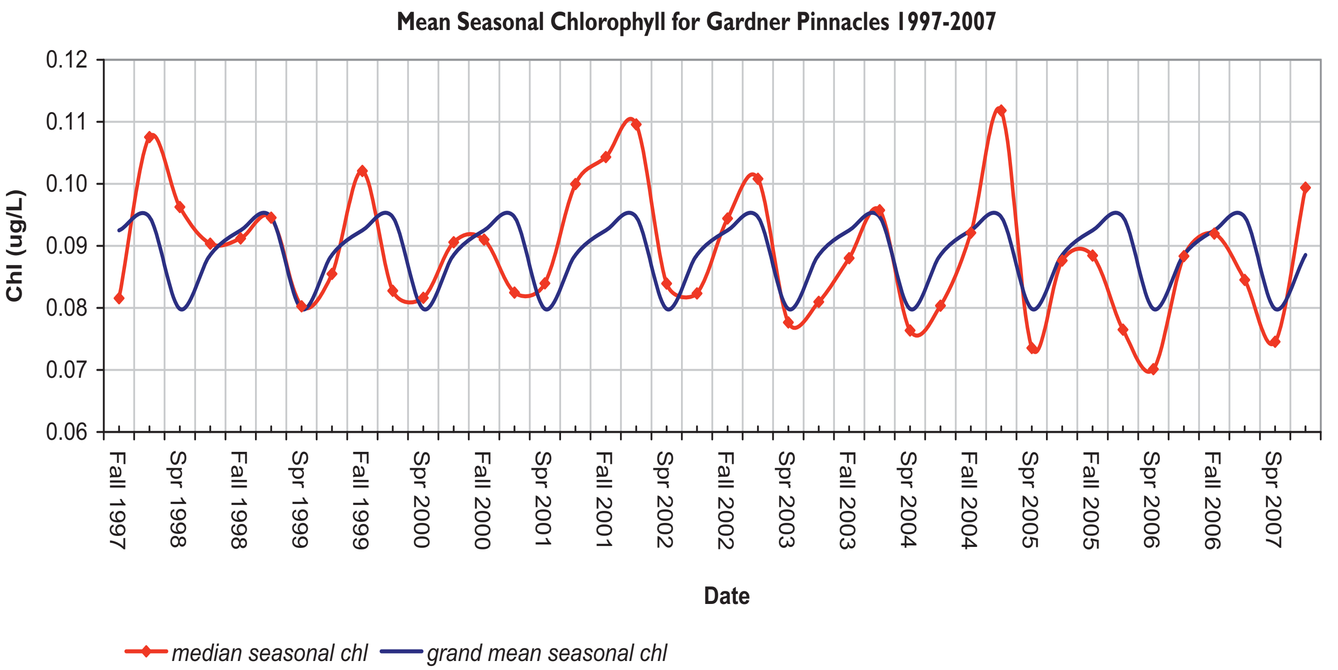
Mean Seasonal Chlorophyll for Gardner Pinnacles 1997-2007
Chl (ug/L)
Date
median seasonal chl
grand mean seasonal chl

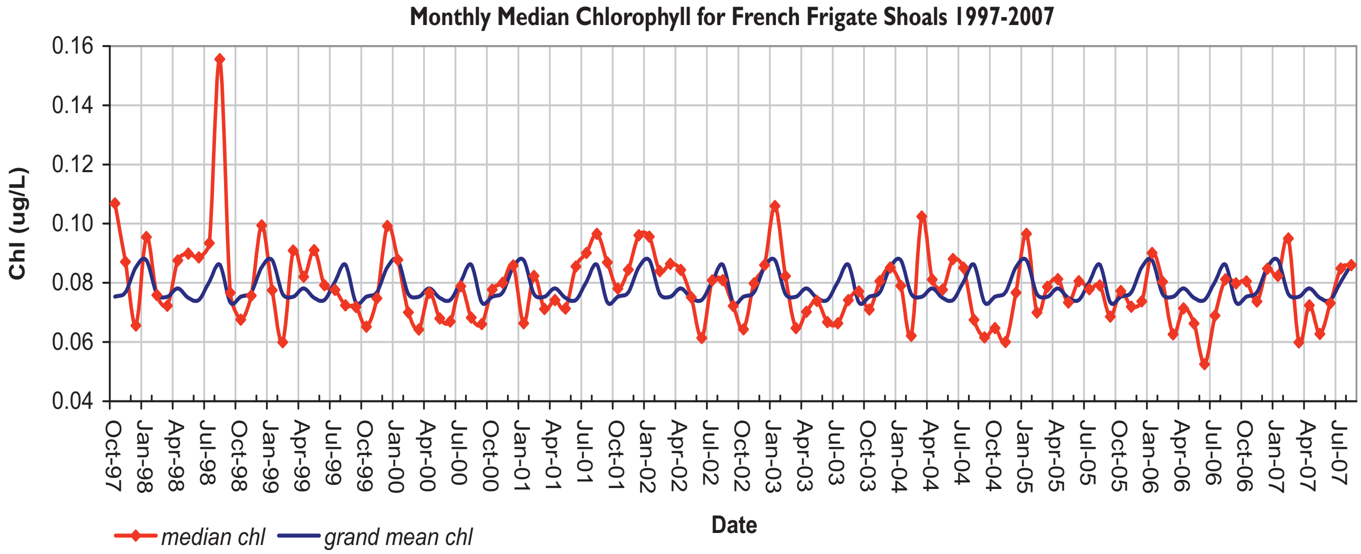
Monthly Median Chlorophyll for French Frigate Shoals 1997-2007
Chl (ug/L)
0.16
0.14
0.12
0.10
0.08
0.06
0.04
Oct-97 Jan-98 Apr-98 Jul-98 Oct-98 Jan-99 Apr-99 Jul-99 Oct-99 Jan-00 Apr-00 Jul-00 Oct-00 Jan-01 Apr-01 Jul-01 Oct-01 Jan-02 Apr-02 Jul-02 Oct-02 Jan-03 Apr-03 Jul-03 Oct-03 Jan-04 Apr-04 Jul-04 Oct-04 Jan-05 Apr-05 Jul-05 Oct-05 Jan-06 Apr-06 Jul-06 Oct-06 Jan-07 Apr-07 Jul-07
Date
median chl
grand mean chl

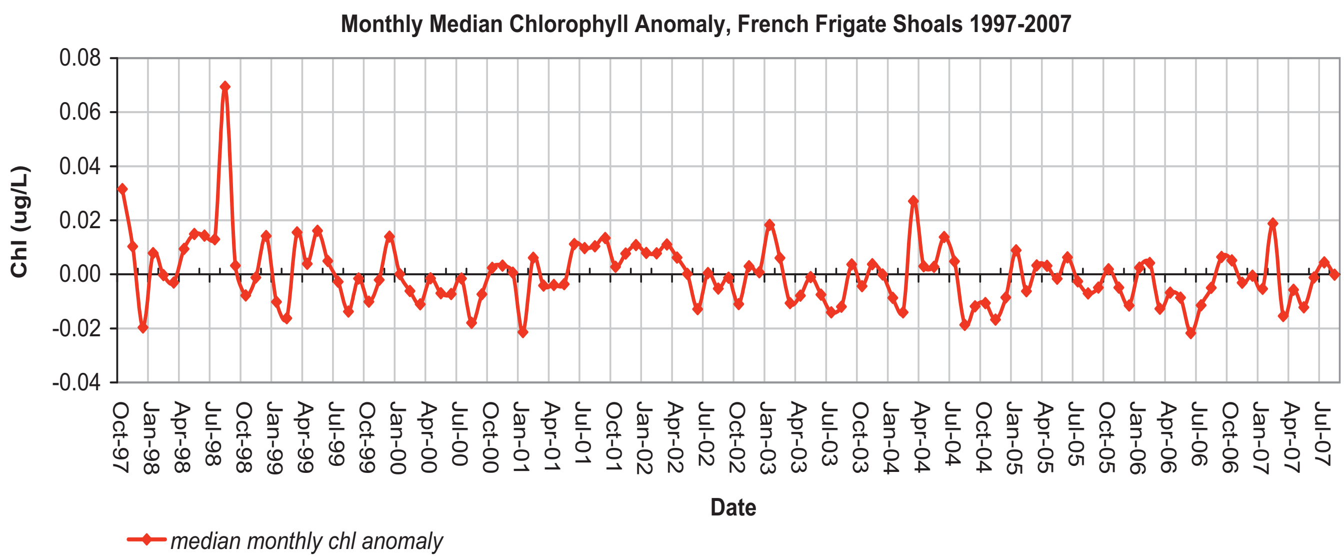
Monthly Median Chlorophyll Anomaly, French Frigate Shoals 1997-2007
Chl (ug/L)
0.08
0.06
0.04
0.02
0.00
-0.02
-0.04
Oct-97 Jan-98 Apr-98 Jul-98 Oct-98 Jan-99 Apr-99 Jul-99 Oct-99 Jan-00 Apr-00 Jul-00 Oct-00 Jan-01 Apr-01 Jul-01 Oct-01 Jan-02 Apr-02 Jul-02 Oct-02 Jan-03 Apr-03 Jul-03 Oct-03 Jan-04 Apr-04 Jul-04 Oct-04 Jan-05 Apr-05 Jul-05 Oct-05 Jan-06 Apr-06 Jul-06 Oct-06 Jan-07 Apr-07 Jul-07
Date
median monthly chl anomaly

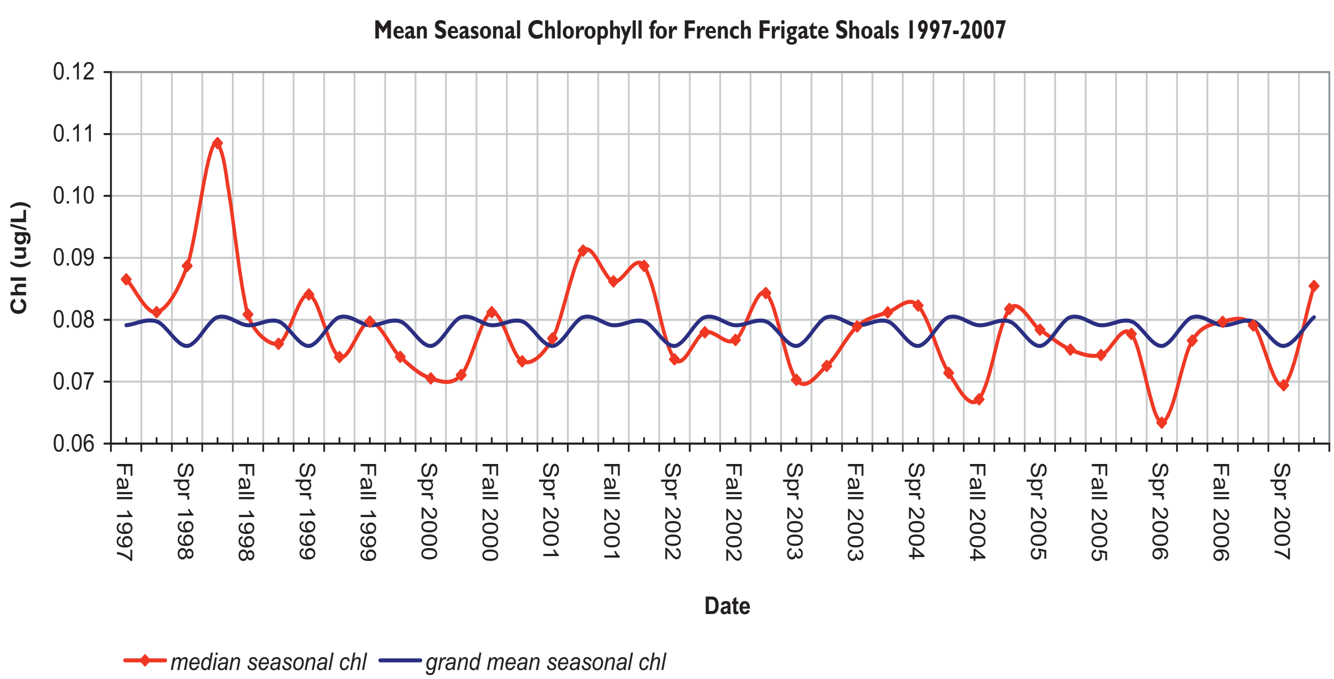
Mean Seasonal Chlorophyll for French Frigate Shoals 1997-2007
Chl (ug/L)
0.12
0.11
0.10
0.09
0.08
0.07
0.06
Fall 1997 Spr 1998 Fall 1998 Spr 1999 Fall 1999 Spr 2000 Fall 2000 Spr 2001 Fall 2001 Spr 2002 Fall 2002 Spr 2003 Fall 2003 Spr 2004 Fall 2004 Spr 2005 Fall 2005 Spr 2006 Fall 2006 Spr 2007
Date
median seasonal chl
grand mean seasonal chl

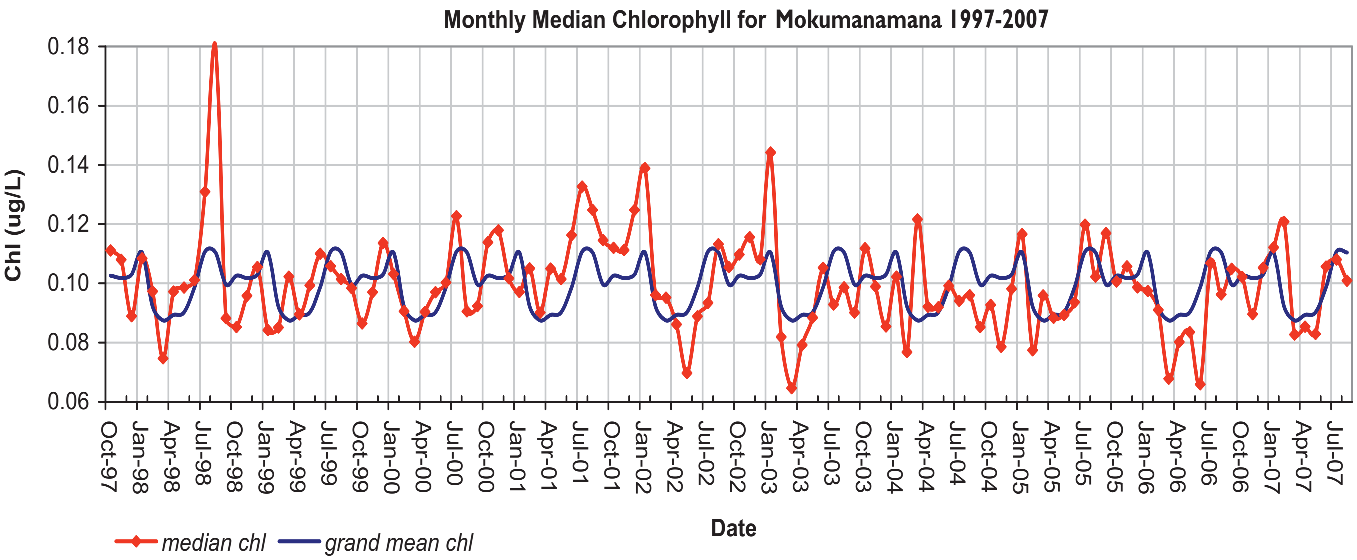
Monthly Median Chlorophyll for Mokumanamana 1997-2007
Chl (ug/L)
0.18
0.16
0.14
0.12
0.10
0.08
0.06
Oct-97 Jan-98 Apr-98 Jul-98 Oct-98 Jan-99 Apr-99 Jul-99 Oct-99 Jan-00 Apr-00 Jul-00 Oct-00 Jan-01 Apr-01 Jul-01 Oct-01 Jan-02 Apr-02 Jul-02 Oct-02 Jan-03 Apr-03 Jul-03 Oct-03 Jan-04 Apr-04 Jul-04 Oct-04 Jan-05 Apr-05 Jul-05 Oct-05 Jan-06 Apr-06 Jul-06 Oct-06 Jan-07 Apr-07 Jul-07
Date
median chl
grand mean chl

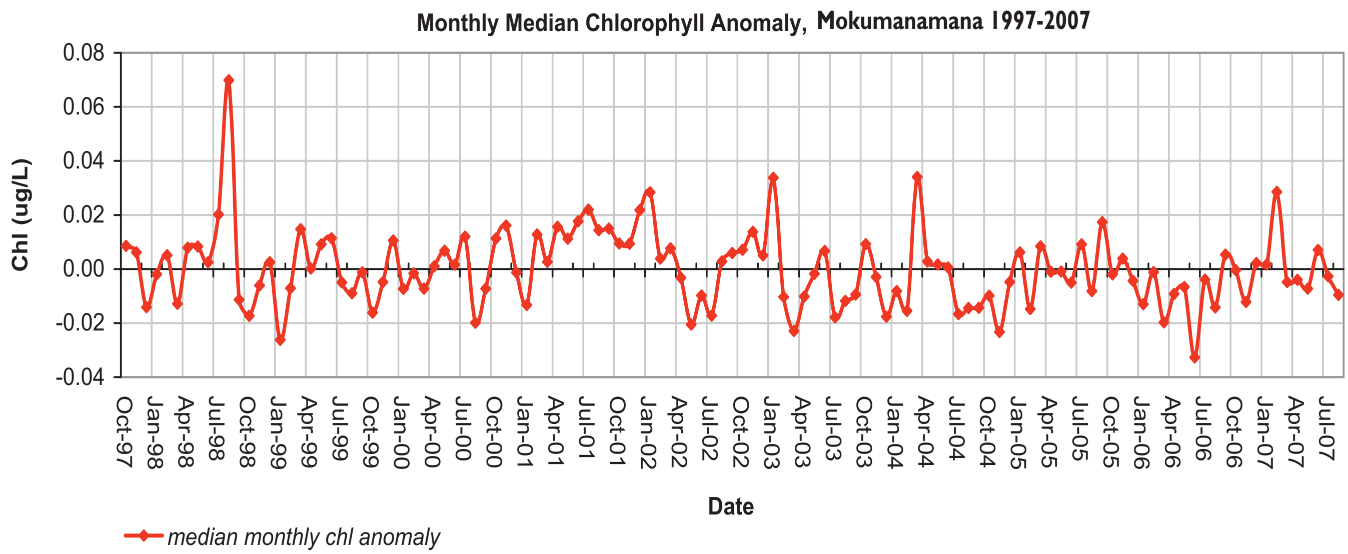
Monthly Median Chlorophyll Anomaly, Mokumanamana 1997-2007
Chl (ug/L)
0.08
0.06
0.04
0.02
0.00
-0.02
-0.04
Oct-97 Jan-98 Apr-98 Jul-98 Oct-98 Jan-99 Apr-99 Jul-99 Oct-99 Jan-00 Apr-00 Jul-00 Oct-00 Jan-01 Apr-01 Jul-01 Oct-01 Jan-02 Apr-02 Jul-02 Oct-02 Jan-03 Apr-03 Jul-03 Oct-03 Jan-04 Apr-04 Jul-04 Oct-04 Jan-05 Apr-05 Jul-05 Oct-05 Jan-06 Apr-06 Jul-06 Oct-06 Jan-07 Apr-07 Jul-07
Date
median monthly chl anomaly

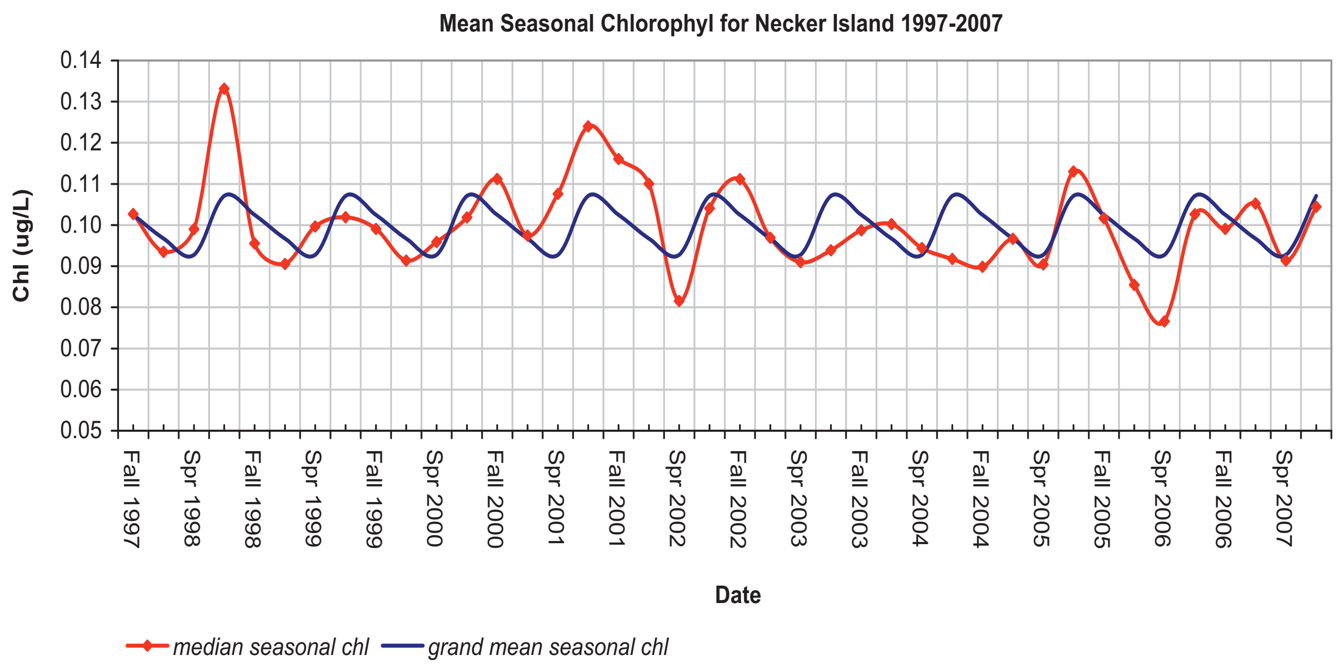
Mean Seasonal Chlorophyl for Necker Island 1997-2007
Chl (ug/L)
0.14
0.13
0.12
0.11
0.10
0.09
0.08
0.07
0.06
0.05
Fall 1997 Spr 1998 Fall 1998 Spr 1999 Fall 1999 Spr 2000 Fall 2000 Spr 2001 Fall 2001 Spr 2002 Fall 2002 Spr 2003 Fall 2003 Spr 2004 Fall 2004 Spr 2005 Fall 2005 Spr 2006 Fall 2006 Spr 2007
Date
median seasonal chl
grand mean seasonal chl

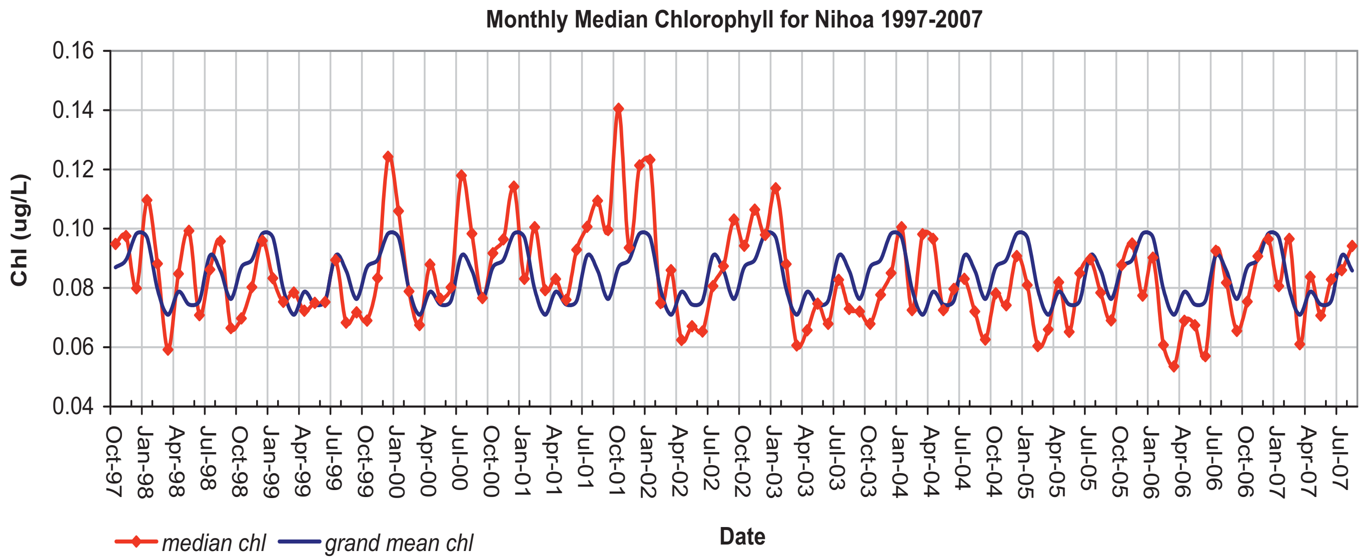
Monthly Median Chlorophyll for Nihoa 1997-2007
Chl (ug/L)
0.16
0.14
0.12
0.10
0.08
0.06
0.04
Oct-97 Jan-98 Apr-98 Jul-98 Oct-98 Jan-99 Apr-99 Jul-99 Oct-99 Jan-00 Apr-00 Jul-00 Oct-00 Jan-01 Apr-01 Jul-01 Oct-01 Jan-02 Apr-02 Jul-02 Oct-02 Jan-03 Apr-03 Jul-03 Oct-03 Jan-04 Apr-04 Jul-04 Oct-04 Jan-05 Apr-05 Jul-05 Oct-05 Jan-06 Apr-06 Jul-06 Oct-06 Jan-07 Apr-07 Jul-07
Date
median chl
grand mean chl

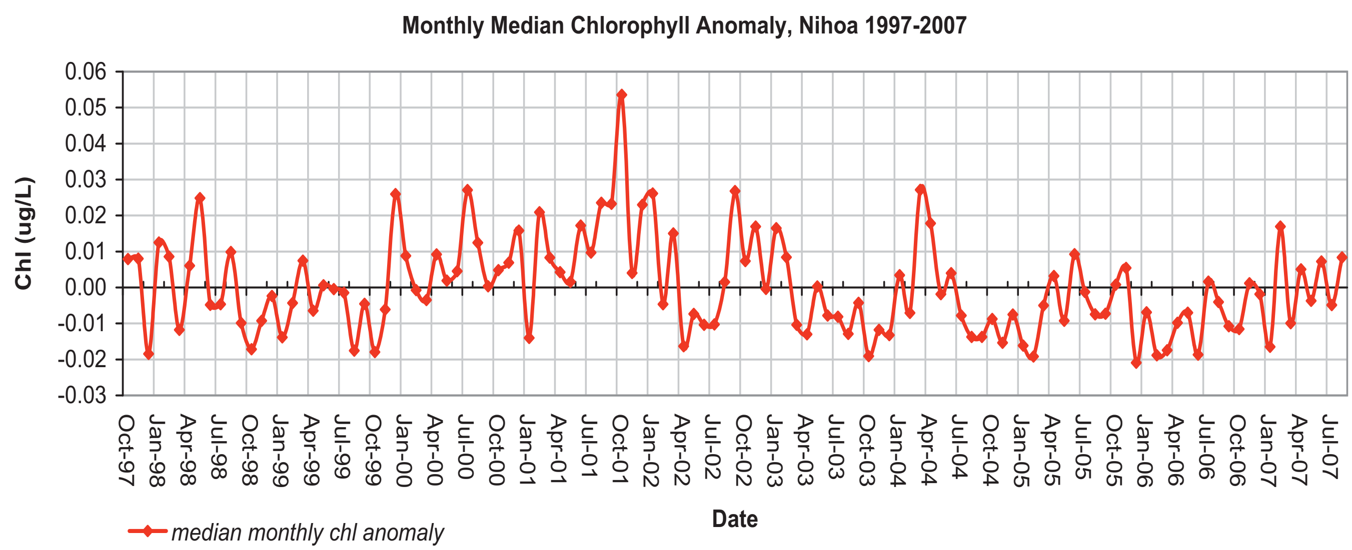
Monthly Median Chlorophyll Anomaly, Nihoa 1997-2007
Chl (ug/L)
0.06
0.05
0.04
0.03
0.02
0.01
0.00
-0.01
-0.02
-0.03
Oct-97 Jan-98 Apr-98 Jul-98 Oct-98 Jan-99 Apr-99 Jul-99 Oct-99 Jan-00 Apr-00 Jul-00 Oct-00 Jan-01 Apr-01 Jul-01 Oct-01 Jan-02 Apr-02 Jul-02 Oct-02 Jan-03 Apr-03 Jul-03 Oct-03 Jan-04 Apr-04 Jul-04 Oct-04 Jan-05 Apr-05 Jul-05 Oct-05 Jan-06 Apr-06 Jul-06 Oct-06 Jan-07 Apr-07 Jul-07
Date
median monthly chl anomaly

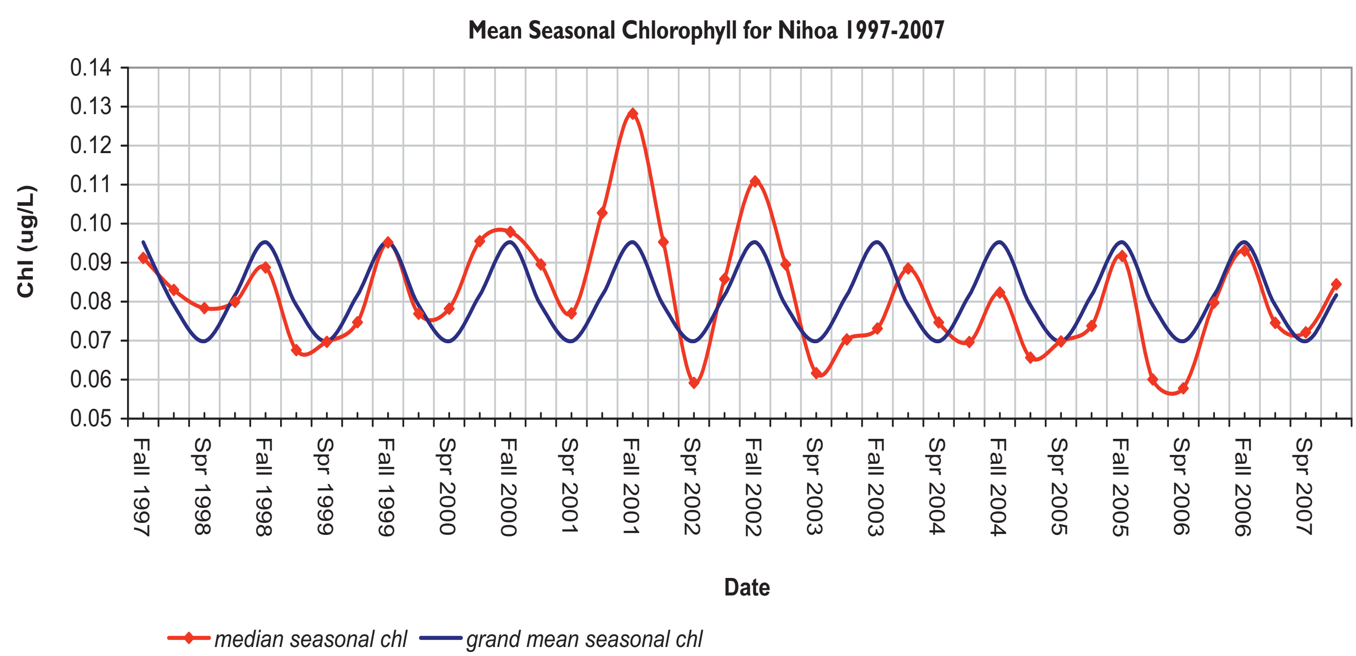
Mean Seasonal Chlorophyll for Nihoa 1997-2007
Chl (ug/L)
0.14
0.13
0.12
0.11
0.10
0.09
0.08
0.07
0.06
0.05
Fall 1997 Spr 1998 Fall 1998 Spr 1999 Fall 1999 Spr 2000 Fall 2000 Spr 2001 Fall 2001 Spr 2002 Fall 2002 Spr 2003 Fall 2003 Spr 2004 Fall 2004 Spr 2005 Fall 2005 Spr 2006 Fall 2006 Spr 2007
Date
median seasonal chl
grand mean seasonal chl

REFERENCES

Aeby G.S., J.C. Kenyon, J.E. Maragos, and D.C. Potts. 2003. First record of mass coral bleaching in the northwestern Hawaiian Islands. Coral Reefs 22: 256.

Amerson, A.B., R.B. Clapp, and W.O. Wirtz. 1974. Atoll Research Bulletin.

Ashmole, N.P. 1963. The Regulation of Numbers of Tropical Oceanic Birds. British Ornithologists Union Volume 103b:3, pp. 458 - 473.

Ashmole N.P. and M.J. Ashmole. 1967. Comparative feeding ecology of sea birds of a tropical oceanic island. Bulletin of the Peabody Museum of Natural History. 24: 1–131.

Bigelow, K. A., C. H. Boggs, and X. He. 1999. Environmental effects on swordfish and blue shark catch rates in the U.S. North Pacific longline fishery. Fish. Oceanogr. 8: 179-198.

Boehlert, G.W. 1993. Fisheries and marine resources of Hawaii and the U.S.-associated Pacific Islands: An introduction. Marine Fisheries Review. Vol. 55, no. 2, pp. 3-6.

Bograd, S.J., D.G. Foley, F.B. Schwing, C. Wilson, R.M. Laurs, J.J. Polovina, E.A. Howell, and R.E. Brainard. 2004. On the seasonal and interannual migrations of the transition zone chlorophyll front. Geophys. Res. Lett. 31: L17204.

Brainard, R.E., R. Hoeke, R.A. Moffitt, K.B. Wong, J. Firing, J. Gove, S. Choukroun, and K. Hogrefe. 2004. Spatial and temporal variability of key oceanographic processes influencing coral reef ecosystems of the Northwestern Hawaiian Islands [Abst]. Northwestern Hawaiian Islands: 3rd Scientific Symposium. Honolulu, HI. Nov. 2-4 2004, p. 18.

Bromirski, P.D., D.R. Cayan, and R.E. Flick. 2005. Wave spectral energy variability in the northeast Pacific. J. Geophys. Res., 110: C03005, doi:10.1029/2004JC002398.

Canny, J. 1986. A computational approach to edge detection. Institute of Electrical and Electronic Engineers (IEE). Transactions on pattern analysis and machine intelligence. No. 8. IEEE, New York. pp. 679–698.

Di Lorenzo, E., N. Schneider, K.M. Cobb, K. Chhak, P.J.S. Franks, A.J. Miller, J.C. McWilliams, S.J. Bograd, H. Arango, E. Curchister, T.M. Powell, and P. Rivere. 2008. North Pacific Gyre Oscillation links ocean climate and ecosystem change. Geophys. Res. Lett., 35, L08607, doi:10.1029/2007GL032838.

DeMartini, E.E. and A.M. Friedlander. 2004. Spatial patterns of endemism in shallow-water reef fishes of the North West Hawaiian Islands. Marine Ecology Progress Series Vol. 271: 281-296

Dollar, S.J. 1982. Wave stress and coral community structure in Hawaii. Coral Reefs 1: 71-81.

Dollar, S.J. and R.W. Grigg. 2004. Anthropogenic and natural stresses on selected coral reefs in Hawaii: A multidecade synthesis of impact and recovery. Pac. Sci. 58(2): 281-304.

Feare, C.J. 1976. Desertion and abnormal development in a colony of Sooty Terns infested by virus-infected ticks. Ibis. 118: 112–115.

Firing, J.B., R. Brainard, and E. Firing. 2004a. Ten years of shipboard ADCP measurements along the Northwestern Hawaiian Islands. Northwestern Hawaiian Islands: 3rd Scientific Symposium, Honolulu. 18 pp.

Firing, J.B., R. Hoeke, R.E. Brainard, and E. Firing. 2004b. Connectivity in the Hawaiian Archipelago and beyond: potential larval pathways. pp. 310. In: Proceedings of the 10th International Coral Reef Symposium, Okinawa.

Flint, E. 1991. Time and energy limits to the foraging radius of sooty terns *Sterna fuscata.* Ibis. 133: 43-46.

Friedlander, A., G. Aeby, R. Brainard, A. Clark, E. DeMartini, S. Godwin, J. Kenyon, R. Kosaki, J. Maragos, and P. Vroom. 2005. The State of the Coral Reef Ecosystem of the Northwestern Hawaiian Islands. pp. 270-311. In: J.E. Waddell (ed.). The State of Coral Reef Ecosystems of the United States and Pacific Freely Associated States: 2005. NOAA Technical Memorandum NOS NCCOS 11. Silver Spring, MD. 522 pp.

Fu, L.-L. 2004. The interannual variability of the North Atlantic Ocean revealed by combined data from TOPEX/Poseidon and Jason altimetric measurements. Geophys. Res. Lett., 31, L23303.

Fu, L.-L., E.J. Christensen, C.A. Yamarone Jr., M. Lefebvre, Y. Ménard, M. Dorrer, and P. Escudier. 1994. TOPEX/POSEIDON mission overview, J. Geophys. Res. 99(C12), 24,369–24,381.

Giambelluca, T.W. and T.A. Schroeder. 1998. Climate. In Atlas of Hawaii (eds. S.P. Juvik and J.O. Juvik). University of Hawaii Press, Honolulu.

Gilson J., D. Roemmich, B. Cornuelle, and L.L. Fu. 1998. The Relationship of TOPEX/POSEIDON altimetric height to the steric height of the sea surface. J. Geophys. Res. 103: 27947-27965.

Hoeke R., R. Brainard, R. Moffitt, and M. Merrifield. 2006. The role of oceanographic condition and reef morphology in the 2002 coral bleaching event in the Northwest Hawaiian Islands. Atoll Research Bulletin. 543.

Houk P., S. Bograd, and R. van Woesik. 2007. The transition zone chlorophyll front can trigger *Acanthaster planci* outbreaks in the Pacific Ocean: Historical confirmation. J. Oceanogr. Vol. 63(1): 149-154(6).

IFREMER. 2002. QuikSCAT Scatterometer Mean Wind Field Products User Manual. Reference: C2-MUT-W-03-IF. Ver. 1.

Johannes, R.E. 1981. Words of the Lagoon: Fishing and marine lore in the Palau District of Micronesia. University of California Press, Berkeley.

Johnson, G.C., M.J. McPhaden, G.D. Rowe, and K.E. McTaggert. 2000. Upper equatorial Pacific Ocean current and salinity variability during the 1996—1998 El Niño-La Niña cycle. J. Geophys. Res. 105: 1037—1053.

Jokiel, P.L. and S.L. Coles. 1990. Response of Hawaiian and other Indo-Pacific reef corals to elevated temperatures associated with global warming. Coral Reefs 8: 155-162.

Jokiel, P.L. and E.K. Brown. 2004. Global warming, regional trends and inshore environmental conditions influence coral bleaching in Hawaii. Global Change Biol. 10: 1627-1641.

Jones, M.S., M. Allen, T. Guymer, and M. Saunders. 1998. Correlations between altimetric sea surface height and radiometric sea surface temperature in the South Atlantic. J. Geophys. Res. 103(C4): 8073–8087.

Kalnay, E., M. Kanamitsu, R. Kistler, W. Collins, D. Deaven, L. Gandin, M. Iredell, S. Saha, G. White, J. Woollen, Y. Zhu, A. Leetmaa, R. Reynolds, M. Chelliah, W. Ebisuzaki, W. Higgins, J. Janowiak, K. Mo, C. Ropelewski, J. Wang, R. Jenne, and D. Joseph. 1996. The NCEP/NCAR 40-Year Reanalysis Project. Bull. Amer. Meteor. Soc. 77: 437–471.

Kazmin, A.S. and M.M. Rienecker. 1996. Variability and frontogenesis in the large-scale oceanic frontal zones. J. Geophysical Research 101 (C1), 907-921.

Kenyon, J.C., G.S. Aeby, R.E. Brainard, J.D. Chojnacki, M.J. Dunlap, and C.B. Wilkinson. 2006. Mass coral bleaching on high-latitude reefs in the Hawaiian Archipelago. pp: 631-634. In: Proceedings of the 10th International Coral Reef Symposium Okinawa 2. Okinawa, Japan. 1,950 pp.

Kenyon, J.C. and R.E. Brainard. 2006. Second recorded episode of mass coral bleaching in the Northwestern Hawaiian Islands. Atoll Research Bulletin 543: 505-523.

Laurs, R.M., P.C. Fiedler, and D.R. Montgomery. 1984. Albacore tuna catch distribution relative to environmental features observed from satellites. Deep-Sea Res., 31(9): 1085-1099.

Leonard, C.L., R.R. Bidigare, M.P. Seki, and J.J. Polovina. 2001. Interannual mesoscale physical and biological variability in the North Pacific Central Gyre. Progress In Oceanography 49(1-4): 227-244.

Mantua, N.J., S.R. Hare, Y. Zhang, J.M. Wallace, and R.C. Francis. 1997. A Pacific decadal climate oscillation with impacts on salmon. Bulletin of the American Meteorological Society. 78: 1069-1079.

NASA. 2004. AVHRR Oceans Pathfinder Sea Surface Temperature Datasets. [Available online] http://podaac.jpl.nasa.gov:2031/DATASET_DOCS/avhrr_pathfinder_sst_v5.html.

NASA. 2005. AVHRR Pathfinder Documentation. [Available online] http://podaac.jpl.nasa.gov/DATA_CATALOG/avhrrinfo.html.

NOAA, NOS, SPO. 1999. Coastal Assessment Framework. Silver Spring, MD.

NOAA. 2004. NOAA-CIRES Climate Diagnostics Center. [available online] http://www.cdc.noaa.gov/.

NOAA. 2005. National Data Buoy Center. [available online] http://www.ndbc.noaa.gov/.

National Weather Service. 2007. Cold and warm episodes by season. http://www.cpc.ncep.noaa.gov/products/analysis_monitoring/ensostuff/ensoyears.shtml.

Nakamura, H. and A.S. Kazmin. 2003. Decadal changes in the North Pacific oceanic frontal zones as revealed in ship and satellite observations. J. Geophysical Research 108 (C3). 3078. doi:10.1029/1999JC000085.

Papahanaumokuakea Marine National Monument Management Plan: Environmental Assessment Volume II. 2008. NOAA, U.S. Fish & Wildlife Service, and the State of Hawaii. 264 pp.

Philander, S.G. 1990. El Niño, La Niña and the Southern Oscillation. Academic Press. San Diego, CA. 293 pp.

Polovina, J.J., D.R. Kobayashi, D.M. Ellis, M.P. Seki, and G.H. Balazs. 2000. Turtles on the edge: movement of loggerhead turtles (*Caretta caretta*) along oceanic fronts in the central North Pacific, 1997–1998. Fisheries Oceanography 9: 71–82.
Polovina, J.J. and Haight. 1999. Climate variation, ecosystem dynamics, and fisheries management in the NWHI. Ecosystem Approaches for Fisheries Management. Alaska Sea Grant College Program AK-SG-99-01.

Polovina J.J., E. Howell, D.R. Kobayashi, and M.P. Seki. 2001. The Transition Zone Chlorophyll Front, a dynamic global feature defining migration and forage habitat for marine resources. Progress in Oceanography 49(1–4): 469–483.

Polovina, J.J., G.T. Mitchum, N.E. Graham, M.P. Craig, E.E. DeMartini, and E.N. Flint. 1994. Physical and biological consequences of a climate event in the central North Pacific. Fish.Oceanogr. 3: 15–21.

Polovina J.J., G.T. Mitchum, and G.T. Evans. 1995. Decadal and basin-scale variation in mixed layer depth and the impact on biological production in the Central and North Pacific, 1960–88. Deep-Sea Research 42: 1701–1716.

Polovina, J.J. 2005. Climate variation, regime shifts, and implications for sustainable fisheries. Bull. Mar. Sci. 76: 233-2144.

Polovina, J.J. and E. Howell. 2005. Ecosystem indicators derived from satellite remotely sensed oceanography data for the North Pacific. ICES. J. Marine Science 62: 319-327.

Polovina, J.J., E. Howell, D.R. Kobayashi, and M.P. Seki. 2001. The transition zone chlorophyll front, a dynamic global feature defining migration and forage habitat for marine resources. Prog. Oceanogr. 49(1-4): 469-483.

Qiu, B. 1999. Seasonal eddy field modulation of the North Pacific Subtropical Countercurrent: TOPEX/Poseidon observations and theory. J. Phys. Oceanogr. 29: 1670-1685.

Roemmich, D. and J. Gilson. 2001. Eddy transport of heat and thermocline waters in the North Pacific: a key to interannual/decadal climate variability? J. Phys. Oceanogr. 13: 675-687.

Savidge, G. 1976. A preliminary study of the distribution of chlorophyll a in the vicinity of fronts in the Celtic and western Irish Sea. Estuarine, Coastal and Marine Science 4: 617–625.

Savidge, G. and P. Foster. 1978. Phytoplankton biology of a thermal front in the Celtic Sea. Nature 271: 155–157.

Seki, M.P., J.J. Polovina, R.E. Brainard, R.R. Bidigare, C.L. Leonard, and D.G. Foley. 2001. Biological enhancement at cyclonic eddies tracked with GOES thermal imagery in Hawaiian waters. Geophys. Res. Letters. 28(8): 1583-1586.

Seki, M.P., J.J. Polovina, D.R. Kobayashi, R.R. Bidigare, and G.T. Mitchum. 2002. An oceanographic characterization of swordfish (*Xiphias gladius*) longline fishing grounds in the springtime subtropical North Pacific. Fisheries Oceanography 11(5): 251-266(16).

Stumpf, R.P., R.A. Arnone, R.W. Gould, Jr., P. Martinolich, and V. Ransibrahmanakul. 2002. A Partially-Coupled Ocean-Atmosphere Model for Retrieval of Water-Leaving Radiance from SeaWiFS in Coastal Waters: In: Patt, F.S., and et al., 2002: Algorithm Updates for the Fourth SeaWiFS Data Reprocessing. NASA Tech. Memo. 2002-206892, Vol. 22, S.B. Hooker and E.R. Firestone, Eds., NASA Goddard Space Flight Center, Greenbelt, Maryland.

Stumpf, R.P., M.E. Culverb, P.A. Testerc, M. Tomlinsona, G.J. Kirkpatrickd, B.A. Pedersond, E. Trubye, V. Ransibrahmanakulf, and M. Soracco. 2003. Monitoring *Karenia brevis* blooms in the Gulf of Mexico using satellite ocean color imagery and other data. Harmful Algae Vol. 2(2): 147-160.

Ullman, D. and P. Cornillon. 1999. Satellite-derived sea surface temperature fronts on the continental shelf off the northeast U.S. coast. J. Geophys. Res. 104(C10): 23459-23478.

Wilson, C. and V. J. Coles. 2005. Global climatological relationships between satellite biological and physical observations and upper ocean properties. J. Geophys. Res. 110, C10001.